

“Life moves pretty fast. You don’t stop and look around once in a while, you could miss it.”
- Ferris Bueller, *Ferris Bueller’s Day Off*

University of Alberta

Analysis of Nitrogen Species in Gas Oils Using High Performance Liquid Chromatography and Fourier Transform Ion Cyclotron Resonance Mass Spectrometry

by

Nicole Elizabeth Oro

A thesis submitted to the Faculty of Graduate Studies and Research
in partial fulfillment of the requirements for the degree of

Doctor of Philosophy

Department of Chemistry

©Nicole Elizabeth Oro

Fall 2012

Edmonton, Alberta

Permission is hereby granted to the University of Alberta Libraries to reproduce single copies of this thesis and to lend or sell such copies for private, scholarly or scientific research purposes only. Where the thesis is converted to, or otherwise made available in digital form, the University of Alberta will advise potential users of the thesis of these terms.

The author reserves all other publication and other rights in association with the copyright in the thesis and, except as herein before provided, neither the thesis nor any substantial portion thereof may be printed or otherwise reproduced in any material form whatsoever without the author's prior written permission.

ABSTRACT

The nitrogen content of products derived from oil sands bitumen is important, as nitrogen causes problems in upgrading and hydrotreating. Normal phase high performance liquid chromatography (HPLC) has been previously used to attempt separation of the nitrogen group types (pyrrole and pyridine) found in petroleum, but complete separation in a single step has not been achieved. High resolution Fourier Transform Ion Cyclotron Resonance Mass Spectrometry (FT-ICR MS) has been used successfully for the detailed analysis of nitrogen content in petroleum samples (petroleomics), but HPLC separation prior to petroleomic analysis has not been exploited.

This thesis explores the use of normal phase HPLC and FT-ICR MS to gain a better understanding of the nitrogen compounds found in gas oil samples derived from oil sands bitumen. Unconventional hypercrosslinked polystyrene stationary phases and a commercial dinitrophenyl (“DNAP”) stationary phase were studied for their nitrogen group-type separation capabilities. Hypercrosslinked polystyrene was found to have unique selectivity for nitrogen compounds. Custom synthesized hypercrosslinked polystyrene was able to separate pyrroles, pyridines and polycyclic aromatic hydrocarbons (PAHs) into three distinct groups, acting via an adsorption mechanism. Polymeric hypercrosslinked polystyrene separates model compounds by both aromaticity and heteroatom content. The “DNAP” column separates nitrogen-containing compounds from PAHs.

Methods were developed in order to analyze HPLC fractions collected offline on an FT-ICR MS system. Concentrating the HPLC fractions and adding strong acid or base prior to analysis were important steps. Contamination from sample handling was found to be an issue, and proper procedures to eliminate sources of contamination are described, including a previously unreported interference from iron-formate ion clusters.

These methods were used to analyze HPLC fractions of gas oil samples on “DNAP” on the FT-MS. The MS data revealed that the chromatographic peak intensity on “DNAP” can be correlated to nitrogen content in the sample, and that alkylation reduces retention of pyrroles and pyridines. “DNAP” separations can also be used to judge the relative efficiency of nitrogen removal processes. Comparison of fraction data to petroleomic analysis of unfractionated samples showed that the HPLC fraction analysis is a compliment to full petroleomic studies of samples.

ACKNOWLEDGMENTS

I would like to thank my supervisor, Dr. Charles Lucy, for his guidance and support throughout my degree. I am grateful for the many travel opportunities he has given me, and for allowing me to be creative and explore my own ideas in my research. I also need to thank Dr. Randy Whittal and Dr. Richard Paproski. I could not have completed this degree without their incredibly patient advice, support and training. I thank the machine shop, especially Dieter Starke, for always repairing parts of my instrument with a sense of humor. I would also like to thank Ping Jiang, for allowing me to use some of her “DNAP” data. Thank you to my committee, for your time and input on this thesis: Dr. Liang Li, Dr. Mariusz Klobukowski, Dr. James Harynuk, Dr. Murray Gray and Dr. Kevin Thurbide.

My sincerest thanks go to the people who have provided emotional support to me during this degree. Thank you to my parents, Kathleen and Bruce. Thank you to my mom, for always listening to me when I needed to talk about anything; you have celebrated my successes and loved me through the complaining. I especially thank Andrew, for constantly pushing me to be better, and for letting me lean on him when I needed to. I have always been encouraged by the desire to make you proud. For the rest of my life I will be grateful to the incredible women I have shared the journey of graduate school with; your friendship has made my life better both inside and outside school. Thank you to Andrea, Margot, Chen, Brandon and Katie for both laughing with me and encouraging me.

This thesis was supported by the University of Alberta, the Natural Sciences and Engineering Council of Canada, Alberta Innovates Technology Futures and Syncrude Canada Ltd.

TABLE OF CONTENTS

CHAPTER ONE. Introduction

1.1	Motivation and Thesis Overview	1
1.2	Chromatography	4
1.2.1	Separations	4
1.2.2	Chromatography Theory	5
1.2.3	Band Broadening.....	9
1.3	Normal Phase Separations	17
1.3.1	Normal Phase High Performance Liquid Chromatography	17
1.3.2	Stationary Phases	19
1.3.3	Nitrogen Group-Type Separations	22
1.3.4	Detection	24
1.4	Mass Spectrometry.....	24
1.4.1	Fourier Transform Ion Cyclotron Resonance Mass Analyzer.....	25
1.4.2	Electrospray Ionization.....	31
1.4.3	The Nitrogen Rule.....	33
1.5	Summary	34
1.6	References.....	35

CHAPTER TWO. Comparison of Hypercrosslinked Polystyrene Columns for the Separation of Nitrogen Group-Types in Petroleum Using HPLC

2.1	Introduction.....	40
2.2	Experimental	44
2.2.1	Apparatus.....	44
2.2.2	Chemicals	45
2.2.3	Column Packing	47
2.2.4	Calculations	48
2.3	Results and Discussion	48
2.3.1	Retention Behavior on Hypercrosslinked Phases.....	50
2.3.1.1	Retention of Standards	50
2.3.1.2	Mechanism of Retention.....	54
2.3.2	Comparison of HC-Tol and HC-C ₈	61
2.3.3	Comparison of HC-Tol and HGN phases.....	63
2.3.4	Separation of Model Compounds on HC-Tol	64
2.4	Conclusions.....	69

2.5	References.....	70
-----	-----------------	----

CHAPTER THREE. High Performance Liquid Chromatographic Separations of Gas Oil Samples and Their Hydrotreated Products Using Commercial Normal Phases

3.1	Introduction.....	74
3.2	Experimental.....	78
3.2.1	Apparatus.....	78
3.2.2	Chemicals.....	79
3.2.3	Calculations.....	79
3.3	Results and Discussion.....	82
3.3.1	HGN: Commercial Hypercrosslinked Polystyrene.....	83
3.3.1.1	Model Compounds.....	83
3.3.1.2	Gas Oil Samples.....	86
3.3.2	Restek Biphenyl Phase.....	92
3.3.3	“DNAP”: Dinitrophenyl Phase.....	95
3.3.3.1	Model Compounds.....	95
3.3.3.2	Gas Oil Samples.....	100
3.4	Conclusions.....	104
3.5	References.....	106

CHAPTER FOUR. Sample Handling and Contamination Encountered When Coupling Offline High Performance Liquid Chromatography Fraction Collection of Petroleum Samples to Fourier Transform Ion Cyclotron Resonance Mass Spectrometry

4.1	Introduction.....	110
4.2	Experimental.....	113
4.2.1	Apparatus.....	113
4.2.2	Chemicals.....	114
4.2.3	Fraction Collection and Sample Preparation.....	117
4.3	Results and Discussion.....	118
4.3.1	Sample Concentration.....	119
4.3.1.1	Sample Screening and Fraction Selection.....	119
4.3.1.2	Sample Preparation.....	123
4.3.2	Contaminants and Interferences.....	130
4.3.2.1	Soaps and Detergents.....	130
4.3.2.2	Molecular Sieves.....	131
4.3.2.3	Plastic.....	134

4.3.2.4 Identified Interferences.....	136
4.4 Conclusions.....	143
4.5 References.....	144

CHAPTER FIVE. Analysis of Nitrogen Content in Distillate Cut Gas Oils and Treated Heavy Gas Oils Using Normal Phase HPLC, Fraction Collection and Petroleomic FT-ICR MS Data

5.1 Introduction.....	148
5.2 Experimental.....	152
5.2.1 Apparatus.....	152
5.2.2 Chemicals.....	152
5.2.3 Mass Spectrum Data Analysis.....	153
5.2.3.1 Composer Parameters.....	158
5.2.3.2 Composer Viewing Options.....	160
5.3 Results and Discussion.....	161
5.3.1 Separations on HC-Tol.....	161
5.3.2 Separations on “DNAP”.....	166
5.3.3 FT-ICR MS Analysis of the “DNAP” Fractions.....	173
5.3.4 Case Study: Comparing Catalysts.....	188
5.4 Conclusions.....	191
5.5 References.....	191

CHAPTER SIX. Conclusions and Future Work

6.1 Conclusions.....	196
6.1.1 Normal Phase HPLC.....	196
6.1.2 High Resolution Mass Spectrometry.....	198
6.2 Future Work.....	200
6.2.1 Improving HPLC Separations.....	200
6.2.2 Petroleomic Data Analysis.....	203
6.2.3 Different MS Ionization Methods.....	204
6.2.4 Response Factors and Quantitative Analysis.....	206
6.2.5 Perspective on Current Research.....	207
6.3 References.....	208

**APPENDIX A. Exporting Chromatograms from Varian's Star Workstation
and Mass Spectra from Bruker's DataAnalysis for Re-plotting**

A.1 Exporting Chromatograms.....213

A.2 Exporting Mass Spectra216

LIST OF TABLES

2-1	Model compounds used to test column retention.....	46
2-2	Correlation coefficients for standards on the HC-Tol and HGN columns.....	59
2-3	Efficiencies and retention on the HC-Tol column	68
3-1	Model compounds used to test column retention.....	80
3-2	Bulk properties of the light and heavy gas oil samples.....	81
3-3	Retention factors of model compounds on the HGN column.....	84
3-4	Retention factors of model compounds on the biphenyl column.....	94
4-1	FT-ICR MS instrument parameters	115-116
4-2	Mass values and sources for positive ion contamination peaks in Figure 4-9.....	133
4-3	Positive ion contamination peaks observed in HPLC fractions.....	137
4-4	Negative ion contamination peaks observed in HPLC fractions	138
5-1	Sample information for light gas oil distillate cut samples.....	154
5-2	Sample information for heavy gas oil distillate cut samples	155
5-3	Sample information for catalyst sample set	156
5-4	Dominant compound classes present in HPLC fractions on the “DNAP” column for selected distillate cut samples	176-177
5-5	Dominant compound classes present in HPLC fractions on the “DNAP” column for selected catalyst samples.....	178-179
5-6	Reduction in HPLC peaks 2 and 3 on the “DNAP” column compared to the feed sample for samples treated with nitrogen removal processes	185
5-7	Sample compositions from MS analysis of a heavy gas oil feed and two catalyst products	190

LIST OF FIGURES

1-1	Illustration of the multiple flow paths in a column.....	10
1-2	Longitudinal diffusion of an analyte as it travels through a column	12
1-3	Effect of the resistance to mass transfer in the stationary phase.....	14
1-4	Van Deemter plot showing the contributions from the three band broadening terms	16
1-5	Schematic of the Varian HPLC instrument.....	20
1-6	Schematic of the Bruker FT-ICR MS system	26
1-7	Ion motion inside an ICR cell	29
1-8	Electrospray ionization process in positive mode.....	32
2-1	Structure of the HC-Tol and HC-C ₈ stationary phases.....	43
2-2	Retention factors of standards on HC-Tol vs. HC-C ₈	51
2-3	Retention factors of standards on HC-Tol vs. HGN	53
2-4	(a) log k vs. log (% DCM) on HC-Tol (b) log k vs. % DCM on HC-Tol	56
2-5	(a) log k vs. log (% DCM) on HGN (b) log k vs. % DCM on HGN	57
2-6	(a) log k vs. log (% DCM) on HC-C ₈ (b) log k vs. % DCM on HC-C ₈	58
2-7	Chromatogram of nitrogen/PAH mixture on HC-Tol.....	65
2-8	Chromatogram of oxygen mixture on HC-Tol	66
3-1	Structures of the HGN, biphenyl and “DNAP” stationary phases.....	76
3-2	Chromatograms of an LGO and two hydrotreated products on HGN	87
3-3	Chromatograms of an HGO and two hydrotreated products on HGN.....	88
3-4	Chromatograms of an HGO at three different detection wavelengths on HGN	90
3-5	Chromatograms of a hydrotreated HGO at three different concentrations on HGN.....	93
3-6	Retention factors for standard compounds on “DNAP” at four different solvent conditions	97
3-7	Chromatogram of nitrogen/PAH mix on “DNAP”	99
3-8	Chromatograms of an LGO and a hydrotreated product on “DNAP”	101
3-9	Chromatograms of an HGO and two hydrotreated products on “DNAP”	102
3-10	Chromatograms of a hydrotreated HGO at three different concentrations on “DNAP”	105
4-1	Positive ion mass spectrum of a hydrotreated HGO	120
4-2	Negative ion mass spectrum of a hydrotreated HGO	121
4-3	Chromatogram of a hydrotreated HGO on HC-Tol, showing the region collected for MS analysis.....	122
4-4	Positive ion mass spectrum of an HGO sample prior to evaporation	124

4-5	Positive ion mass spectrum of an HGO sample following evaporation ..	125
4-6	Charge creation processes in ESI for nitrogen-containing species	127
4-7	Positive ion mass spectra of an HPLC fraction before (a) and after (b) adding formic acid.....	128
4-8	Three negative ion mass spectra of an HPLC fraction showing the effect of collecting multiple HPLC runs	129
4-9	Positive mode spectrum of an HPLC fraction showing soap and plastic contamination peaks	132
4-10	Positive mode mass spectra of methanol (a) dried over molecular sieves; (b) not dried with molecular sieves	135
4-11	Positive mode mass spectra of an HPLC fraction illustrating the removal of iron-formate cluster peaks	140
4-12	(a) Observed and (b) simulated isotope patterns for an iron-formate cluster.....	141
5-1	Chromatograms of distillate cut gas oils on HC-Tol	163
5-2	Chromatograms of catalyst samples on HC-Tol	164
5-3	Chromatogram showing the four peak regions analyzed with MS on “DNAP”	167
5-4	Chromatograms of distillate cut gas oils on “DNAP”	168
5-5	Chromatograms comparing the effect of adsorptive denitrogenation treatment on “DNAP”	170
5-6	Chromatograms showing the effect of using different sections of a fixed bed reactor on “DNAP”	171
5-7	Chromatograms showing the effect of different catalyst systems on “DNAP”	172
5-8	Representative mass spectra of HPLC fractions in positive and negative ionization mode	175
5-9	Relative abundance of double bond equivalents by fraction for HPLC fractions, positive and negative mode.....	182
5-10	Abundance of carbon numbers by fraction for HPLC fractions, positive and negative mode.....	183
5-11	Abundance of nitrogen species by fraction for an HGO and two treated products	187

LIST OF SYMBOLS AND ABBREVIATIONS

Symbol	Parameter
2D	Two dimensional
A	Multipath band broadening term
A	Solute hydrogen bond donating ability
<i>Abs.</i>	Absorbance
ADN	Adsorptive denitrogenation
amu	Atomic mass unit
APPI	Atmospheric pressure photoionization
au	Arbitrary units
Avg	Average
B	Longitudinal diffusion band broadening term
<i>B</i>	Solute hydrogen bond accepting ability
<i>b</i>	Flow cell pathlength
B_M	Applied magnetic field
[C]	Analyte concentration
C	Resistance to mass transfer band broadening term
C#	Carbon number
Cat	Catalyst
CE	Capillary electrophoresis
$C_{i,M}$	Concentration of analyte <i>i</i> in the mobile phase
$C_{i,S}$	Concentration of analyte <i>i</i> in the stationary phase
Da	Daltons

DBE	Double bond equivalent
DCM	Dichloromethane
D_M	Diffusion coefficient of analyte in the mobile phase
DM-CMPES	Dimethylchloromethylphenylethylchlorosilane
“DNAP”	Dinitrophenyl stationary phase
DNAP	Dinitroanilinopropyl stationary phase
d_p	Particle diameter
E	Solute polarizability
e^-	Electron
ESI	Electrospray ionization
f	Frequency
$f(p,k)$	Function of pressure and retention
FT	Fourier Transform
FT-ICR	Fourier Transform Ion Cyclotron Resonance
GC	Gas chromatography
H	Plate height
$H(f)$	Frequency domain function
$h(t)$	Time domain function
H_A	Plate height contribution from the A-term
H_B	Plate height contribution from the B-term
HC	Hypercrosslinked
HC-C ₈	Hypercrosslinked polystyrene with octyl group stationary phase
HC-Tol	Hypercrosslinked polystyrene with toluene group stationary phase

HGN	Polymeric hypercrosslinked polystyrene stationary phase
HGO	Heavy gas oil
H_M	Plate height contribution from mass transfer in mobile phase
HPLC	High performance liquid chromatography
H_S	Plate height contribution from mass transfer in stationary phase
H_{SM}	Plate height contribution from mass transfer in stagnant mobile phase
i	Analyte
IBP	Initial boiling point
IET	Ion evaporation theory
i_M	Analyte i in the mobile phase
IPA	Isopropyl alcohol
i_S	Analyte i in the stationary phase
j	Analyte
k	Retention factor
k_B	Retention factor of solute in pure eluent B
k_i	Retention factor of analyte i
k_j	Retention factor of analyte j
k_w	Retention factor in pure weak solvent
L_C	Length of column
LC	Liquid chromatography
LGO	Light gas oil
LSERs	Linear solvation energy relationships
M	Mobile phase

m	Ion mass
m/z	Mass to charge ratio
m_1	Peak in a mass spectrum
m_2	Peak in a mass spectrum
Me	Methyl
MeOH	Methanol
min	Minutes
MS	Mass spectrometry
N	Efficiency
n	Number of molecules of solvent B displaced by solute
$n_{i,M}$	Moles of analyte i in the mobile phase
$n_{i,S}$	Moles of analyte i in the stationary phase
NP	Normal phase
P	Column pressure
PAH	Polycyclic aromatic hydrocarbon
PASH	Polycyclic aromatic sulfur heterocycles
ppm	Parts per million
PS	Pumping station
q	Ion charge
QNP	Quasi-normal phase
R	Functional group
R	Resolving power of a mass spectrometer
R^2	Correlation coefficient

Ref.	Reference
RF	Radio frequency
RPLC	Reversed phase liquid chromatography
R_S	Resolution
S	Stationary phase
S	Slope of log k vs. ϕ
S	Solute dipolarity
SIDT	Single ion in droplet theory
SP	Equivalent to log k
T	Temperature
t	Time
t_0	Dead time of column
t_D	Time the analyte spends in the stationary phase
t_i	Retention time for analyte i
t_j	Retention time for analyte j
t_R	Retention time
UHPLC	Ultra high pressure liquid chromatography
UV	Ultraviolet
V	Volts
V	Solute molecular size
v/v%	Volume percent
V_M	Volume of mobile phase
V_S	Volume of stationary phase

w_h	Width of peak at half height
w_i	Width of peak at half height for analyte i
w_j	Width of peak at half height for analyte j
W_S	Weight of stationary phase
wt	Weight
$x_{A \text{ or } B}$	Volume fraction of solvent
X_B	Mole fraction of strong eluent
$\alpha_{i,j}$	Separation factor
β	Phase ratio
γ_o	Obstruction factor
γ_t	Tortuosity factor
ΔP	Change in pressure
ε	Molar absorptivity
η	Viscosity
$\eta_{A \text{ or } B}$	Solvent viscosity
κ	Distribution coefficient
v	Linear velocity of the mobile phase
$\sigma^2_{X,i}$	Variance of analyte i
φ	Volume fraction of strong eluent
ω	Cyclotron frequency
ω_A	Packing factor (A-term)
ω_C	Packing factor (C-term)

CHAPTER ONE. Introduction

1.1 Motivation and Thesis Overview

Petroleum products and fossil fuels are the most important global source of energy in our society today. They provide the bulk of our energy needs for all aspects of living, and in 2010 Canadians consumed 1.8 million barrels of oil per day [1]. The oil and gas industry employs 550 000 people in Canada, and Syncrude Canada's oil production has the capacity to fill 15% of Canada's petroleum requirements [1, 2]. In recent years, conventional oil and gas reserves have become depleted, with oil sands and other heavy oil becoming a prominent source of fuel in an energy-hungry economy [3, 4]. The upgrading of heavy oil is more complex than its lighter counterparts, as heavy oil is rich in heteroatoms and complex aromatics that need to be broken down before being made into consumable fuel and petroleum products [5, 6]. Oil sands bitumen contains approximately 83% carbon, 10% hydrogen, 0.4% nitrogen, 1% oxygen and 5% sulphur [5]. A heavy gas oil derived from bitumen can contain thousands of different individual molecules, making analysis of the sample a non-trivial task.

Despite constituting a very small percentage of bulk content, nitrogen-containing compounds are the proverbial thorn in the side of the petroleum industry. Nitrogen compounds cause a host of problems, including the production of NO_x species as air pollution [7], deactivation of catalysts [8, 9], corrosion and storage instability [10-12]. Nitrogen compounds are also resistant to hydrotreating, meaning that it is difficult to remove them from heavy oil streams

to upgrade the product [13]. An important push in the study of nitrogen compounds is determining those compounds that are present following hydrotreating, with the goal of identifying common structural or chemical characteristics [11-14]. In this way it is hoped that catalysts can be designed that remove the resistant species.

Chromatography is a common analytical method used to analyze petroleum samples [3, 15, 16]. There have been a number of studies using high performance liquid chromatography (HPLC) to separate hydrocarbon group-types [15, 16], but the use of HPLC to study nitrogen compounds has been less successful (Section 1.3.3). Gas chromatography (GC) is a popular and long standing choice for the analysis of petroleum and fuel samples, and is popular for lower boiling ($< 200^{\circ}\text{C}$) samples [5]. Oil sands bitumen is high boiling, with most material boiling at temperatures of 350°C and greater [5]. For this reason, GC experiments on oil sands samples usually involve prior separation techniques of heavier fractions, and can employ two-dimensional GCxGC separations to fully analyze samples [3].

Over the past 12 years high resolution mass spectrometry (MS) has found application in the analysis of petroleum samples, giving rise to a field termed petroleomics. The goal of petroleomics is to determine the full structural content of samples, and then use that information to predict the behaviour of that sample in processing and upgrading steps [17, 18]. Petroleomics has become a valuable and powerful tool for determining the structures of compounds in petroleum and continues to advance with new ionization methods and studies of more difficult

samples [3]. One area of research that has not seen much development is the use of HPLC to fractionate samples prior to MS analysis. Petroleomic analysis of HPLC fractions can simplify samples based on the HPLC separation, and is also an excellent way to enhance understanding of chromatograms of petroleum samples.

This thesis explores analytical approaches for the study of nitrogen compounds in gas oils derived from Athabasca oil sands bitumen. The overarching goal of the work was to achieve a nitrogen group-type separation of samples with HPLC, and then analyze the different peaks of the separation with high resolution MS (petroleomics). In Chapter 2, three hypercrosslinked polystyrene HPLC stationary phases are compared for their abilities to separate nitrogen compounds, and their retention behaviours are characterized. In Chapter 3, three commercially available HPLC columns are also studied for their separation of nitrogen compounds, and separations of gas oil samples are used to evaluate their practical separation capabilities. In Chapter 4, the methods developed to analyze offline HPLC fractions on a Fourier Transform Ion Cyclotron Resonance mass spectrometer (FT-ICR MS) system are described. Chapter 4 also identifies sources of contamination in the MS analysis and their elimination. In Chapter 5, two HPLC columns (one custom made, one commercial) are evaluated for their separations of a wide variety of distillate cut and hydrotreated gas oil samples. Full petroleomic analysis of the HPLC fractions from the commercial column is performed, and the meaning of the data is discussed in the context of the samples.

1.2 Chromatography

The simplest explanation for what an analytical chemist does is to say that they find out what chemicals are in something and how much is there. At the heart of analytical chemistry is the separation of components in a sample to make determination and quantification easier. The first report of chromatography as we know it today was by Russian botanist Mikhail Tswett, who separated plant pigments by column liquid chromatography [19, 20]. He called the process chromatography, stemming from the Greek *chroma* (color) and *graphein* (to write) [21]. In 1952 A.J.P. Martin and R.L.M. Synge won the Nobel prize for their development of partition chromatography [22], and the field has only advanced since then. In 1963, J.C. Giddings published an article describing LC conditions with high pressure, and HPLC was born [23]. This thesis adds one small piece to the body of knowledge that has been built over the past 50+ years.

1.2.1 Separations [24-26]

The primary goal of chromatography is to separate sample mixtures into their individual components. A sample is injected into a fluid mobile phase, and is then carried into a column containing an immiscible stationary phase. The different components of the sample (analytes) equilibrate between the mobile phase and the stationary phase to various extents, depending on the structural or chemical characteristics of the analytes. When an analyte is sorbed onto the stationary phase, it becomes immobile. Analytes that are in the mobile phase travel through the column at the same velocity as the mobile phase. When

analytes do not sorb onto the stationary phase at all, they elute first from the column and are said to be unretained. Analytes that do sorb onto the stationary phase elute from the column at a later time, and are said to be retained by the column. The sorption of analytes onto the stationary phase varies with the structural and chemical characteristics of each analyte, and as a result their retention is different. This allows the components of the sample to be separated based on the time it takes them to elute from the column (retention time, t_R).

The stationary phases used in this thesis were both commercially prepared columns and home-packed columns. The particles in these columns ranged in size from 4.5-5.5 μm , and were held in place in the column with porous frits. The mobile phases used were mixtures of hexane and dichloromethane, and mixtures of hexane and isopropyl alcohol. The mode of chromatography used in this thesis was normal phase chromatography, as will be discussed in detail in Section 1.3.

1.2.2 Chromatography Theory [24-26]

The mechanism for a chromatographic separation is based on the equilibrium of an analyte, i , between a mobile phase (M) and an immiscible stationary phase (S). A thermodynamic equilibrium is established and can be expressed by the following:



The further this equilibrium is shifted to the right, the stronger the retention of the analyte on the column. This equilibrium can be described by a distribution coefficient, κ_i , as follows:

$$K_i = \frac{C_{i,S}}{C_{i,M}} \quad (\text{Equation 1-2})$$

where $C_{i,S}$ and $C_{i,M}$ are the concentrations of analyte in the stationary phase and the mobile phase, respectively. Retention can also be quantified using the retention factor, k_i :

$$k_i = \frac{n_{i,S}}{n_{i,M}} = \frac{K_i}{\beta} \quad (\text{Equation 1-3})$$

where $n_{i,S}$ and $n_{i,M}$ are the moles of analyte in the stationary phase and the mobile phase, respectively. β is the phase ratio, which is the ratio of the mobile phase volume (V_M) to the stationary phase volume (V_S):

$$\beta = \frac{V_M}{V_S} \quad (\text{Equation 1-4})$$

V_M is also known as the dead volume. The weight of the stationary phase (W_S) can also be used in place of volume, as long as the units are not omitted. The retention factor can also be calculated from chromatographic data, and is more commonly expressed in the following form:

$$k_i = \frac{t_R - t_0}{t_0} \quad (\text{Equation 1-5})$$

where t_R is the retention time of the analyte and t_0 is the dead time of the column (the time it takes for an unretained compound to elute from the column).

Along with quantifying the extent of retention on a column, it is important to quantify the difference in retention between two analytes. The term used to express this difference is referred to as the separation factor (also called the selectivity factor), $\alpha_{i,j}$:

$$\alpha_{i,j} = \frac{k_j}{k_i} \quad (\text{Equation 1-6})$$

where k_j is the retention factor of the later eluting analyte (j) and k_i is the retention factor for the earlier eluting analyte (i). The substitution of Equation 1-5 into Equation 1-6 yields:

$$\alpha_{i,j} = \frac{t_{R,j}-t_0}{t_{R,i}-t_0} \quad (\text{Equation 1-7})$$

Another important measurement is the quantification of how narrow the analyte bands are as they elute off the column. It is easier to separate and quantify narrow analyte bands that give sharp Gaussian peaks than it is to analyze broad analyte bands. Band broadening is measured by plate height, H , and is expressed by the following equation:

$$H = \frac{\sigma_{x,i}^2}{L_C} \quad (\text{Equation 1-8})$$

where $\sigma_{x,i}^2$ is the variance of analyte i in distance units squared, and L_C is the length of the column. A smaller plate height indicates a narrower analyte band. Band broadening can also be measured by N , which is called the efficiency:

$$N = \frac{L_C}{H} = \frac{L_C^2}{\sigma_{x,i}^2} \quad (\text{Equation 1-9})$$

Using plate height to measure band broadening is preferable to efficiency because plate heights are corrected for column length. This allows direct comparisons of plate heights from columns of different length. The efficiency of a peak can be directly measured from chromatographic data using the width-at-half-height method:

$$N = 5.54 \left(\frac{t_R}{w_h} \right)^2 \quad (\text{Equation 1-10})$$

where w_h is the width of the peak at 50% of the peak height.

The retention factor, separation factor and efficiency are the measures that determine how well two analytes will be separated. These variables can be combined into an equation that expresses the amount of separation, the resolution (R_S):

$$R_S = \frac{\sqrt{N}}{4} \cdot \frac{(\alpha_{i,j}-1)}{\alpha_{i,j}} \cdot \frac{k_j}{(k_j+1)} \quad (\text{Equation 1-11})$$

The resolution equation shows how resolution can be increased by changing parts of the separation. An improvement in resolution results from an increase in efficiency (decrease of plate height), an increase in the separation factor, or an increase in the retention factor. When resolution is 1.5 or greater, two equally sized Gaussian peaks are considered to be baseline resolved, meaning that the signal intensity between the two peaks reaches the baseline of the separation. The efficiency has a square root dependence, meaning that a two-fold improvement in resolution will require a four-fold increase in efficiency. It can be difficult to achieve such an increase without making the separation or column length excessively long. When the retention factor is increased to improve resolution, the returns are diminishing. As k_j increases, analysis times increase, and the retention factor term in Equation 1-11 approaches one. With these considerations in mind, the best way to improve resolution is to increase the separation factor. The separation factor can be changed by modifying variables like the stationary phase, mobile phase and column temperature.

To calculate resolution from two Gaussian peaks, chromatographic data can be used with this equation:

$$R_S = \frac{2(t_j - t_i)}{1.699(w_j + w_i)} \quad (\text{Equation 1-12})$$

where t_j and t_i are the elution times of later and earlier eluting analytes j and i , and w_j and w_i are the peak widths at half height for the same analytes j and i .

1.2.3 Band Broadening [24-26]

As analytes move down a column, their bands broaden irreversibly. A common descriptor of this band broadening is the van Deemter equation:

$$H = A + \frac{B}{v} + Cv \quad (\text{Equation 1-13})$$

where H is the plate height, A , B and C are different band broadening processes and v is the linear velocity of the mobile phase, which is proportional to the flow rate. While other models have been developed to explain band broadening [27-29], the van Deemter model is a simple and accurate way to represent the processes occurring to analytes in the column.

The A-term of the van Deemter equation is often called the multipath band broadening term, and describes the broadening that occurs as analyte molecules take different flow paths through the column. This process is illustrated in Figure 1-1. Some analytes will take a very straight path through the particles in the column, arriving at the detector first (1 in Figure 1-1). The average analyte molecule will take a moderately straight path through the column (2 in Figure 1-1), and some molecules will take a meandering path through the column, eluting later than the average analyte molecule (3 in Figure 1-1).

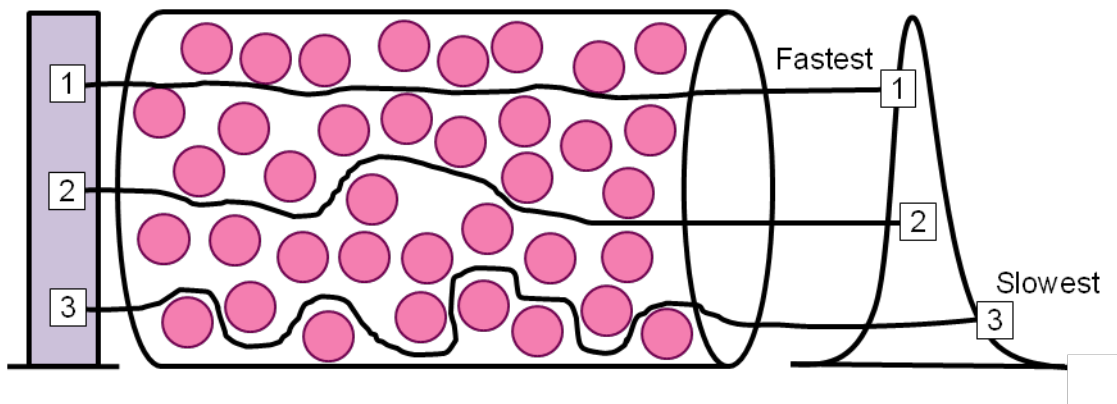


Figure 1-1. Illustration of the multiple flow paths in a column resulting in A-term band broadening. Adapted from Reference [25].

Multipath band broadening is caused by anything that contributes to a non-uniform flow profile through the column, including poorly packed columns, voids in the column and any particulate matter of different retention character. Multipath band broadening is independent of flow rate and is present in all packed columns. The plate height contribution from the A-term, H_A is expressed by:

$$H_A = 2\omega_A d_p \quad (\text{Equation 1-14})$$

where ω_A is the packing factor, and d_p is the particle diameter. The packing factor describes how the column is packed, and is larger for loosely packed columns. The terms in Equation 1-14 show that the A-term contribution to band broadening can be reduced by better quality column packing and smaller particle diameter.

The B-term in the van Deemter equation is the longitudinal diffusion term. It describes how analyte molecules diffuse away from the center of the analyte band (high concentration to low) as the band moves along the column. The longitudinal diffusion of an analyte band is illustrated in Figure 1-2. The analyte will experience greater diffusion if it spends more time in the mobile phase, and consequently, the B-term scales inversely with the velocity of the mobile phase (flow rate). The contribution to plate height from longitudinal diffusion, H_B , is:

$$H_B = \frac{2\gamma_o D_M}{v} \quad (\text{Equation 1-15})$$

where γ_o is the obstruction factor and D_M is the diffusion coefficient of the analyte in the mobile phase. Diffusion coefficients in liquids are small, and as a result H_B can generally be ignored in HPLC.

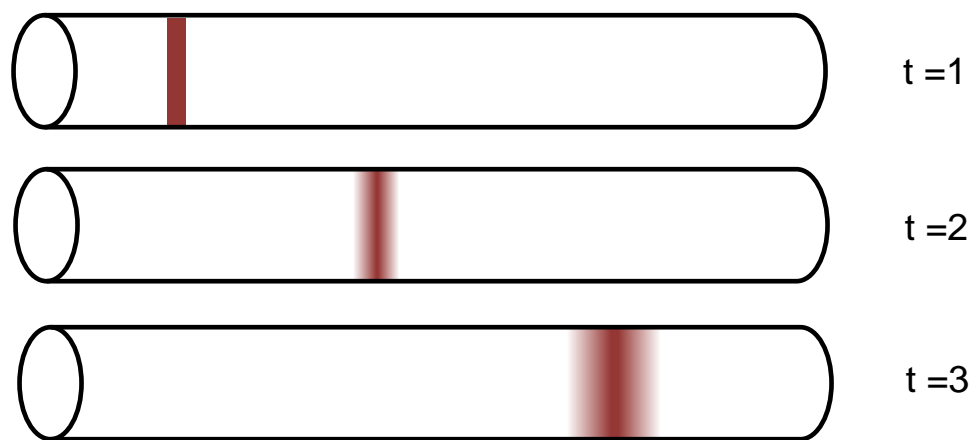


Figure 1-2. Longitudinal diffusion of an analyte as it travels through a column at times $t=1$, $t=2$ and $t=3$.

However H_B cannot be ignored when operating under conditions of low flow rates and high temperatures, as well as under UHPLC (ultra high pressure LC) conditions where the contributions from the A and C terms have been minimized.

The third term of the van Deemter equation is the C-term, the resistance to mass transfer term. The mass transfer of analytes within the column is not instantaneous, and the C-term is the most significant contributor to band broadening in HPLC. There are three band broadening processes that occur due to limited mass transfer. The first process is the time it takes analyte molecules to transfer from the stationary phase to the stagnant mobile phase that is contained in the pores of stationary phase particles. The contribution to plate height from this first process is termed H_S and is expressed as follows:

$$H_S = \frac{2k}{(1+k)^2} t_D v \quad (\text{Equation 1-16})$$

where k is the retention factor, and t_D is the time the analyte spends in the stationary phase. When the analyte molecules are at equilibrium, they are distributed equally in the mobile phase and stationary phase (Figure 1-3A), but as the band moves down the column, the molecules in the stationary phase lag behind those in the mobile phase. Figure 1-3B shows the band broadening that results from this process. When flow rate is increased, the band moves further down the column before the analyte molecules in the stationary phase can move back into the mobile phase, resulting in greater band broadening at higher flow rates.

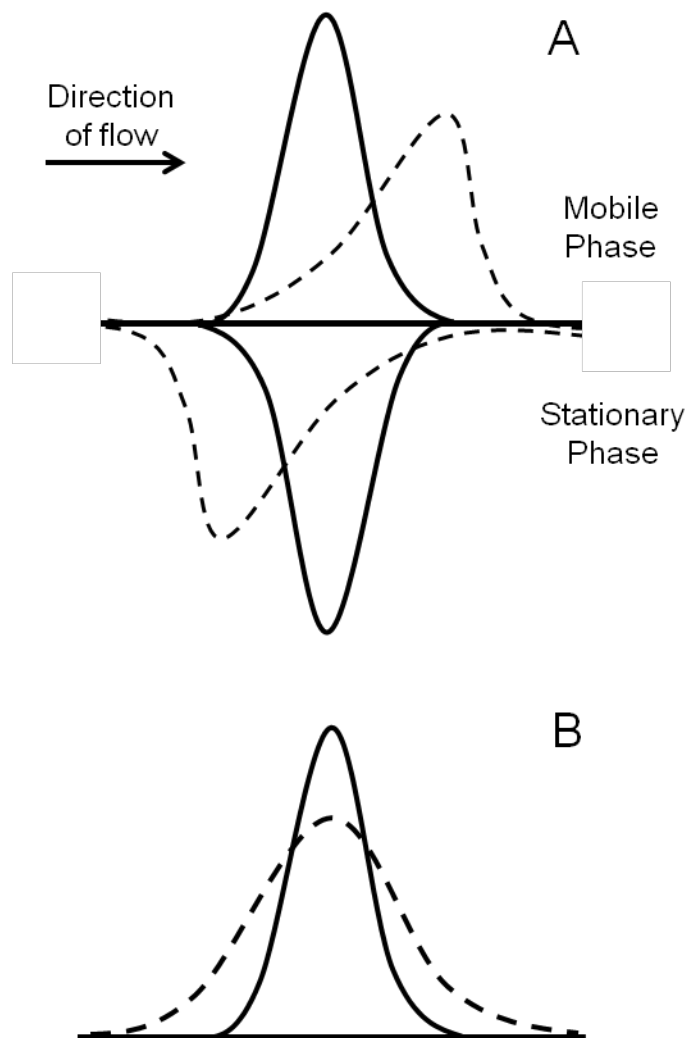


Figure 1-3. Illustration showing (A) the resistance to mass transfer in the stationary phase and (B) the resulting band broadening on a Gaussian peak. The area under the curves is proportional to moles of analyte; solid lines represent a case with no resistance to mass transfer, and dotted lines represent a case with resistance to mass transfer.

The second term caused by resistance to mass transfer is from the slow diffusion of analyte molecules within the stagnant mobile phase contained in the pores of the stationary phase. The contribution to plate height from this process is termed H_{SM} , and given by the following:

$$H_{SM} = \frac{f(p,k)d_p^2}{\gamma_t D_M} \nu \quad (\text{Equation 1-17})$$

where $f(p,k)$ is a function of pressure and retention, and γ_t is the tortuosity factor. This term represents that analyte molecules must diffuse through stagnant mobile phase in order to reach the surface of the stationary phase, and also to exit the stationary phase and re-enter the flowing mobile phase. The H_{SM} term can be decreased by decreasing flow rate, decreasing particle size and increasing the diffusion coefficient of the analyte.

The third and final resistance to mass transfer term is from the slow transfer of analyte molecules in the mobile phase moving between the particles of the stationary phase. This contribution is designated H_M and is expressed by:

$$H_M = \frac{\omega_C d_p^2}{D_M} \nu \quad (\text{Equation 1-18})$$

where ω_C is the packing factor; ω_C is smaller for uniformly packed beds. Similar to H_{SM} , H_M can be decreased by decreasing particle diameter, decreasing flow rate, and increasing the diffusion coefficient of the analyte. All three resistance to mass transfer terms have the same linear dependence on flow rate, so they are combined and treated together as the C-term in the van Deemter equation.

To obtain a van Deemter plot, plate height is plotted against linear flow velocity (or flow rate). A van Deemter plot is illustrated in Figure 1-4.

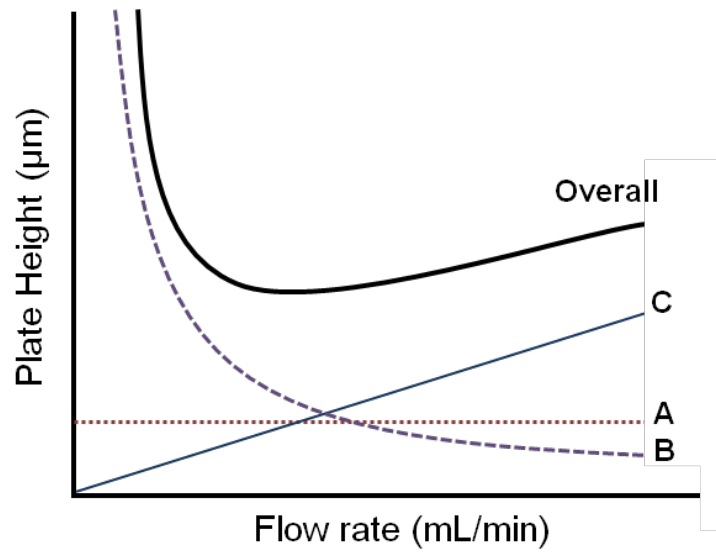


Figure 1-4. Plot of plate height versus flow rate, showing the contributions from the three band broadening terms of the van Deemter equation (Equation 1-13).

Each of the three terms contributes to the overall plate height (shown in black). At low flow rates, the plate height is dominated by the B-term (longitudinal diffusion), and at high flow rates, the plate height is dominated by the C-term (resistance to mass transfer). At intermediate flow rates, a minimum in the plate height is achieved. This minimum is considered the optimum flow rate and is where the least band broadening and the highest efficiency occur. In practice however, the system is usually operated at a higher flow rate than the minimum on the van Deemter curve, as the trade off for a shorter analysis time is worth the slight decrease in efficiency. A general rule is that the minimum plate height is approximately 2-3 times the particle diameter for a well-packed column.

Finally, band broadening can also originate from sources outside the column. This is referred to as extra-column band broadening, and can be caused by the extra volume in injection loops, connection tubing and detectors and the detector response time. Problems with extra-column band broadening can be reduced or eliminated by thoughtful and purposeful instrument design; minimizing the volumes associated with extra-column tubing and using a fast detector response time all help reduce extra-column band broadening.

1.3 Normal Phase Separations

1.3.1 Normal Phase High Performance Liquid Chromatography [24-26]

Separations performed under normal phase mode use a polar stationary phase and relatively non-polar mobile phases. The term “normal” stems from the first uses of chromatography with polar stationary phases such as silica and

alumina and non-polar mobile phases such as hexane. In the 1970s chromatography was developed with non-polar stationary phases and polar mobile phases and was termed “reversed” phase, being opposite in polarity to normal phase. In normal phase, polar analytes (or analytes with higher polarizability, e.g. aromatic hydrocarbons) are retained on the stationary phase, while analytes of low polarity interact weakly with the stationary phase and experience weak retention. Solvents such as hexane are often used as mobile phases, with the strong eluent in mixtures being the more polar solvent (dichloromethane, for example). Organic solvents are used in normal phase, as water can bind strongly to the polar stationary phase and negatively affect reproducibility. In some extreme cases, water can even dissolve the stationary phase itself on normal phase columns (e.g. an aminopropyl stationary phase) [30].

When stationary phases do not have a distinct polar site for retention but are still used in normal phase mode, the term quasi-normal phase has been coined to describe the retention occurring [31-33]. Put another way, quasi-normal phase describes the adsorption of solutes on a largely non-polar stationary phase under normal phase conditions. This term is relevant for this thesis because the hypercrosslinked polystyrene stationary phases used in Chapters 2 and 3 have no discrete polar sites for adsorption, but are used with normal phase solvent systems and conditions. The reasons for using normal phase and quasi-normal phase HPLC in this thesis are two-fold. First, the goal was to study polar (nitrogen-containing) compounds, and it makes sense to retain them on a polar stationary phase. Second, petroleum samples do not easily dissolve in aqueous solutions,

while they are easily diluted with organic solvents. The organic solvent systems used in normal phase are a natural fit to petroleum samples.

A schematic of the HPLC system used in this thesis is shown in Figure 1-5. Two high pressure pumps (A and B) are used to draw solvent from two reservoirs, and the solvents are mixed in a high pressure mixer. The mobile phase is carried into the autosampler, where a few microliters of the sample to be analyzed are injected into the mobile phase stream and carried to the HPLC column. The column is contained in a column oven (maximum temperature 150°C) to maintain a constant temperature throughout analysis. The column separates individual components in the sample, and the effluent is carried to a flow cell that is connected to a UV detector via a fibre optic cable. The detector measures the absorbance of ultraviolet light by the compounds eluting off the column, and outputs the data to a computer to create a chromatogram. After exiting the flow cell, the column effluent passes through the fraction collector, where desired HPLC fractions can be either collected in vials (Chapters 4 and 5) or diverted to waste (Chapters 2 and 3).

1.3.2 Stationary Phases [25, 26]

In normal phase chromatography, the most common and widely used stationary phase is amorphous and porous bare silica. The surface of the silica particles are covered with silanol groups (Si-OH), giving highly polar sites for adsorption and retention of analytes. The silanol groups interact with analytes through hydrogen bonds, dipole-dipole and dipole-induced dipole interactions.

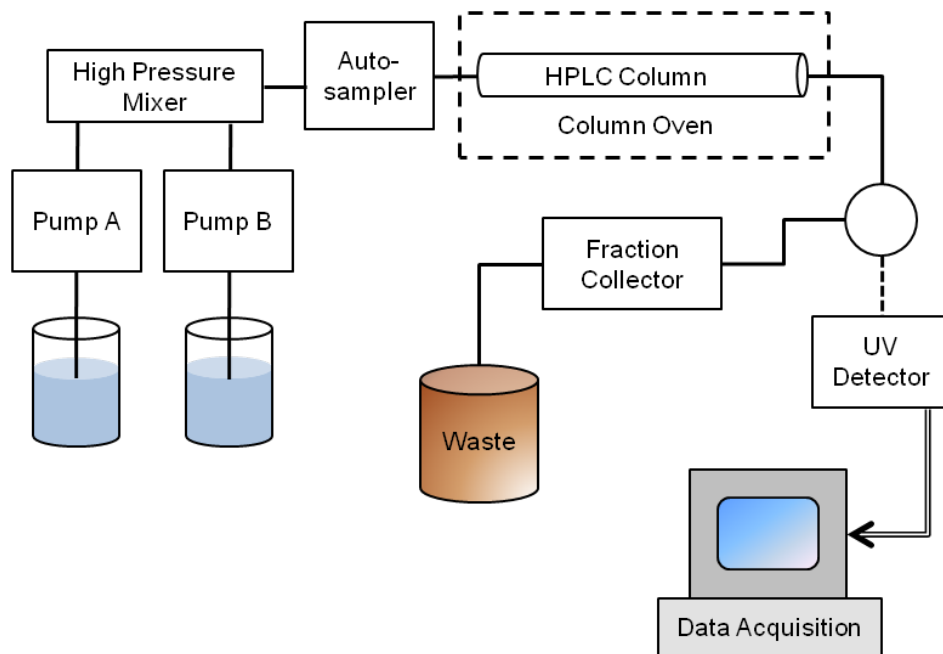


Figure 1-5. Schematic of the Varian ProStar HPLC instrument used in Chapters 2-5.

However, problems can arise from the interaction of small polar molecules with the surface silanols. These problems include poor separation reproducibility, slow column equilibration times and high sensitivity to trace water content in the mobile phase. Strong interactions of the silanols with basic analytes can also result in peak tailing and poor peak efficiency.

The problems with using silica as a normal phase stationary phase can be avoided by using polar bonded phases. Bonded phases have a functional group covalently attached to the silica particles. Common bonded normal phases are cyano columns ($-(\text{CH}_2)_3\text{-C}\equiv\text{N}$ ligands), diol columns ($-(\text{CH}_2)_3\text{-O-CH}_2\text{-CHOH-CH}_2\text{OH}$ ligands) and amino columns ($-(\text{CH}_2)_3\text{-NH}_2$ ligands). The bonded groups provide a more homogeneous surface than bare silica. As a result bonded phases are less sensitive to water and give better reproducibilities and better peak shapes than bare silica, especially with basic analytes.

The work in this thesis uses one polar bonded phase (dinitrophenyl, “DNAP”, Chapters 3 and 5) and three hypercrosslinked polystyrene stationary phases (Chapter 2, 3 and 5). The “DNAP” phase has a dinitrophenyl group bonded to silica particles, and is a variation of a popular dinitroanilinopropyl bonded phase that has been most commonly used in the past 30 years for the normal phase separation of polycyclic aromatic hydrocarbons (PAHs) [34-41]. A detailed discussion of the “DNAP” stationary phase and its use in published literature can be found in Section 3.1, with the structure shown in Figure 3-1. Chapters 3 and 5 explore the capabilities of the “DNAP” column for its ability to separate nitrogen group-types.

The hypercrosslinked polystyrene phases used in this thesis are unconventional normal phase stationary phases, in that they lack a polar group for retention (Section 1.3.1). Prior to this work, two of the phases (HC-Tol and HC-C₈) had never been used under normal phase conditions [42]. These HC phases consist of a thin layer of hypercrosslinked polystyrene polymer on a silica particle [43, 44]. Sections 2.1 and 2.3 discuss the synthesis and motivation for the creation of the HC hypercrosslinked polystyrene phases, and Figure 2-1 illustrates their structures. The third hypercrosslinked polystyrene column studied (HGN, Figure 3-1) is a fully polymeric stationary phase, and had previously shown interesting selectivity for gas oil resins under a quaternary solvent gradient in our research group [31]. Chapters 2 and 3 study this column under binary solvent gradients for the separation of nitrogen group-types, and details of its use in the literature can be found in Section 2.1.

1.3.3 Nitrogen Group-Type Separations

The nitrogen content in petroleum samples is important, as it makes hydrotreatment and upgrading more difficult (Section 1.1). The objective of nitrogen group-type separations is not to resolve individual nitrogen compounds, but to baseline separate the two different groups of nitrogen compounds found in petroleum (pyrroles and pyridines). Such group-wise separation allows for more accurate determination of the distribution and type of nitrogen compounds present in a sample compared to bulk nitrogen determination. In this thesis, model

compounds are used in Chapters 2 and 3 to assess the nitrogen group-type separation capabilities of different stationary phases.

The separation of nitrogen group-types using HPLC has proven to be a challenge that has been met with limited success. After reviewing the literature it is apparent that silica and the common normal phase bonded phases are not sufficiently selective to differentiate between pyrroles and pyridines. Open column separations have been a popular choice for the concentration and isolation of nitrogen compounds, but require time, multiple steps and suffer from poor control over sorbent activity [45, 46]. A group-type separation of pyrroles and pyridines was performed on a dimethylaminopropyl silica column, but required open column pre-separation and column back flushing [47]. An alumina column was used to analyze diesel oil, but pyrroles co-eluted with the hydrocarbons, and total analysis time was over 100 minutes [48]. DNAP bonded phase columns have been used for the separation of polar compounds from hydrocarbons, but demonstrated no separation of nitrogen group types [37, 38, 45]. Previous work in the Lucy group studied the separation of standards and heavy gas oil samples on bare silica and zirconia columns and found that pyridine compounds were irreversibly retained [49]. Separations on an aminopropyl bonded phase showed a nitrogen group-type separation, but follow-up work indicated that the results could not be reproduced on a new column [49].

For these reasons, this thesis pursued new (“DNAP”) and unconventional (hypercrosslinked polystyrene) stationary phases for nitrogen group-type separation.

1.3.4 Detection [50-52]

In this thesis, one mode of on-line detection is used for chromatography. Ultraviolet (UV) absorbance detection is the most widely used method of detection for HPLC, and is the detector used in this thesis. When using a UV detector, any analytes that possess a chromophore will provide a signal that is directly proportional to its concentration. UV light shines through a flow cell that carries column effluent, and analyte molecules absorb some of the UV light. Beer's Law can be used to describe the amount of light absorbed:

$$Abs. = \epsilon b[C] \quad \text{(Equation 1-19)}$$

where *Abs.* is the absorbance, ϵ is the molar absorptivity, *b* is the pathlength of the flow cell, and [*C*] is the concentration of the analyte. The molar absorptivity of an analyte depends on the wavelength of light and the structure of the analyte. The instrument used in this thesis has a monochromator and a deuterium lamp, allowing for the selection of one wavelength of light to be monitored in the flow cell. More complex detectors have a diode array that allows a range of wavelengths to be monitored simultaneously. Because the molar absorptivity varies for different analytes, it can be difficult to perform quantitative analysis using a UV detector.

1.4 Mass Spectrometry [53, 54]

Mass spectrometry is an analytical technique that measures the mass-to-charge ratio (*m/z*) of ions produced from elements and compounds. At the heart of the mass spectrometer is the mass analyzer, where the motion of ions under an

electric or magnetic field is used to measure their m/z . Samples are introduced to the system, ionized, carried to the mass analyzer, and the ions are detected. A spectrum is produced with ion intensity on the y-axis and m/z on the x-axis. The unique masses of ions of molecules and the fragmented pieces of molecules are used to identify compounds. There are many different types of mass analyzers, including quadrupoles, ion traps, sector instruments and time-of-flight instruments. This thesis uses a Fourier Transform Ion Cyclotron Resonance (FT-ICR) MS instrument, which has the highest resolving power and mass accuracy of any available mass spectrometer.

The resolving power (or resolution) of a mass spectrometer is its ability to separate ions of two adjacent mass peaks, and for FT-ICR MS is defined as:

$$R = \frac{m_1}{m_2 - m_1} \quad (\text{Equation 1-20})$$

where m_1 and m_2 are two adjacent peaks in a mass spectrum. For FT-ICR MS, an R of 10 000 is routine, and $R = 1\,000\,000$ is possible. The high resolving power of an FT-ICR MS system makes it ideal for the analysis of complex samples such as petroleum, as it is able to distinguish between peaks with mass differences as small as 0.0034 Da [18].

1.4.1 Fourier Transform Ion Cyclotron Resonance Mass Analyzer [54-57]

Following ionization, sample ions were detected with an FT-ICR mass analyzer. Figure 1-6 is a schematic of the Bruker 9.4 T FT-ICR MS used in this thesis.

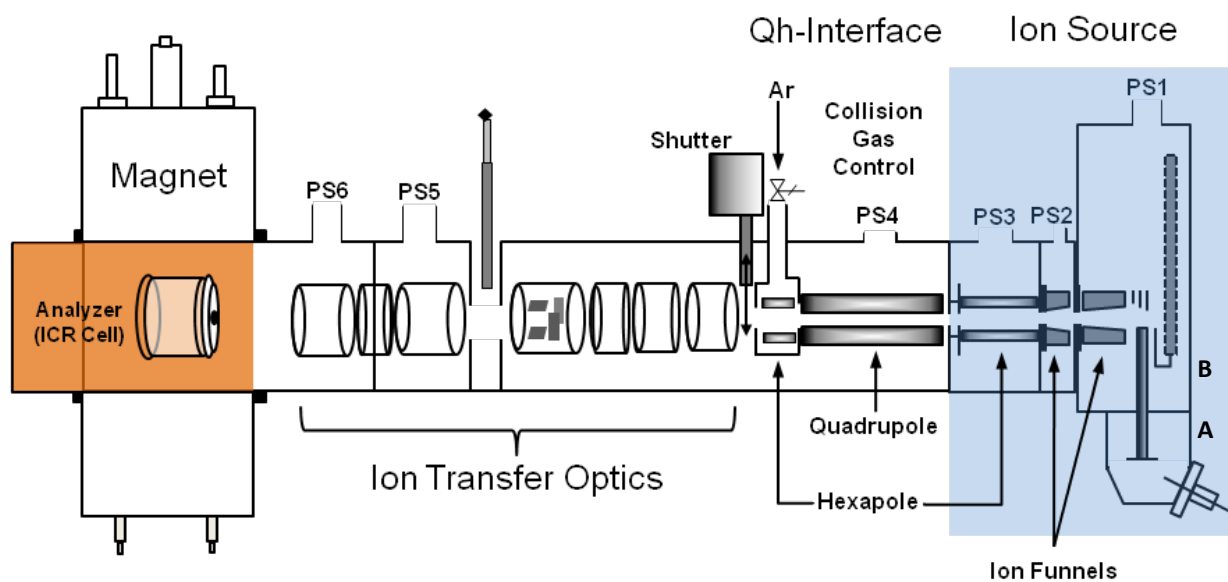


Figure 1-6. Schematic of Bruker's FT-ICR MS system, used in Chapters 4 and 5. PS = Pumping station. A and B indicate the two vacuum stages of the ESI source. Adapted from reference [58].

The ions are transported to the ICR cell via a series of optics and then detected. The principle behind the FT-ICR is ion cyclotron motion, which results from the trapping of an ion in an ion cell that has an applied magnetic field. The cyclotron frequency ω is described by:

$$\omega = \frac{qB_M}{m} \quad (\text{Equation 1-21})$$

where q is the charge on the ion, B_M is the applied magnetic field and m is the mass of the ion. The cyclotron frequency in Equation 1-21 is expressed in units of radians/s. To express the frequency f in Hz, ω is divided by 2π . If the magnetic field B_M is converted to Tesla and the m/z is expressed in Daltons, the frequency can be calculated by:

$$f = 1.53567 \times 10^7 \frac{zB_M}{m} \quad (\text{Equation 1-22})$$

When examining Equations 1-21 and 1-22 it is apparent that all ions of the same m/z rotate at the same frequency, independent of their velocities. This insensitivity to the kinetic energy of an ion gives FT-ICR its ultra-high resolving power.

The ions in the ICR cell are detected by the image current signals they generate. To begin detection, all of the ions in a cell are accelerated with an RF “chirp”, which is a high to low frequency sweep over a few milliseconds. The frequencies in the chirp match the frequencies of the ions in the cell, and excite the ions to larger cyclotron orbits. The subsequent decaying orbit of the ions induces an alternating current in two opposing detector plates, which is called an image current. Figure 1-7 illustrates the incoherent orbit of the ions in the cell as they are excited (Left side, Excite), and the coherent and detectable cyclotron

motion in the cell resulting from the application of an electric field (Right side, Detect). The amplitude of the image current is proportional to the number of ions in the cell, and the frequency of the image current is the same as the cyclotron frequency of the ions. The transient signal from the image current is a composite of all the cyclotron frequencies of all the ions in the ICR cell. This signal is amplified, digitized and stored.

The detected image current is then converted into a mass spectrum via a Fourier Transform (FT). The FT algorithm extracts the frequency and amplitude for each frequency component from the time-domain image current. The theoretical transformation of the time-domain function $h(t)$ to the frequency-domain $H(f)$ function is described by:

$$H(f) = \int_{-\infty}^{\infty} h(t)e^{-i2\pi ft} dt \quad (\text{Equation 1-23})$$

where i is $\sqrt{-1}$, t is time, and f is frequency. This conversion is possible because the frequency of the ions is directly related to their mass to charge ratio (m/z , Equation 1-22).

The resolving power of the FT-ICR is proportional to the magnetic field strength applied to the cell, with larger field strength resulting in higher resolving power, and acquisition time. The acquisition time is the duration of time that transient signal is being recorded, with longer acquisition times giving larger data sets and higher resolving power. To avoid collisions with gas particles and deactivation of ions, the ICR cell is kept at a high vacuum ($<10^{-8}$ torr).

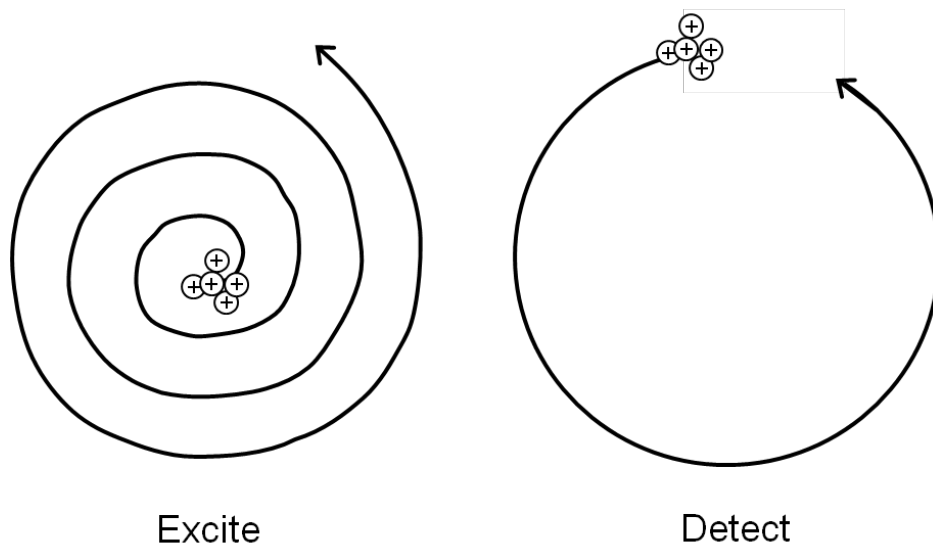


Figure 1-7. Ion motion inside the ICR cell during excitation and the subsequent coherent rotation following excitation. Adapted from reference [57].

FT-ICR is capable of both high resolving power and high mass accuracy. The measurement of ICR frequencies can be accurately done at a part-per-billion level, which allows for high accuracy for the measurement of m/z , as the frequencies are converted to mass-to-charge ratios (Equation 1-23) [18]. To obtain m/z measurements that are at the sub-part-per-million level, a mass calibration is necessary. The conversion from frequency to m/z is determined from the measured frequencies and known masses of calibration ions in the mass spectrum (minimum two ions). The analytes and the calibration ions in the mass spectrum experience the same excitation and detection processes. This means that when the spectrum is internally calibrated, the mass accuracy is of the highest possible for any MS technique. The mass accuracy of FT-ICR is highest when there are few ions in the trap (low trapping potential). To acquire high resolution spectra of petroleum samples, multiple scans of low trapping potential are usually averaged together [18]. If too many ions are trapped in the ICR cell, the performance of the instrument is negatively affected. When a high density of ions is trapped, ion repulsion occurs and disrupts ion trajectories. The peaks in the mass spectrum can broaden and resolution is decreased. The measured frequency of ions can also be affected by the space charge of the ions trapped; therefore calibration is the most accurate when approximately the same number of ions are trapped for both calibration and the collection of experimental data.

1.4.2 Electrospray Ionization [50, 53, 54, 58, 59]

The ionization method used in this thesis is electrospray ionization (ESI). ESI is a popular “soft” ionization technique done at atmospheric pressure that is popular for studying the molecular ions of petroleum compounds. The ESI process produces few fragment ions, and can operate in either positive or negative mode, producing positive ions or negative ions, respectively. The electrospray process is illustrated in Figure 1-8. Liquid enters the steel nebulizer capillary, along with a co-axial flow of nitrogen gas. When the mode is set to positive, the capillary is held at 0 V and the spray chamber is held at a highly negative voltage; for negative mode, the spray chamber is held at a highly positive voltage. The high voltage creates charge separation of analytes in solution, and (in positive mode) the positive charges drift to the liquid surface. A Taylor cone of liquid is formed and will become unstable. Downstream from the Taylor cone, a fine filament of liquid is formed, which eventually breaks up into small charged droplets. Solvent evaporation, accompanied by droplet fission, results in the formation of smaller, highly charged droplets. Fission of the droplets occurs when they reach the Rayleigh limit, the point at which surface tension of the droplet is equal to the Coulombic repulsion of the surface charge. The Bruker instrument used in this thesis generates ions in a spray chamber that is separated into two separate vacuum stages, at ~4 mbar and 0.1 mbar (A and B in Figure 1-6, respectively). Solvent is removed from the ions with nitrogen drying gas, and ions are introduced to the first ion funnel stage orthogonally before being focussed and carried towards the ICR analyzer cell.

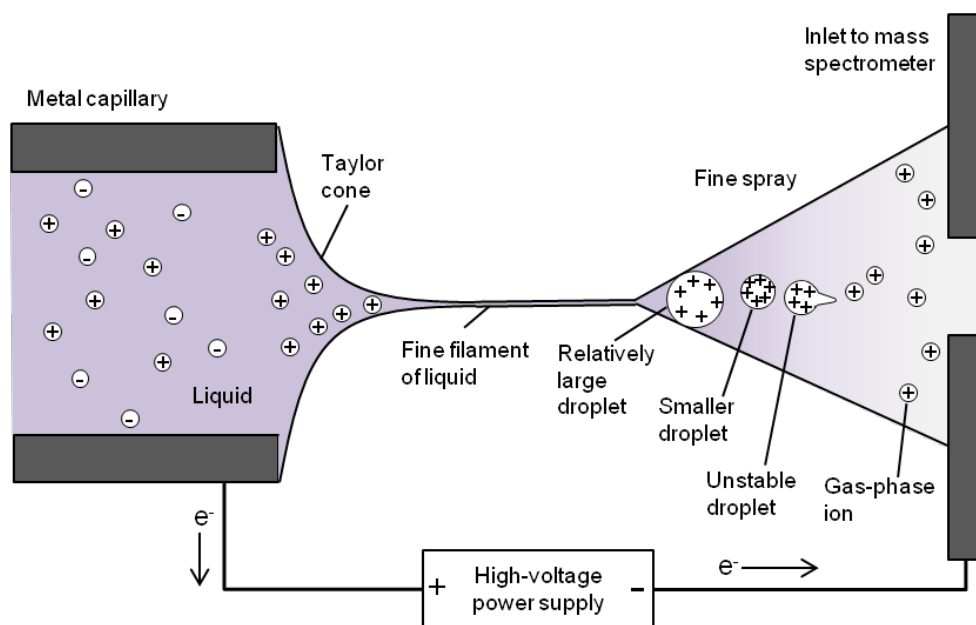


Figure 1-8. Electro spray ionization process in positive mode. Adapted from Reference [50].

There are two proposed mechanisms for the process by which gas phase ions are produced from the small charged droplets of liquid. These mechanisms are the single ion in droplet theory (SIDT) and the ion evaporation theory (IET). The SIDT, proposed by Dole and coworkers [60], assumes that ions are formed by successive evaporation and fission steps, to the point where extremely small droplets (radius ~ 1 nm) containing only one ion are formed. Consequent evaporation of these droplets leads to the gas phase ion. IET was developed by Iribarne and Thomson, and is based on transition state theory [61]. IET proposes that the electric field at the surface of the droplet becomes so high that the ions “escape” from the liquid phase into the gas phase. Emission of gas phase ions is maintained by successive evaporation of the droplet. Although neither mechanism has been proved conclusively, a recent editorial in LC-GC North America suggests that IET is likely the more correct mechanism [62].

1.4.3 The Nitrogen Rule [63]

Interpreting meaning from a mass spectrum is somewhat of an art. It takes experience and some sense of intuition to understand the meaning of the sometimes overwhelming number of peaks in a spectrum. The assignment of peaks to the spectra produced in this thesis is discussed in detail in Section 5.2.3, but there is one general guideline to interpreting mass spectra that is especially applicable to this work.

The nitrogen rule can be a valuable tool when trying to decide on peak assignments for a mass spectrum. The electrospray process creates even-electron

ions consisting of molecules with proton or other adducts. The nitrogen rule states that for even-electron ions, even-mass ions contain an odd number of nitrogen atoms. Put simply, in an ESI spectrum, even-mass peaks contain one or three nitrogen atoms, and odd-mass peaks contain no nitrogen atoms or two nitrogen atoms. When looking for nitrogen-containing pyrrole compounds (negative mode) or pyridine compounds (positive mode), a cursory examination of an ESI spectrum for even-mass peaks can reveal their presence or absence.

1.5 Summary

This thesis uses both HPLC and FT-ICR to gain a better understanding of problematic nitrogen-containing compounds in gas oil samples that are derived from Athabasca bitumen. The literature is lacking in simple and comprehensive HPLC methods that are capable of separating nitrogen group-types. Chapters 2 and 3 work to achieve this separation in normal phase mode, studying both unconventional hypercrosslinked polystyrene columns and commercially available columns. Chapters 4 and 5 exploit the powerful capabilities of high resolution mass spectrometry and develop methods to analyze fractions from the HPLC separations for nitrogen content. The analysis of nitrogen compounds by double bond equivalent and carbon number gives a better understanding of the type of compounds that resist hydrotreating and also gives insight into the HPLC retention mechanism. It is hoped that these methods will enable future technology to more efficiently produce petroleum products from bitumen.

1.6 References

- [1] Canadian Association of Petroleum Producers Basic Statistics, available online at <http://www.capp.ca/library/statistics/basic/Pages/default.aspx>, accessed on March 14, 2012.
- [2] Syncrude Canada available online at <http://www.syncrude.ca/users/folder.asp?FolderID=5617>, accessed on March 14, 2012.
- [3] R.P. Rodgers, A.M. McKenna, *Analytical Chemistry* **2011**, 83, 4665-4687.
- [4] J.R. Woods, J. Kung, G. Pleizier, L.S. Kotlyar, B.D. Sparks, J. Adjaye, K.H. Chung, *Fuel* **2004**, 83, 1907-1914.
- [5] J.G. Speight, *The Chemistry and Technology of Petroleum*, 4th ed., CRC Press, 2007.
- [6] K. Qian, R.P. Rodgers, C.L. Hendrickson, M.R. Emmett, A.G. Marshall, *Energy & Fuels* **2001**, 15, 492-498.
- [7] B. Wen, M.Y. He, C. Costello, *Energy & Fuels* **2002**, 16, 1048-1053.
- [8] H.V. Drushel, A.L. Sommers, *Analytical Chemistry* **1966**, 38, 19-&.
- [9] E. Furimsky, F.E. Massoth, *Catalysis Today* **1999**, 52, 381-495.
- [10] A.Z. Fathoni, B.D. Batts, *Energy & Fuels* **1992**, 6, 682-693.
- [11] T. Kekalainen, J.M.H. Pakarinen, K. Wickstrom, P. Vainiotalo, *Energy & Fuels* **2009**, 23, 6055-6061.
- [12] Z. Wu, R.P. Rodgers, A.G. Marshall, J.J. Strohm, C. Song, *Energy & Fuels* **2005**, 19, 1072-1077.
- [13] G.C. Klein, R.P. Rodgers, A.G. Marshall, *Fuel* **2006**, 85, 2071-2080.

- [14] J. Fu, G.C. Klein, D.F. Smith, S. Kim, R.P. Rodgers, C.L. Hendrickson, A.G. Marshall, *Energy & Fuels* **2006**, *20*, 1235-1241.
- [15] B.N. Barman, V.L. Cebolla, L. Membrado, *Critical Reviews in Analytical Chemistry* **2000**, *30*, 75-120.
- [16] M. Kaminski, R. Kartanowicz, E. Gilgenast, J. Namiesnik, *Critical Reviews in Analytical Chemistry* **2005**, *35*, 193-216.
- [17] O.C. Mullins, E.Y. Sheu, A. Hammami, A.G. Marshall, *Ashphaltenes, Heavy Oils and Petroleomics*, 1st ed., Springer Science, New York, 2007.
- [18] R.P. Rodgers, T.M. Schaub, A.G. Marshall, *Analytical Chemistry* **2005**, *77*, 20A-27A.
- [19] H.H. Strain, J. Sherma, *Journal of Chemical Education* **1967**, *44*, 235-237.
- [20] M. Tswett, *Die Berichte der deutschen botanischen Gesellschaft* **1906**, *24*, 384-393.
- [21] L.S. Ettre, *LC GC North America* **2003**, *21*, 458-467.
- [22] A.J.P. Martin, R.L.M. Synge, *Biochemical Journal* **1941**, *35*, 1358-1368.
- [23] J.C. Giddings, *Analytical Chemistry* **1963**, *35*, 2215-2216.
- [24] C.A. Lucy, *Analytical Separations Class Notes*, University of Alberta, Edmonton, 2006.
- [25] J.M. Miller, *Chromatography: Concepts and Contrasts*, 2nd ed., John Wiley & Sons, Inc, 2005.
- [26] L.R.K. Snyder, J.J.; Dolan, J.W., *Introduction to Modern Liquid Chromatography*, 3rd ed., Wiley, Hoboken, New Jersey, 2010.
- [27] C. Horvath, H.J. Lin, *Journal of Chromatography* **1978**, *149*, 43-70.

- [28] J.H. Knox, H.P. Scott, *Journal of Chromatography* **1983**, 282, 297-313.
- [29] J.C. Giddings, *Analytical Chemistry* **1962**, 34, 1186-1192.
- [30] U.D. Neue, *HPLC Columns: Theory, Technology, and Practice* 1st ed., Wiley-VCH, 1997.
- [31] P. Arboleda, *Characterization of Gas Oil Resins Using High Performance Liquid Chromatography*, M.Sc. Thesis, 2007.
- [32] V. Davankov, C.S. Sychov, M.M. Ilyin, K.O. Sochilina, *Journal of Chromatography A* **2003**, 987, 67-75.
- [33] C.S. Sychov, M.M. Ilyin, V.A. Davankov, K.O. Sochilina, *Journal of Chromatography A* **2004**, 1030, 17-24.
- [34] L. Carbognani, *Journal of Chromatography A* **1994**, 663, 11-26.
- [35] P. Ghosh, B. Chawla, P.V. Joshi, S.B. Jaffe, *Energy & Fuels* **2006**, 20, 609-619.
- [36] P.L. Grizzle, J.S. Thomson, *Analytical Chemistry* **1982**, 54, 1071-1078.
- [37] C.S. Hsu, M.A. McLean, K. Qian, T. Aczel, S.C. Blum, W.N. Olmstead, L.H. Kaplan, W.K. Robbins, W.W. Schulz, *Energy & Fuels* **1991**, 5, 395-398.
- [38] C.S. Hsu, K. Qian, *Energy & Fuels* **1993**, 7, 268-272.
- [39] L. Nondek, M. Minarik, J. Malek, *Journal of Chromatography* **1979**, 178, 427-434.
- [40] D.M. Padlo, R.B. Subramanian, E.L. Kugler, *Fuel Processing Technology* **1996**, 49, 247-258.
- [41] J.S. Thomson, J.W. Reynolds, *Analytical Chemistry* **1984**, 56, 2434-2441.

- [42] N.E. Oro, C.A. Lucy, *Journal of Chromatography A* **2010**, 1217, 6178-6185.
- [43] Y. Zhang, Y.M. Huang, P.W. Carr, *Journal of Separation Science* **2011**, 34, 1407-1422.
- [44] L.J. Ma, H. Luo, J. Dai, P.W. Carr, *Journal of Chromatography A* **2006**, 1114, 21-28.
- [45] C.S. Hsu, K.N. Qian, W.K. Robbins, *Hrc-Journal of High Resolution Chromatography* **1994**, 17, 271-276.
- [46] P.L. Jokuty, M.R. Gray, *Energy & Fuels* **1991**, 5, 791-795.
- [47] H. Carlsson, C. Ostman, *Journal of Chromatography A* **1997**, 790, 73-82.
- [48] J. Mao, C.R. Pacheco, D.D. Traficante, W. Rosen, *Journal of Chromatography A* **1994**, 684, 103-111.
- [49] R.E. Paproski, C. Liang, C.A. Lucy, *Energy & Fuels* **2011**, 25, 4469-4478.
- [50] D.C. Harris, *Quantitative Chemical Analysis*, 6th ed., W.H. Freeman and Company, New York, 2003.
- [51] E.S. Yeung, R.E. Synovec, *Analytical Chemistry* **1986**, 58, 1237A-1256A.
- [52] D.A. Skoog, F.J. Holler, T.A. Nieman, *Principles of Instrumental Analysis*, 5th ed., Thomson Learning, 1998.
- [53] A.I. Mallet, S. Down, *Dictionary of Mass Spectrometry*, 1st ed., John Wiley & Sons, 2009.
- [54] L. Li, *Analytical Mass Spectrometry Class Notes*, University of Alberta, Edmonton, AB, 2007.
- [55] I.J. Amster, *Journal of Mass Spectrometry* **1996**, 31, 1325-1337.

- [56] M.L. Easterling, C.B. Lebrilla, I.J. Amster, R. Zubarev, *FTMS: Principles and Applications*, ASMS, Philadelphia, PA, 2009.
- [57] A.G. Marshall, C.L. Hendrickson, G.S. Jackson, *Mass Spectrometry Reviews* **1998**, *17*, 1-35.
- [58] *Qh-Interface User and Service Manual*, Bruker Daltonics, 2006.
- [59] P. Kebarle, L. Tang, *Analytical Chemistry* **1993**, *65*, A972-A986.
- [60] M. Dole, L.L. Mack, R.L. Hines, *Journal of Chemical Physics* **1968**, *49*, 2240-&.
- [61] J.V. Iribarne, B.A. Thomson, *Journal of Chemical Physics* **1976**, *64*, 2287-2294.
- [62] *LC GC North America* **2012**, *30*, 182-182.
- [63] F.W. McLafferty, F. Tureek, *Interpretation of Mass Spectra*, 4th ed., University Science Books, 1993.

CHAPTER TWO. Comparison of Hypercrosslinked Polystyrene Columns for the Separation of Nitrogen Group-Types in Petroleum Using HPLC*

2.1 Introduction

As discussed in Section 1.1, petroleum is a complex mixture of many hundreds of thousands of compounds. In particular, compounds containing nitrogen cause refining problems, corrosion and catalyst fouling [1-4]. High performance liquid chromatography (HPLC) enables the separation of the individual components of petroleum, allowing partial identification of which compounds or classes of compounds are present at different refining stages. The majority of the current published literature concerning petroleum based separations focuses on polycyclic aromatic hydrocarbons (PAHs) and the different ways to separate them [5, 6]. While this information is useful, more work is needed in the separation and analysis of the polar compounds, particularly nitrogen, in petroleum. Due to the complex nature of petroleum samples, the separation of individual compounds is not realistic. Therefore, the goal is to separate N-containing compounds by their group (pyrrole vs. pyridine). This class-specific separation will enhance the information content of analyses that are performed on the samples, such as high-resolution mass spectrometry (MS), as the sample itself will be quite simplified compared to the original petroleum sample [2].

* A version of this chapter has been published. Oro N.E., Lucy C.A.; *Journal of Chromatography A* **2010**, *1217*, 6178-6185.

HPLC separations of petroleum compounds are generally done in normal phase (NP) mode, due to the solubility of oil and petroleum samples in organic solvents. The published methods for polar compounds tend to be long, complicated, and involve multiple clean-up steps or columns. For instance, open column separations are used to concentrate and isolate nitrogen compounds from petroleum [7, 8] but suffer from long separation times, poor control over sorbent activity and being labour intensive. Carlsson and Östman achieved HPLC separation of pyrrole and pyridine groups on a dimethylaminopropyl silica stationary phase [9], but their procedure involved open-column pre-separation, as well as backflushing of the column. Another experiment used an alumina NP (HPLC) column to analyze nitrogen compounds in diesel oil without any sample clean-up, and was able to separate neutral nitrogen groups from hydrocarbons, but had a run time of over 100 min, and was unable to resolve basic nitrogen compounds from hydrocarbons [1].

Group classification of sulphur compounds has also been carried out. Polycyclic aromatic sulphur heterocycles (PASHs) have been oxidized to sulfones prior to HPLC separation, in order to separate them from the PAHs [10]. Alternately, a Pd-containing stationary phase can separate PASHs from PAHs. The PASHs can then be separated according to their number of aromatic double bonds on a β -cyclodextrin phase [3].

It is clear that a simple HPLC method to separate polar compounds in petroleum is needed. This chapter focuses on the use of hypercrosslinked polystyrene phases for the group-type separation of polar compounds in

petroleum. Hypercrosslinked polystyrene has been used in SPE cartridges, HPLC packings and as an adsorbant for the concentration of organic compounds [11-18]. Hypercrosslinked polystyrene is characterized by long polystyrene chains that have been crosslinked with methyl groups between the phenyl groups of polystyrene [12] (Figure 2-1). The resultant structure is rigid and dense, with a high inner surface area and wide mobile phase compatibility. The retention mechanism (reversed phase vs. normal phase) may be changed simply by changing the mobile phase [11, 12].

Recently, Peter Carr's group has synthesized a new family of highly pH and temperature stable stationary phases for reversed phase HPLC. These "HC" (hypercrosslinked) phases are silica based, and are synthesized as a thin monolayer on the surface of the silica [19-25] (Figure 2-1). The motivation for their synthesis was to create a stationary phase that is stable under extremes of temperature and acidic conditions, and they have been used to successfully separate basic drugs and non-electrolytes [22, 25]. Of the HC phases, the two that are relevant to this work are designated HC-C₈ and HC-Tol (Figure 2-1). The primary difference between the two is in the last step of synthesis; in the HC-C₈ phase, the hypercrosslinked polystyrene is derivatized with an octyl phenyl group, while in the HC-Tol phase it is derivatized with toluene [25]. The HC-Tol phase was shown to have equivalent stability, and better efficiency than the HC-C₈ phase. While these phases were designed for RPLC, they are compatible with NP conditions, but prior to this work have not been used for quasi-normal phase (QNP) separations.

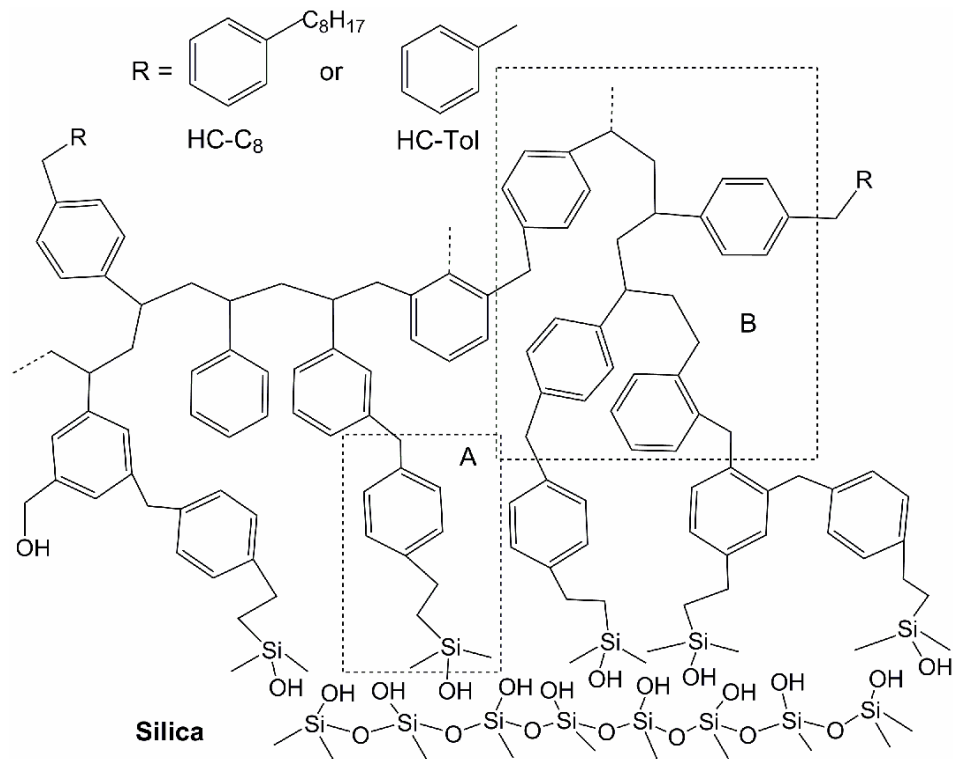


Figure 2-1. Structure of the HC-Tol and HC-C₈ stationary phases. Box A refers to the initial silanization step, and box B highlights the crosslinking step. Adapted from references [21] and [22].

Our interest in hypercrosslinked polystyrene for petroleum separations arose from previous studies in our group with the commercial 5-HGN packing for the separation of gas oil resins into fractions containing aromatics, sulphur compounds and nitrogen compounds [26]. The packing showed unique selectivity for compounds in petroleum. The work presented in this chapter studies both purely polymer and silica based hypercrosslinked polystyrene. A suite of 21 model compounds found in petroleum were analyzed on the commercial polymer packing, an HC-Tol column, and two HC-C₈ columns. Discussion will focus primarily on the group type separation of N-containing compounds, with some discussion of other polar functionalities based on sulphur and oxygen.

2.2 Experimental

2.2.1 Apparatus

All experiments were performed on a Varian ProStar HPLC system (Varian, Palo Alto, CA, USA). A schematic diagram of the HPLC is shown in Chapter 1 (Figure 1-5). Eluents were sparged with helium (<5 ppm water, Praxair, Mississauga, ON) before and during the experiments, and the helium was dried with an in-line gas dry filter trap (Chromatography Research Supplies, Louisville, KY, USA). Two Varian 210 ProStar pumps were used to pump at 1.0 mL/min. All tubing and fittings were stainless steel. Sample injections were performed with a Varian ProStar 410 autosampler equipped with a 1 µL sample loop. To maintain a consistent 35°C column temperature, an Eppendorf CH-30 column oven (Mississauga, ON) was used. Detection was performed at 254 nm with a 0.1

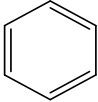
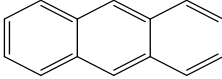
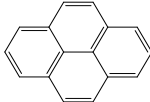
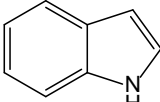
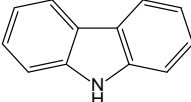
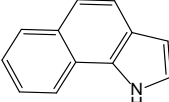
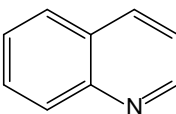
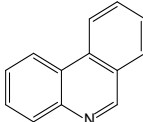
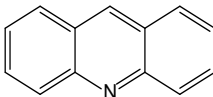
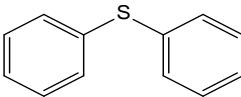
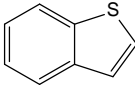
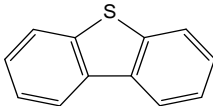
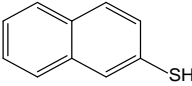
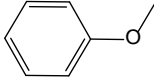
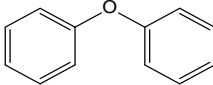
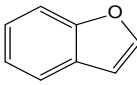
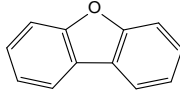
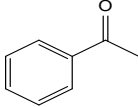
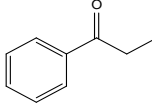
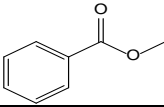
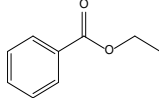
s rise time with a Knauer Smartline 2500 UV detector (Knauer-ASI, Franklin, MA, USA), fit with a 2 μ L flow cell connected via fibre optic cables. Data acquisition was performed using Varian Star Chromatography Workstation version 6.20 software, at a rate of 20 Hz.

2.2.2 Chemicals

Optima grade dichloromethane (DCM) and hexanes (Fisher Chemicals, Fairlawn, NJ, USA) were pre-dried by adding 50 g of Type 3A, 8-12 mesh molecular sieves (EMD Chemicals, Gibbstown, NJ, USA) to a 4 L bottle 24 hours before use. All chromatographic solutes were of >90% purity (Sigma-Aldrich, St. Louis, MO, USA), and were prepared according to their ring size. One-ring compounds were prepared at 10 mg/mL, and multiple-ring compounds were prepared at 1 mg/mL. Indole and carbazole were dissolved in dichloromethane, and the remaining solutes were dissolved in hexane and a minimum amount of dichloromethane to allow full dissolution. A list of these compounds along with their structures and group types can be found in Table 2-1.

Chromalite 5-HGN hypercrosslinked polystyrene particles were a gift from Purolite (Purolite International Limited, Wales, UK and Bala Cynwyd, PA, USA). The particles have a mean diameter of 4.5 – 5.5 μ m, and their surface area is 1100 – 1500 m²/g. The HC-Tol phase was synthesized on Type-B Zorbax silica particles, with a particle diameter of 5.0 μ m and a surface area of 180 m²/g [25].

Table 2-1. Model compounds used in this work.

Group	Compounds	Structure
PAH	benzene (1)	
	anthracene (2)	
	pyrene (3)	
N, pyrrole	indole (4)	
	carbazole (5)	
	1H-Benzo[g]indole (6)	
N, pyridine	quinoline (7)	
	phenanthridine (8)	
	acridine (9)	
S, sulfide	phenyl sulfide (10)	
S, thiophene	benzothiophene (11)	
	dibenzothiophene (12)	
S, thiol	2-naphthalenethiol (13)	
O, ether	anisole (14)	
	phenyl ether (15)	
O, furan	2,3-benzofuran (16)	
	dibenzofuran (17)	
O, ketone	acetophenone (18)	
	propiofenone (20)	
O, ester	methyl benzoate (19)	
	ethyl benzoate (21)	

The HC-C₈ stationary phase was synthesized on HiChrom silica particles, and the particle diameter is also 5.0 μm, and the surface area is 250 m²/g [19, 22]. The HC columns were a gift from Peter Carr (University of Minnesota).

2.2.3 Column Packing

The 5-HGN particles were home-packed, and the column was labelled HGN-01. The packing was performed using a Haskel air-driven liquid pump (DSF-122-87153, Haskel, Burbank, CA, USA). 2.2 grams of particles were slurried in 40 mL of dichloromethane and sonicated for 15 minutes. This slurry was placed in an 80 mL reservoir (Lab Alliance, State College, PA, USA) and packed in the downward direction into a 5.0 x 0.46 cm ID stainless steel column jacket (Grace Davison Discovery Science, Deerfield, IL, USA) using dichloromethane as the packing solvent. The pressure was increased from 0 psi to ~3200 psi over one minute, and then maintained at 3200 psi until 300 mL of dichloromethane had passed through the column. The pressure was released and the column was fitted with stainless steel frits (2 μm pore size, Grace Davison Discovery Science, Deerfield, IL, USA) and flushed with the desired solvent mixture for two hours prior to first use. The column efficiency was 1140, which corresponds to a plate height of 44 μm, and was used to gauge the quality of the packing, where higher efficiency and a lower plate height are desirable. This is superior to the 190 μm observed for a 25 cm column packed with 5-HGN [26].

2.2.4 Calculations

Retention times and peak widths at half-height were determined using Varian's Star Chromatography Workstation software, version 6.20. The dead time was determined by the refractive index peak caused by injection of hexane in dichloromethane and confirmed by injection of dichloromethane in a hexane mobile phase. The column efficiency (N) was calculated based on the width-at-half-height (Equation 1-10), and retention factors (k) were calculated using Equation 1-5.

2.3 Results and Discussion

The stationary phases used in this chapter are all hypercrosslinked polystyrene. The hypercrosslinked phase is rigid, and has many $-\text{CH}_2-$ bridges linking the phenyl groups of polystyrene [12, 21, 22]. The absence of polar groups on the stationary phase means that there are no specific adsorption sites on the surface. For this reason, we use Davankov's term *quasi-normal phase chromatography* to describe the adsorption of solutes on a largely non-polar stationary phase under normal phase conditions [11, 12, 26]. There are two types of hypercrosslinked polystyrene studied in this chapter; the HGN phase is a bed of the hypercrosslinked material (phenyl groups of polystyrene linked with methyl groups) [12], while the HC phases have hypercrosslinked polystyrene surrounding the silica surface of the stationary phase (Figure 2-1). The HC phases are synthesized in a multi-step process, and their somewhat more complicated structure bears further explanation. Silica is silanized with an agent such as

dimethylchloromethylphenylethylchloro-silane (DM-CMPES) (“A” in Figure 2-1), which is then polymerized and crosslinked with a styrene heptamer (“B” in Figure 2-1). Some self-condensation also occurs during this process. The phase is derivatized with the desired moiety (R in Figure 2-1), and is finally acid washed for increased stability [21, 22]. The resultant polymer phase is a thin layer, rather than a bed of material. The siloxane bonds with the surface of the silica are broken to eliminate any acid-labile bonds on the stationary phase. The hypercrosslinked polystyrene surrounds the silica particles and is not washed off, despite the lack of bonds holding the polystyrene to the silica.

The HGN polymeric phase is a gel-type polymer, meaning it has to swell to be used in chromatography [27]. One unique property of hypercrosslinked polymers is that they are able to swell in any solvent, and once they are swollen, they are not sensitive to changes in eluent [11, 12, 27]. The changes in pressure observed with our HGN column with different solvent mixtures are consistent with what we would expect from viscosity changes. No additional pressure change indicates that the phase is not swelling or shrinking. The pressure in an HPLC column in relation to viscosity can be described by [28]:

$$P \approx \frac{1.25L_C^2\eta}{t_o d_p} \quad (\text{Equation 2-1})$$

where P is pressure in psi, L_C is column length in mm, η is viscosity in cP, t_o is the column dead time in minutes and d_p is the particle diameter in μm . The change in pressure, ΔP can be calculated by:

$$\Delta P = P_2 - P_1 \approx \frac{1.25L^2}{t_o d_p} (\eta_2 - \eta_1) \quad (\text{Equation 2-2})$$

where η_1 and η_2 are the viscosities of two different solvent mixtures. The viscosity of a binary solvent mixture of a regular solution can be calculated using [29]:

$$\eta = x_A^2\eta_A + x_B^2\eta_B + x_Ax_B\eta', \quad \eta' = \eta_A + \eta_B \quad (\text{Equation 2-3})$$

where x is the volume fraction (1 = 100%) of solvent A or B, and η_A and η_B are the pure solvent viscosities.

2.3.1 Retention Behavior on Hypercrosslinked Phases

2.3.1.1 Retention of Standards

The HC-Tol and HC-C₈ phases are very similar in terms of their structure. At the derivitization step of the synthesis, the HC-Tol is derivatized with toluene, while the C₈ phase uses octyl benzene (Figure 2-1). Figure 2-2 compares the QNPLC retention of model compounds on these two columns, with k for HC-C₈ plotted on the x-axis, and k for HC-Tol plotted on the y-axis. As expected, the retention behavior of model compounds on these phases is quite similar. Most remarkably, PAH standards show very weak retention on both of the columns (■ in Figure 2-2), with $k < 1$ on both columns. Figure 2-2 also shows that as retention increases on one column, it generally increases on the other, and that different polar groups are generally grouped together in terms of retention. On the two HC columns, the order of elution for the N groups is the same, with the pyrrole compounds (▲ in Figure 2-2) eluting after the PAHs (■), followed by the pyridine compounds (not shown in Figure 2-2 due to very strong retention on the C₈ phase).

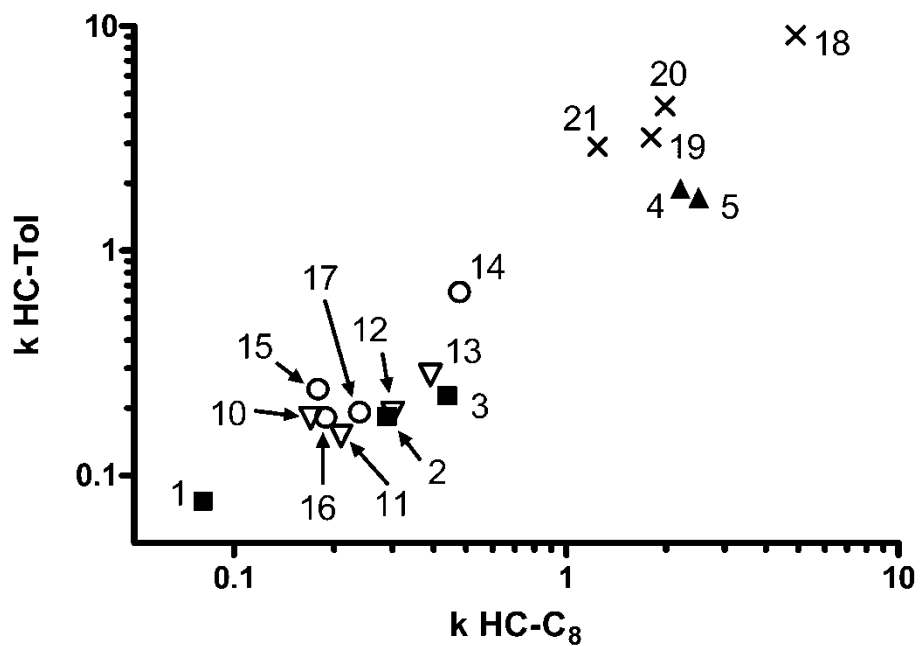


Figure 2-2. Retention factors of standards on the HC-Tol column versus the HC-C₈ column, at a solvent strength of 25% DCM in hexane. Numbering corresponds to the compounds listed in Table 2-1. The size of the data points includes error. k values are the average of three runs.

■ PAHs, ▲ pyrroles, ▽ S compounds, ○ ethers and furans, × ketones and esters

The retention of groups is overall higher on the C₈ column than the Tol column, but the groups occupy comparable “windows” in the chromatograms between the two columns. The most notable difference between HC-Tol and HC-C₈ is the retention of the pyridine groups, in that the retention on the C₈ phase is so strong for this group that essentially they are not eluted. This stronger retention on the C₈ phase will be discussed in more detail in Section 2.3.2.

On both HC columns, the model sulphur compounds experience very weak retention (∇ in Figure 2-2), clustering below a k of 0.4, and overlapping with the PAHs. The ether and furan oxygen groups are weakly retained ($k < 1$) at all solvent strengths (ranging from 100% DCM in hexane to 5% DCM in hexane) on the HC columns (\circ), but the ketone and ester oxygen groups (\times) experience much more retention and are well separated from the rest of the oxygen and sulphur compounds, with retention comparable to the pyrroles. In summary, both HC columns show the same retention trend for all oxygen and sulphur standards. This is contrary to what is observed for the nitrogen standards.

Figure 2-3 compares retention on the HC-Tol and HGN columns. The retention of standards on the HGN column is similar to the HC phases in that the PAHs elute before the pyrroles. Like the HC-C₈ phase, the pyridines are also irreversibly retained at all solvent strengths on the HGN column. Figure 2-3 also shows that there is no distinct group-type separation of the compounds on HGN, and that these groups will overlap in the chromatograms. While different groups are separated on the HC-Tol column, the HGN column has a scattering of groups across the range of k values.

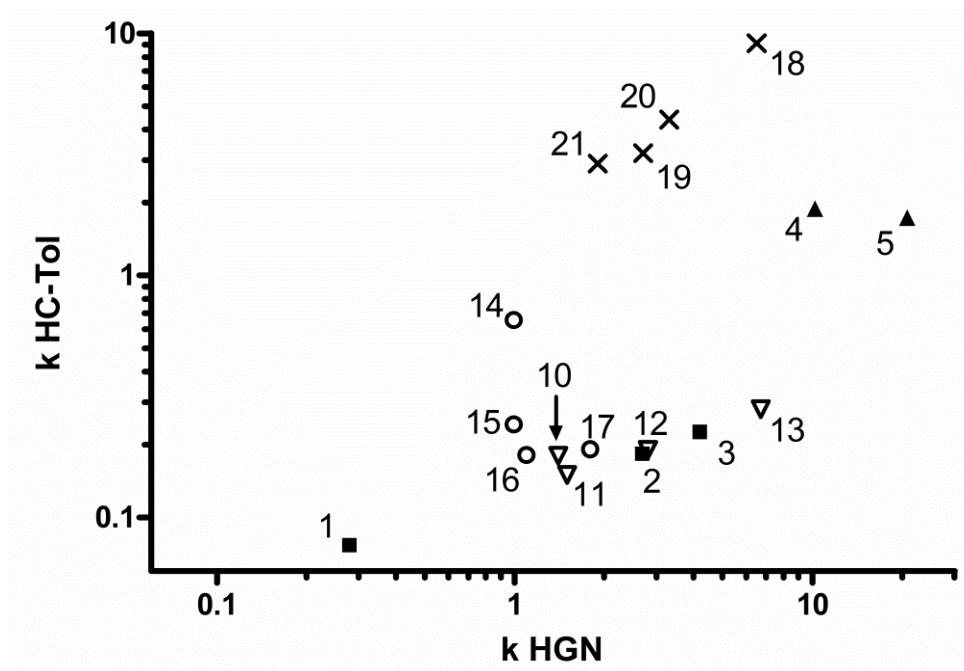


Figure 2-3. Retention factors of standards on the HC-Tol column versus k on the HGN column, at a solvent strength of 25% DCM in hexane. Numbering corresponds to the compounds listed in Table 2-1. The size of the data points includes error in the point. k values are the average of three runs.
 ■ PAHs, ▲ pyrroles, ▽ S compounds, ○ ethers and furans, × ketones and esters

This type of phase shows notable retention for the PAHs, as well as the sulphur and oxygen standards, which can be seen with the spread of points along the x-axis of Figure 2-3. The pyrroles are slightly separated from the rest of the compounds, but not enough to be considered a group-type separation. The detailed retention mechanism for this phase is discussed in Section 2.3.1.2.

2.3.1.2 Mechanism of Retention

Hemström and Irgum present an excellent discussion on the use of simple equations to describe retention behavior [30]. Retention behavior on an HPLC column can be classified as either partition or adsorption, where partitioning can be thought of as a dissolving in and out of the stationary phase, and adsorption as a surface interaction on the stationary phase. When a partitioning mechanism is occurring, the linear solvent strength model can be used [31]:

$$\log k = \log k_w - S\phi \quad (\text{Equation 2-4})$$

where k is the retention factor in the chosen eluent, k_w is the retention factor in pure weak solvent, ϕ is the volume fraction of the strong eluent, and S is the slope of a plot of $\log k$ vs. ϕ derived from a linear regression.

Similarly, a competitive adsorption mechanism can be described by the Snyder-Soczewinski equation [28, 32] :

$$\log k = \log k_B - n \log X_B \quad (\text{Equation 2-5})$$

where k_B is the retention factor of the solute in pure eluent B, n is the number of molecules of solvent B displaced by the solute, and X_B is the mole fraction of solvent B, the stronger eluent. These two models can be used to determine

whether or not retention is behaving under a partition mechanism, or an adsorption mechanism. Plots can be made of $\log k$ vs. % DCM (partition) and $\log k$ vs. \log % DCM (adsorption), and linear behavior for either of the plots will indicate which mechanism is dominant [30].

To gain more insight into the retention mechanism of the columns, these plots were made for both HC columns, as well as the HGN column. Figures 2-4, 2-5 and 2-6 show these plots for the HC-Tol column, the HGN column and the HC-C₈ column. The plots corresponding to partition behavior (Equation 2-4, Figures 2-4B, 2-5B and 2-6B) show clear curvature for the HC-Tol, HGN and HC-C₈ columns, while the adsorption plots (Equation 2-5, Figures 2-4A, 2-5A and 2-6A) are much more linear. The data points for both types of plots were fit to a linear regression, and the correlation coefficient (R^2) values for the adsorption plots are all closer to one than the partition plots for both HC-Tol and HGN (Table 2-2). The correlation coefficient is used to assess quality of fit; therefore, the adsorption plots are more linear than the partition plots. Based on this data and Equations 2-4 and 2-5, we assume that the retention mechanism of the hypercrosslinked phases in QNP is that of adsorption.

In previous work by Trammell and co-workers, application of the linear solvent strength model (Equation 2-4) demonstrated that the HC-C₈ column behaves under a partition mechanism in RPLC [22]. The HC columns are therefore able to act under either adsorption or partition mechanisms, depending on whether NP or RP conditions are used. Similar behavior has also been observed on the HGN-type hypercrosslinked phases [11, 12].

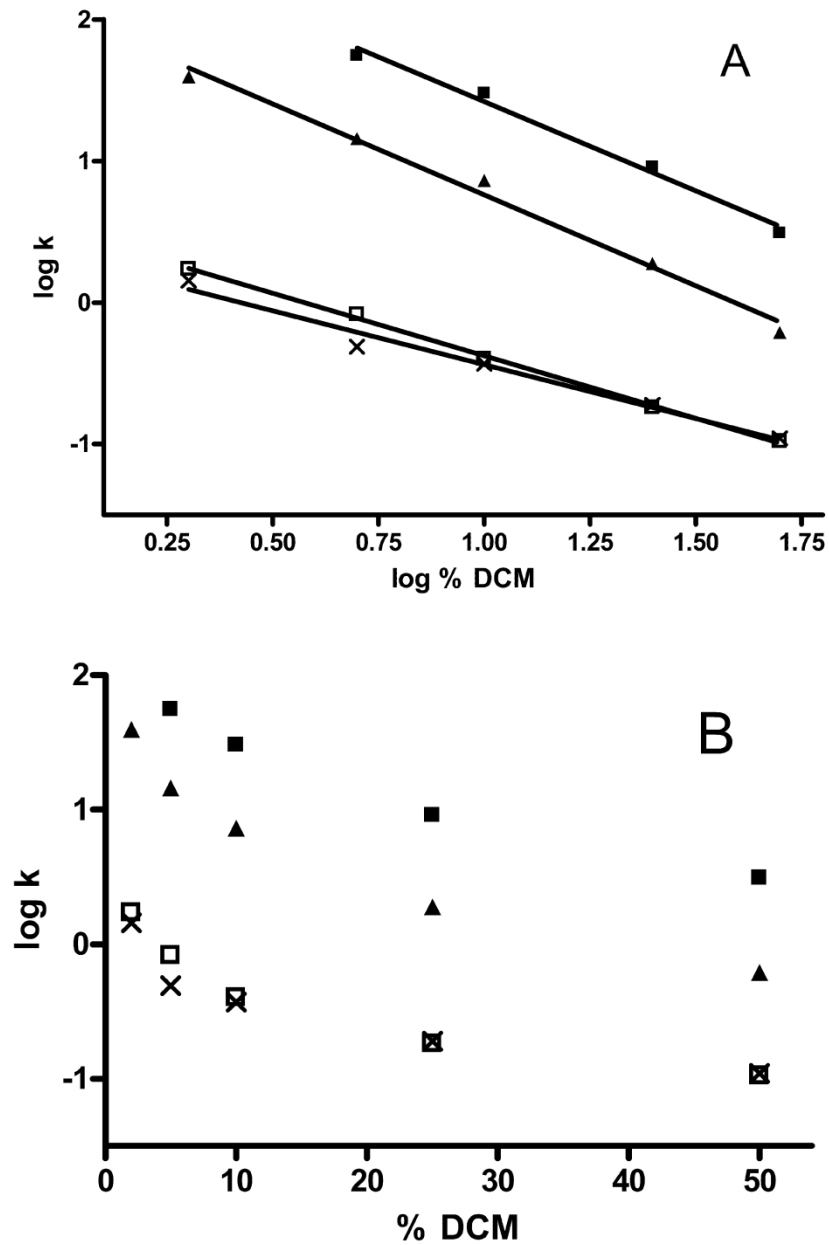


Figure 2-4. (a) Plot of log k vs. log (% DCM) on the HC-Tol column (adsorption). The lines are a linear fit to the data. (b) Plot of log k vs. % DCM on the HC-Tol column (partition). The size of the data points includes the error in the data.

▲ indole, □ anthracene, ■ acetophenone, × dibenzothiophene

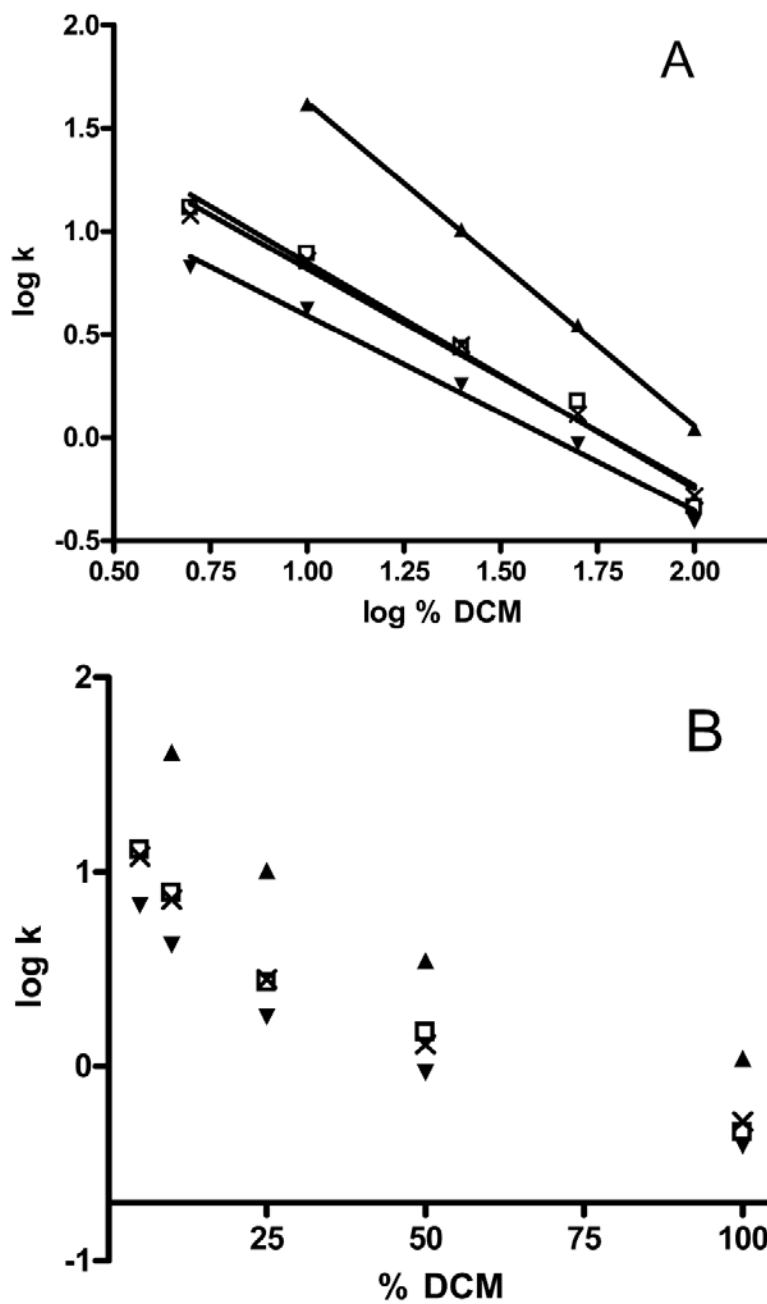


Figure 2-5. (a) log k vs. log % DCM for HGN column (adsorption). The lines are a linear fit to the data. (b) log k vs. % DCM for HGN column (partition). The size of the data points includes error.

▲ indole, □ anthracene, ▼ dibenzofuran, × dibenzothiophene

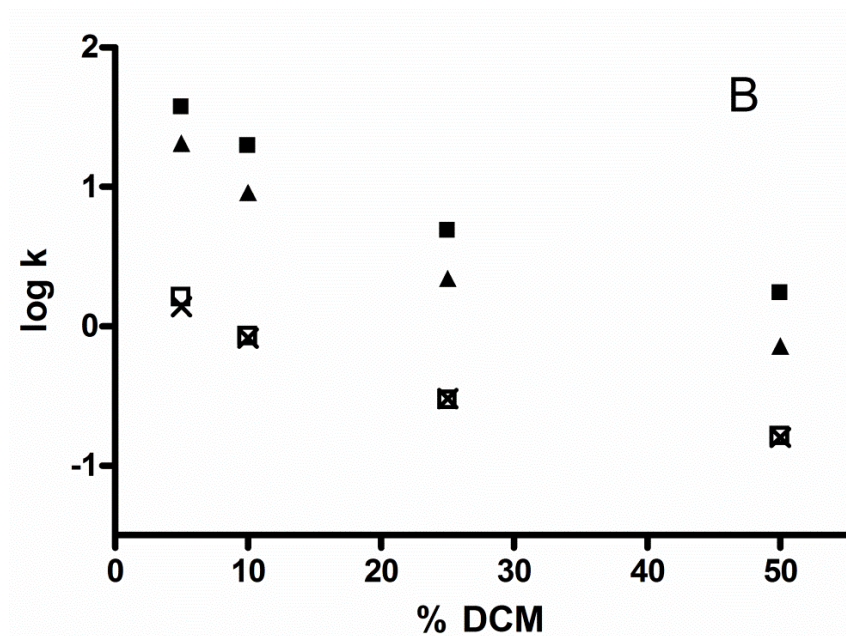
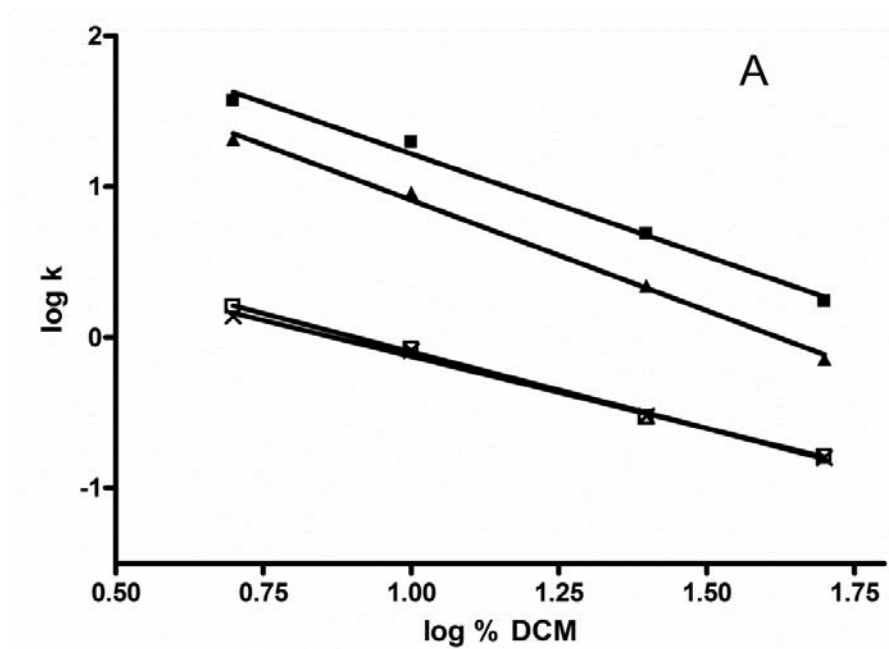


Figure 2-6. (a) Plot of $\log k$ vs. $\log (\% \text{ DCM})$ on the HC-C₈ column (adsorption). The lines are a linear fit to the data. (b) Plot of $\log k$ vs. $\% \text{ DCM}$ on the HC-Tol column (partition). The size of the data points includes the error in the data.

▲ indole, □ anthracene, ■ acetophenone, × dibenzothiophene

Table 2-2. Correlation coefficients for all standards on the HC-Tol and HGN columns.*

Compound	R ²			
	HC-Tol		HGN	
	Adsorption	Partition	Adsorption	Partition
pyrene	0.991	0.922	0.983	0.927
indole	0.992	0.954	0.907	0.956
carbazole	0.994	0.951	0.995	0.985
benzene	0.922	0.715	0.872	0.693
anthracene	0.997	0.884	0.982	0.924
acetophenone	0.989	0.962	0.991	0.900
Me-benzoate	0.985	0.961	0.990	0.911
anisole	0.993	0.945	0.987	0.915
benzofuran	0.985	0.958	0.979	0.938
diphenyl ether	0.997	0.938	0.982	0.931
dibenzofuran	0.979	0.957	0.990	0.916
dibenzothiophene	0.985	0.961	0.991	0.911
Ph-sulfide	0.996	0.930	0.980	0.938
naphthalenethiol	0.995	0.946	0.997	0.979
thianaphthalene	0.96	0.922	0.985	0.926

* The R² values are for a linear fit to a plot of either log k vs. % DCM (partition, Equation 2-4) or log k vs. log (% DCM) (adsorption, Equation 2-5).

The major retention mechanism on the HGN stationary phases has been reported to be an interaction of π electrons (π - π) between the analyte and the stationary phase [12, 15, 18, 26]. To confirm this for the current work, the retention of PAH standards on the HGN phase was investigated. If a π - π mechanism is occurring, we would expect retention to increase with the number of aromatic rings in the compound [18]. Indeed, at 10% DCM, the k values for benzene, anthracene and pyrene are 0.7, 7.8 and 12.3, respectively. This is an excellent indicator that the π - π interactions are a major contributor to retention on the HGN column. π - π interactions are dominant in non-polar solvents (hexane in this case), and are weakened by the presence of a more polar solvent (DCM) [12, 18]. The retention for all compounds on the HGN column decreases with the addition of more DCM in the mobile phase, consistent with expectations for π - π interactions.

Other polymeric hypercrosslinked polystyrene stationary phases (MN-200) have been described as acting under a π - π mechanism [15]. On the MN-200 stationary phase, there are also oxygen groups on the surface that can cause additional retention of heteroatom-containing compounds [33]. The HGN phase is synthesized in a similar manner to MN-200. Thus, it is possible that similar oxygen functionalities exist on the HGN phase, causing retention beyond what we would expect from just π - π interactions. However, studies have concluded that no such groups are present on HGN [11, 34].

If the HC columns were acting under the same π - π mechanism, we would see similar increasing retention for the PAHs as they increase in size. However, as shown previously, the PAHs all experience very weak retention on the HC

columns, with very little dependence on ring size. This indicates that the HC columns experience an adsorptive mechanism that is not π - π .

Polymeric hypercrosslinked polystyrene can be used for size exclusion chromatography [15, 35-37], but we do not believe this to be occurring with the HC phases. On the HC phases, at all solvent strengths examined, there is an increase in retention with the size of the solute for PAHs (i.e. benzene to anthracene to pyrene). On both HC columns, we see much stronger retention of carbazole than of benzene (i.e. k of 16.4 vs. 0.3 at 5% DCM in hexane on HC-Tol). Carbazole is two rings larger than benzene (Table 2-1). If an exclusion mechanism were occurring, we would expect to see less retention of a larger solute, which is opposite to what is observed on the HC columns.

2.3.2 Comparison of HC-Tol and HC-C₈

The retention of compounds is generally stronger on the HC-C₈ phase when compared to the HC-Tol phase. The difference between the structures of the HC-Tol and the HC-C₈ phases is the moiety used in the final derivitization step. The HC-C₈ phase is derivatized with octylbenzene, while the Tol phase with toluene. Essentially, the C₈ phase has an eight carbon chain attached to the surface at various positions, while the Tol phase has only one carbon, as illustrated in Figure 2-1 [21]. The motivation for the creation of the HC phases was to make phases that are stable under acidic and high temperature conditions for use as the second dimension in 2D-LC [19, 21, 25, 38]. The HC-Tol phase is one generation beyond the HC-C₈, and was made because toluene facilitates an

easier reaction; it is more reactive than octylbenzene, and can be used as the solvent in the derivitization step [25].

The HC-C₈ phase is structurally very similar to the HC-Tol phase, but the synthesis steps as well as the underlying silica used are different. The surface area of the HC-C₈ phase is also greater than the HC-Tol phase (250 m²/g vs. 180 m²/g) [19, 22, 25]. These two factors may account for the differences in retention observed between these two columns.

In comparing the two phases, it is useful to revisit Figure 2-2, which is at a solvent strength of 25% DCM in hexane. Due to their strong retention on HC-C₈, the pyridines were not plotted. The pyrroles (▲) are isolated from the rest of the compounds on both columns. The similarity in retention between the Tol and C₈ phases is indicated by a correlation coefficient for the k values of 0.87. The sulphur (▽), ether and furan (○) and PAH (■) compounds experience very weak retention on both HC phases (k < 0.5).

A contributing factor towards retention on the HC phases may be silanols available on the surface that are not shielded by the hypercrosslinked polystyrene. Silanols can interact strongly with many polar compounds. The HC-Tol phase is designed, in part, to have fewer activated silanols than the HC-C₈ phase [25]. This could contribute to the different retention observed on the two phases. The silanols may also be part of the strong retention of the ketones and esters (×) observed in Figure 2-2. However, the HGN phase also strongly retains ketones and esters, so we cannot disregard the selectivity of the hypercrosslinked polystyrene itself.

2.3.3 Comparison of HC-Tol and HGN phases

As discussed in Sections 2.3.1.1 and 2.3.1.2, the retention mechanism and characteristics of the HGN column are different than the HC columns. This can be partly attributed to the π - π retention mechanism on the HGN column. Aromatic rings in all of the standards causes them to be retained on the HGN phase where they may experience very little retention on the HC-Tol phase.

As in the comparison of the two HC columns, a plot of the k values on HC-Tol vs. k on HGN at 25% DCM reveals a lot about the retention on these two phases (Figure 2-3). On this figure, there is a very distinct scatter of points. There is overlap of all the groups on the HGN column, and the standards experience more retention on the HGN column. Where the majority of the compounds on HC-Tol have a k of less than one, almost all of the compounds have a k greater than one on HGN. There is almost no correlation in retention between the two columns ($R^2 = 0.05$). This reinforces the notion that the HC-Tol column is not acting under a π - π mechanism as was the HGN [12, 15, 18, 26]. As the main goal of this study was to separate N-containing groups, the inability to elute the pyridine-type compounds, as well as the overlap of groups, points to the conclusion that the HGN packing was not the best choice. However, the exceptional orthogonality exhibited by these two phases indicates that they may be used together in a 2D-LC experiment, to perhaps attain even better resolution and group separation of the compounds in petroleum.

2.3.4 Separation of Model Compounds on HC-Tol

The HC-Tol phase is ideal for the type of separation we want to achieve because both nitrogen groups as well as aromatic compounds have different retention on the column. To illustrate the abilities of this column, a mix of nine compounds (three PAHs, three pyridines and three pyrroles) was analyzed under a step gradient (Figure 2-7). The gradient is necessary because of the strong retention of the pyridine groups relative to the pyrrole and PAH groups, and a step gradient was used because it gave sharper later eluting peaks than a linear gradient. An equilibration time of 12 minutes was used; 10 minutes was insufficient to return the column to equilibrium after the separation, but increasing the time beyond 12 minutes did not show any additional improvement. The aromatic compounds are essentially unretained, while the two different nitrogen groups show very different selectivity. Within the pyrrole group, two peaks are visible. The pyridine group elutes as a single peak, as does the PAH group. However this is not a problem, as the objective with petroleum analysis is to separate groups, not compounds within a group.

The HC-Tol phase also exhibits unique selectivity for oxygen-containing compounds (Figure 2-8). A separation of eight oxygen compounds was achieved using a similar step gradient. There is better resolution between compounds, and it would appear that the HC-Tol phase has a different selectivity for oxygen group-types as well.

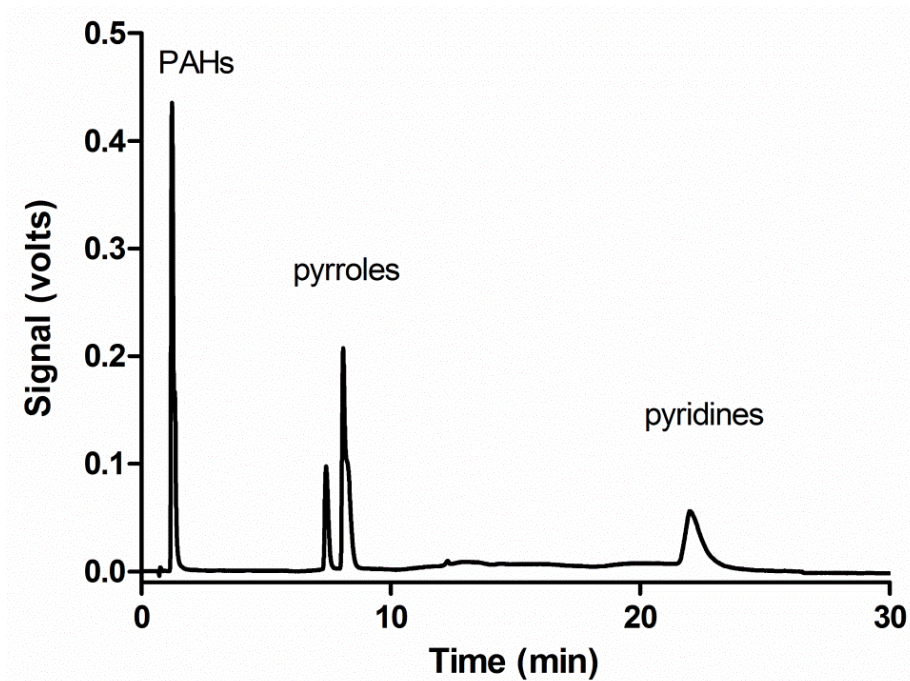


Figure 2-7. Chromatogram of nitrogen/PAH mix under a step gradient on the HC-Tol column. Temperature was 35°C, at a flow rate of 1 mL/min, detection wavelength of 254 nm. PAHs: benzene, pyrene, anthracene. Pyrroles: indole, carbazole, 1H-benzo[g]indole. Pyridines: quinoline, phenanthridine, acridine. Step gradient was 20 minutes long, with 12 minutes of equilibration time. Initial solvent condition was 5% DCM in hexane, increasing by 20% DCM every four minutes.

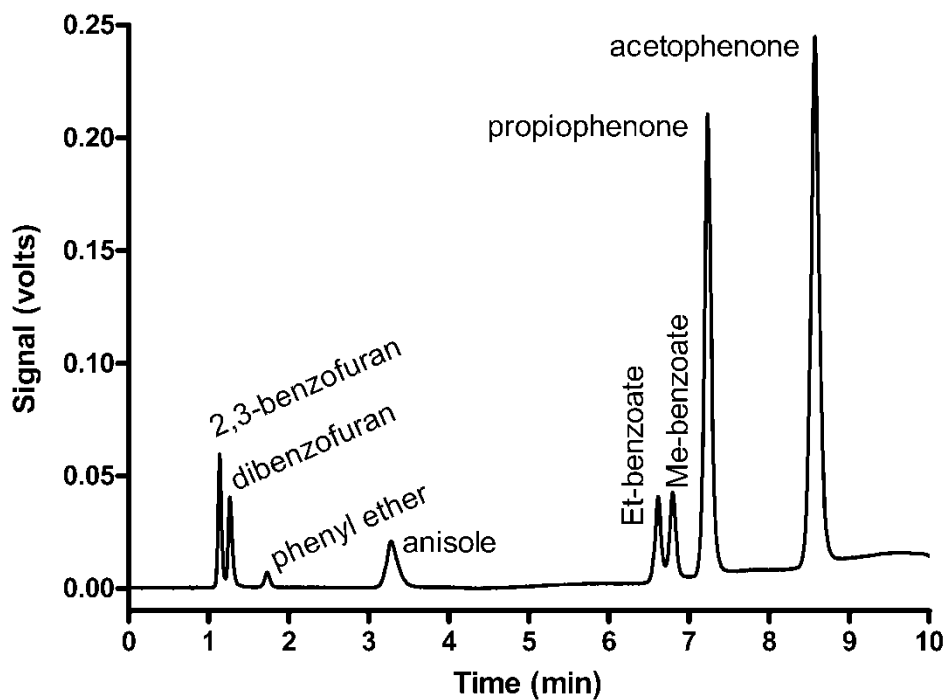


Figure 2-8. Chromatogram showing the separation of oxygen-containing model compounds on the HC-Tol column. Conditions: 35°C, 1 mL/min, detection wavelength of 254 nm. A step gradient was used, beginning at 5% DCM in hexane, increasing 20% DCM every two minutes up to 100% DCM. Equilibration time was 12 minutes between each gradient separation.

Although this was not the target of this study, this may prove useful in the future. Figure 2-8 also reveals more about the retention mechanism on the HC-Tol column. The HGN column acts under a π - π mechanism [12, 15, 18, 26], with compounds with more aromatic rings experiencing more retention. On the HC-Tol column, anisole and phenyl ether elute in an order opposite to what would be expected based on a π - π mechanism. Anisole, which has only one ring, is retained stronger than phenyl ether, which has two rings. This would suggest that the retention is based on the polar group, as the phenyl ether has more steric hindrance around the oxygen than the anisole. A similar elution order is observed with ethyl and methyl benzoate, with methyl benzoate experiencing stronger retention. This theory is further confirmed by the elution of a highly sterically hindered N standard (t-butyl pyridine) in the PAH region of the chromatogram ($t_R \sim 1$ min). Efficiencies were calculated for the HC-Tol phase for anthracene, carbazole and methyl benzoate. As the compounds become more retained, the efficiencies of the standards decrease, but the peak shapes remain the same (Table 2-3a). These efficiencies are lower than the 3560 – 4210 observed in RP mode [25].

All of the standards were run at a high concentration (up to 10 mg/mL) during the experiments, and a suite of four compounds were run at one-third the elevated concentration to see if the concentration had any effect on retention and efficiency. The retention of the weakly retained anthracene, dibenzofuran and dibenzothiophene were the same within error at both concentrations.

Table 2-3. (a) Efficiencies and retention on the HC-Tol column with varying solvent strengths.

(b) Efficiencies and retention on the HC-Tol column, from retention data collected at a solvent strength of 2 % DCM in hexane. k values are an average of three runs.

a)

Conditions	Compound					
	Anthracene		Carbazole		Me-benzoate	
	N	k	N	k	N	k
50% DCM	2500	0.11	2000	0.51	2400	1.2
25% DCM	2500	0.18	1100	1.7	1600	3.2
10% DCM	1100	0.40	730	7.2	870	10.7
5% DCM	1800	0.83	770	16.4	600	17.6
2% DCM	840	1.7				

b)

	1.0 mg/mL		0.3 mg/mL	
	N	k	N	k
anthracene	840	1.7	1300	1.8
indole	420	39.4	800	45.3
dibenzothiophene	1800	1.4	2000	1.5
dibenzofuran	2200	1.5	2400	1.5

However retention of the strongly retained indole decreased with an increase in concentration (Table 2-3b). Qualitatively, the peak shapes are the same between the different concentrations, despite the shift in retention time. This suggests that overload is not a problem here. Unfortunately, the signal-to-noise is too poor to allow for a quantitative comparison of asymmetry.

Previous work completed in our group had shown that an aminopropyl bonded silica NP column was capable of group-type separation of N compounds in petroleum [39]. However, when these experiments were repeated on a new column, it was found that the chemistry of the previous column had somehow been altered by harsh solvent and temperature conditions, and that retention was due to residual silanols. The hypercrosslinked columns in this chapter have shown to be far more useful than an aminopropyl column, serving to separate the N groups from each other, as well as from PAHs that may interfere with further analysis.

2.4 Conclusions

The HC-Tol stationary phase provides unique and useful selectivity for N-containing groups in petroleum. Using a step gradient, pyrrole and pyridine group-types can be separated in under 25 minutes, with PAHs, sulphur compounds and the majority of oxygen compounds weakly retained and well separated from the N compounds. The HC-Tol phase also provides an excellent separation of oxygen standards.

The HC-C₈ and HGN packings show similar retention characteristics to HC-Tol, but both retain pyridine compounds with such strength that they are unable to provide a group-based separation. This strong retention could be a concern when using real petroleum samples, as irreversible adsorption could occur in the column. The HGN column also retains PAH compounds, which may overlap with the N fractions we wish to analyze. Both of these types of columns have been used in reversed phase and normal phase mode, which speaks to their potential for a very wide variety of applications and solvent conditions.

2.5 References

- [1] J. Mao, C.R. Pacheco, D.D. Traficante, W. Rosen, *Journal of Chromatography A* **1994**, 684, 103-111.
- [2] R.P. Rodgers, T.M. Schaub, A.G. Marshall, *Analytical Chemistry* **2005**, 77, 20A-27A.
- [3] S.K. Panda, W. Schrader, J.T. Andersson, *Journal of Chromatography A* **2006**, 1122, 88-96.
- [4] J.R. Woods, J. Kung, G. Pleizier, L.S. Kotlyar, B.D. Sparks, J. Adjaye, K.H. Chung, *Fuel* **2004**, 83, 1907-1914.
- [5] M. Kaminski, R. Kartanowicz, E. Gilgenast, J. Namiesnik, *Critical Reviews in Analytical Chemistry* **2005**, 35, 193-216.
- [6] P.A. Sutton, P.N. Nesterenko, *Journal of Separation Science* **2007**, 30, 2900-2909.
- [7] P.L. Jokuty, M.R. Gray, *Energy & Fuels* **1991**, 5, 791-795.

- [8] C.S. Hsu, K.N. Qian, W.K. Robbins, *Hrc-Journal of High Resolution Chromatography* **1994**, *17*, 271-276.
- [9] H. Carlsson, C. Ostman, *Journal of Chromatography A* **1997**, *790*, 73-82.
- [10] J. Bundt, W. Herbel, H. Steinhart, *Hrc-Journal of High Resolution Chromatography* **1992**, *15*, 682-685.
- [11] V. Davankov, C.S. Sychov, M.M. Ilyin, K.O. Sochilina, *Journal of Chromatography A* **2003**, *987*, 67-75.
- [12] C.S. Sychov, M.M. Ilyin, V.A. Davankov, K.O. Sochilina, *Journal of Chromatography A* **2004**, *1030*, 17-24.
- [13] N.A. Penner, P.N. Nesterenko, A.V. Khryashevsky, T.N. Stranadko, O.A. Shpigun, *Mendeleev Communications* **1998**, 24-27.
- [14] M.P. Tsyurupa, M.M. Ilyin, A.I. Andreeva, V.A. Davankov, *Fresenius Journal of Analytical Chemistry* **1995**, *352*, 672-675.
- [15] N.A. Penner, P.N. Nesterenko, M.M. Ilyin, M.P. Tsyurupa, V.A. Davankov, *Chromatographia* **1999**, *50*, 611-620.
- [16] X. Zhang, S.H. Shen, L.Y. Fan, *Journal of Materials Science* **2007**, *42*, 7621-7629.
- [17] N.A. Penner, P.N. Nesterenko, *Analyst* **2000**, *125*, 1249-1254.
- [18] C.S. Sychov, V.A. Davankov, N.A. Proskurina, A.J. Mikheeva, *LC GC Europe* **2009**, *22*, 20-27.
- [19] L.J. Ma, H. Luo, J. Dai, P.W. Carr, *Journal of Chromatography A* **2006**, *1114*, 21-28.
- [20] B.C. Trammell, L.J. Ma, H. Luo, D.H. Jin, M.A. Hillmyer, P.W. Carr, *Analytical Chemistry* **2002**, *74*, 4634-4639.

- [21] H. Luo, P.W. Carr, *Analytical and Bioanalytical Chemistry* **2008**, 391, 919-923.
- [22] B.C. Trammell, L.J. Ma, H. Luo, M.A. Hillmyer, P.W. Carr, *Journal of Chromatography A* **2004**, 1060, 61-76.
- [23] B.C. Trammell, L.J. Ma, H. Luo, M.A. Hillmyer, P.W. Carr, *Journal of the American Chemical Society* **2003**, 125, 10504-10505.
- [24] H. Luo, L.J. Ma, C. Paek, P.W. Carr, *Journal of Chromatography A* **2008**, 1202, 8-18.
- [25] Y. Zhang, Y. Huang, P.W. Carr, *Journal of Separation Science* **2011**, 34, 1407-1422.
- [26] P. Arboleda, *Characterization of Gas Oil Resins using High Performance Liquid Chromatography*, M.Sc. Thesis, 2007.
- [27] V. Davankov, M. Tsyurupa, M. Ilyin, L. Pavlova, *Journal of Chromatography A* **2002**, 965, 65-73.
- [28] L.R.K. Snyder, J.J.; Dolan, J.W., *Introduction to Modern Liquid Chromatography*, 3rd ed., Wiley, Hoboken, New Jersey, 2010.
- [29] M.P. Saksena, Harminder, S. Kumar, *Journal of Physics C-Solid State Physics* **1975**, 8, 2376-2381.
- [30] P. Hemstrom, K. Irgum, *Journal of Separation Science* **2006**, 29, 1784-1821.
- [31] L.R. Snyder, J.W. Dolan, J.R. Gant, *Journal of Chromatography* **1979**, 165, 3-30.
- [32] E. Soczewinski, *Journal of Chromatography A* **2002**, 965, 109-116.
- [33] M.S. Streat, L.A., *Process Safety and Environmental Protection* **1998**, 76(B), 115-126.

- [34] V. Davankov, *Reactive Polymers* **1990**, *13*, 27-42.
- [35] V. Davankov, M. Tsyurupa, *Journal of Chromatography A* **2005**, *1087*, 3-12.
- [36] Purolite, *Hyperscrosslinked Gel-type Polystyrene Resin Application Guide*, Purolite, Purolite, 2004.
- [37] V.A. Davankov, M.P. Tsyurupa, N.N. Alexienko, *Journal of Chromatography A* **2005**, *1100*, 32-39.
- [38] M.P. Tsyurupa, V.A. Davankov, *Reactive & Functional Polymers* **2006**, *66*, 768-779.
- [39] R.E. Paproski, C. Liang, C.A. Lucy, *Energy & Fuels* **2011**, *25*, 4469-4478.

CHAPTER THREE. High Performance Liquid Chromatographic Separations of Gas Oil Samples and Their Hydrotreated Products Using Commercial Normal Phases*

3.1 Introduction

Understanding the composition of petroleum helps make the upgrading and refining of petroleum more efficient, and in turn reduces waste and pollution. Due to the complexity of petroleum samples, it is beneficial to simplify samples prior to analysis, thus increasing the information gained from analysis and making it easier to look at target compounds. High performance liquid chromatography (HPLC) enables users to separate petroleum samples by compound type. When coupled with fraction collectors and high resolution mass spectrometry, identification of individual compounds becomes possible [1].

As in Chapter 2, the goal of this chapter is the HPLC separation of compounds containing nitrogen in petroleum, as these compounds cause problems such as catalyst fouling and corrosion during upgrading and refining processes [1-4]. One way to identify problem-causing nitrogen compounds is to develop separation methods that are selective for N-containing compounds. Our ideal separation would be one where polycyclic aromatic hydrocarbons (PAHs) and other heteroatomic compounds are separated from the nitrogen-containing compounds, and where the N-species are further separated into their two classes (pyrroles and pyridines).

* A version of this chapter has been published. Oro N.E., Lucy C.A.; *Journal of Chromatography A* **2011**, 1218, 7788-7795.

Chapter 2 studied custom hypercrosslinked polystyrene columns for this nitrogen group-type separation. However, for a method to be widely useful in the petroleum industry, the column must be easily available. Thus in Chapter 3 we examine three commercially available columns for their ability to separate nitrogen compounds from other compound classes in gas oil samples. All work in this chapter was done in normal phase or quasi-normal phase mode. The term quasi-normal phase refers to separations carried out under normal phase conditions on stationary phases that lack any specific polar sites for adsorption [5-7].

The first stationary phase studied was 5-HGN, a polymeric hypercrosslinked polystyrene from Purolite that was also studied in Chapter 2 (Figure 3-1A). Hypercrosslinked polystyrene has long polystyrene chains crosslinked with methyl groups on the phenyl rings of polystyrene [7]. HGN is a robust phase tolerant of either normal phase or reversed phase conditions [6, 7]. Hypercrosslinked polystyrene has been used as an HPLC packing material [5-12], as well as in solid phase extraction cartridges and as an adsorbant for concentrating organic compounds [9-11, 13, 14]. HGN has been previously studied in our group for the group-type separation gas oil samples [5], but the separation procedure used a quaternary solvent gradient, and the methods developed did not completely separate nitrogen compounds from PAHs and other polar compounds. This chapter expands on the work performed in Chapter 2, using a 2-propanol/hexane mobile phase and gas oil samples on the HGN phase, along with some additional model compound data.

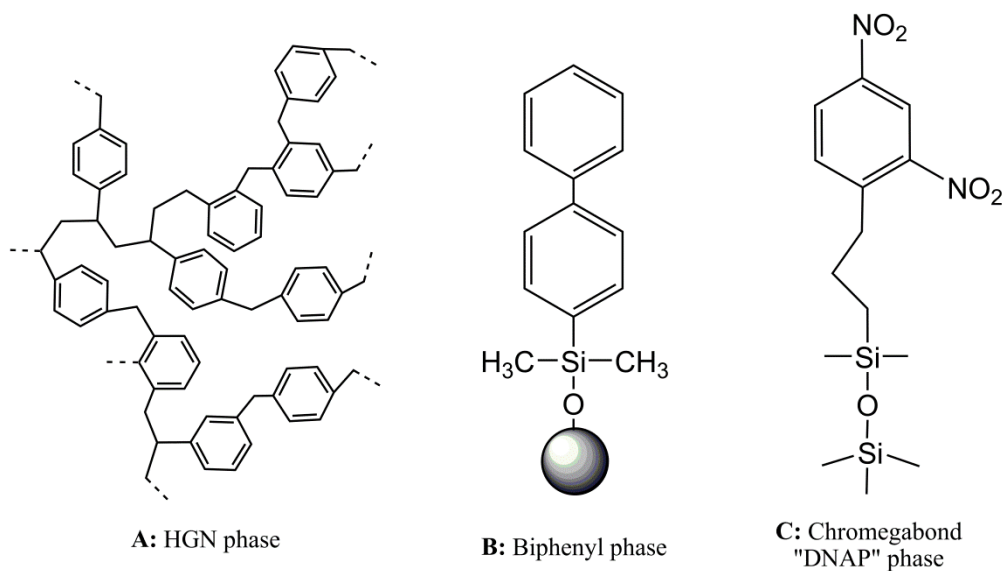


Figure 3-1. Structures of the stationary phases used in this work. A: HGN phase (adapted from reference [7]); B: Biphenyl phase (adapted from reference [15]); C: Chromegabond "DNAP" phase (adapted from references [16, 17]).

The second stationary phase studied was a biphenyl phase from Restek. We selected this phase due to its structural similarity to the HGN phase; the biphenyl phase has two phenyl rings attached to each silica group (Figure 3-1B) [15]. Recent published work for biphenyl phases uses them in a number of reversed phase separations, generally for biological applications [18-21]. The biphenyl phase is not conventionally used in normal phase chromatography or for petroleum analysis.

The final stationary phase studied was the Chromegabond “DNAP” column from ES Industries. The “DNAP” phase is marketed for petroleum analysis, and provides an interesting comparison to our less conventional stationary phases. For the past 30 years, DNAP (dinitroanilinopropyl) phases have been used for the separation of petroleum samples. The most common separation performed is that of PAHs, with separation occurring by ring size [22-29]. When using DNAP to separate polar compounds, the experimental procedures become more complicated. Ternary solvent gradients have been used to elute a polar fraction following the PAH separation [25, 28, 30]. For the separation of coal-derived liquids, a DNAP column was used in a three-column set up for the analysis of aromatics, with polar compounds and aliphatics trapped on separate columns [23]. DNAP columns have also been used as part of LC-MS experiments on petroleum-related samples [25, 28, 30, 31]. The DNAP stationary phase has a dinitrophenyl group attached to the silica via an amine group and a propyl linker chain [17]. The Chromegabond “DNAP” column studied in this paper has a slightly different structure, lacking the amine group between the

dinitrophenyl group and the linker chain (Figure 3-1C), and was named “DNAP” to match with the historical naming of this type of phase [16]. For clarity, when we refer to the Chromegabond dinitrophenyl column, the label “DNAP” will be used, and when referring to previous publications on the dinitroanilinopropyl stationary phase, DNAP without quotations will be used. We wish to maintain the “DNAP” label, as this is the name of the column as it is available from the manufacturer. This is the first study we are aware of that uses this specific variation of the DNAP stationary phase for petroleum analysis.

The ability of these three columns to separate nitrogen group types in petroleum samples is explored herein. Twenty model compounds are used to determine suitability for real samples, and retention data is presented for each column. Separations of both heavy and light gas oil samples are shown. Discussion is focussed on the ability of the phases to separate nitrogen compounds, and their general separation capabilities for gas oil samples.

3.2 Experimental

3.2.1 Apparatus

All experiments were performed on a Varian ProStar HPLC system, as described in Section 2.2.1. UV detection was performed at 254 nm unless otherwise stated.

3.2.2 Chemicals

Optima grade dichloromethane (DCM), 2-propanol (IPA) and hexanes were used as solvents (Fisher Chemicals, Fairlawn, NJ, USA). All chromatographic solutes were prepared as described in Section 2.2.2. An updated list of these compounds for this chapter can be found in Table 3-1.

The HGN column used in this chapter was the same as described in Chapter 2, and the packing procedure can be found in Section 2.2.3. The biphenyl column was an Ultra II Biphenyl (Restek Corporation, Bellefonte, PA, USA), and the “DNAP” column was a Chromegabond “DNAP” phase (ES Industries, West Berlin, NJ, USA). Both columns had 5 μm particles and dimensions of 5.0 x 0.46 cm.

Gas oil samples were provided by Syncrude Canada Ltd. Five samples were analyzed: a light gas oil (LGO) and its hydrotreated product, and a heavy gas oil (HGO) and its hydrotreated products at temperatures T1 and T2. The LGO samples were prepared at 50 mg/mL in hexane, and the HGO samples were prepared at 50 mg/mL in 50/50 v/v% DCM/hexane to permit full dissolution. Table 3-2 lists the bulk composition properties of these samples.

3.2.3 Calculations

Retention times were determined using Varian’s Star Chromatography Workstation software, version 6.20.

Table 3-1. Model compounds used in this chapter.

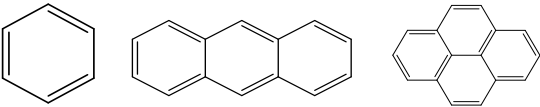
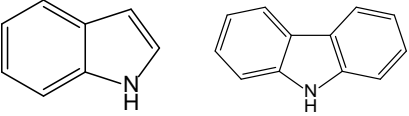
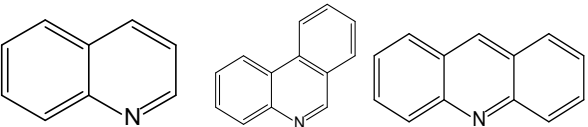
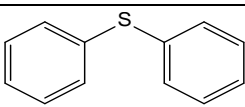
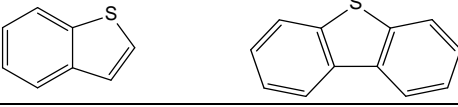
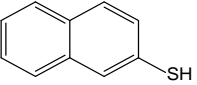
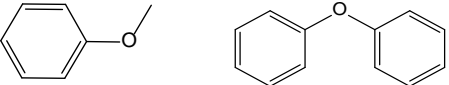
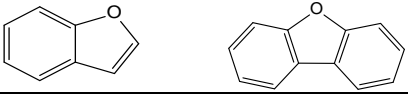

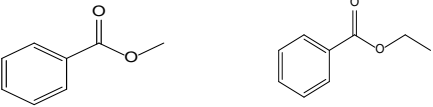
Group	Compounds	Structure
PAH	benzene (1) anthracene (2) pyrene (3)	
N, pyrrole	indole (4) carbazole (5)	
N, pyridine	quinoline (6) phenanthridine (7) acridine (8)	
S, sulfide	phenyl sulfide (9)	
S, thiophene	benzothiophene (10) dibenzothiophene (11)	
S, thiol	2-naphthalenethiol (12)	
O, ether	anisole (13) phenyl ether (14)	
O, furan	2,3-benzofuran (15) dibenzofuran (16)	
O, ketone	acetophenone (17) propiophenone (18)	
O, ester	methyl benzoate (19) ethyl benzoate (20)	

Table 3-2. Bulk properties of the light and heavy gas oil samples, as provided by Syncrude Canada.

Sample	Density (g/mL)	Avg wt% C	Avg wt% H	S (ppm)	N (ppm)	Simulated Distillation Results (°C)		
						5% mass	50% mass	95% mass
LGO feed	0.91	85.6	11.4	24000	1240	202.5	313.5	438.5
LGO first stage product	0.87	87.3	12.7	258	23	174.5	296	425
HGO feed	0.99	84.6	9.8	36800	3490	341.5	449	623
HGO T1 product	0.94	87.4	11.4	5060	2140	280.5	423	534.5
HGO T2 product	0.93	87.4	11.7	3040	1640	256.5	417	530.5

Dead times were determined by the refractive index peak caused by injecting dichloromethane with hexane as the mobile phase, or by injection of hexane in an isopropyl alcohol or dichloromethane mobile phase. Retention factors (k) were calculated using Equation 1-5.

3.3 Results and Discussion

The stationary phases used in this chapter are all commercially available, selected with the dual purpose of achieving nitrogen group-type separation as well as to look at the different columns possible for petroleum analysis. Figure 3-1 shows the structures of the stationary phases. The HGN phase was shown by previous work in our group [5] to have unique selectivity for different group-types in petroleum samples, and it was a logical choice to explore it further. HGN is a highly crosslinked polymeric phase of polystyrene [7], containing many aromatic rings (Figure 3-1A). We also studied a biphenyl phase (Figure 3-1B), to see if the selectivity observed on the HGN phase could be attributed to the aromatic rings. Finally, we also chose the Chromegabond “DNAP” column, as this column is sold specifically for petroleum analysis, and would provide an interesting comparison to our less traditional phases. It is worth further emphasis that the “DNAP” column examined in this chapter is not the same stationary phase structure as the DNAP (dinitroanilinophenyl) columns in the literature [16]. The Chromegabond “DNAP” contains the dinitrophenyl functional group, but lacks the amino group linking the alkyl chain to the phenyl ring (Figure 3-1C).

3.3.1 HGN: Commercial Hypercrosslinked Polystyrene

3.3.1.1 Model Compounds

When hypercrosslinked polystyrene is used with non-aqueous solvents, we refer to it as a quasi-normal phase separation, in that while the column behaves in a normal phase fashion there are no polar groups on the stationary phase that would act as specific adsorption sites [5-7]. The dominant retention mechanism on HGN is π - π adsorption, where π electrons in solutes interact with π electrons on the aromatic groups of the stationary phase [5, 7, 8, 14, 32]. Chapter 2 described work with the HGN phase where DCM was used as the strong solvent for the elution of model petroleum compounds. The data from Chapter 2 is used as a comparison against the new experiments in this chapter. When DCM was used as a strong solvent, the π - π mechanism was dominant, with no group-wise separation of components and very strong retention of pyridine compounds. As shown in Table 3-3, the HGN phase separated pyrroles from the other model compounds using a 25% DCM in hexane mobile phase, but the k for pyridines exceeded 65. When using a weaker mobile phase (5% DCM in hexane), the pyrroles began to co-elute with oxygen-containing compounds and the pyridine compounds were not eluted at all. For these reasons this study used isopropyl alcohol (IPA) as a strong solvent.

IPA elutes all of the model petroleum compounds studied (Table 3-3). When using 20% IPA the retention of the PAHs (benzene, anthracene and pyrene) increases with ring size, indicating that π - π interactions between the compounds and the stationary phase are occurring.

Table 3-3. Retention factors of model compounds on the HGN column under isocratic conditions of 20% isopropyl alcohol (IPA) in hexane and 25% dichloromethane (DCM) in hexane. The DCM data is reproduced from Chapter 2, and included for completeness.

Compound	k			
	5% IPA	20% IPA	5% DCM	25% DCM
benzene	1.0	1.2	0.8	0.28
anthracene	15.1	16.0	13.0	2.7
pyrene	22.9	25.3	21.3	4.2
carbazole	-	25.3	-	20.8
indole	32.7	11.7	36.1	10.2
phenanthridine	-	27.9	-	>65
acridine	-	22.7	-	>65
acetophenone	-	6.0	37.6	6.5
propiophenone	-	4.6	28.7	3.3
Me-benzoate	-	4.0	13.1	2.7
dibenzofuran	-	8.2	6.7	1.8
dibenzothiophene	-	14.5	12.0	2.8

The same trend is observed with pyrroles; carbazole has an additional aromatic ring and its k value is 25.3 compared to 11.7 for indole. The greater retention of heteroatomic compounds relative to the corresponding PAHs indicates that retention is due to their heteroatom as well as the aromatic π electrons. Anthracene and acridine have the same ring structure (Table 3-1), but acridine has a k value of 22.7, while anthracene's k is 16.0. The combination of retention based on π - π interactions and heteroatoms means that there is no group-wise separation.

The solvent selectivity triangle developed by Snyder, Carr and Rutan [33] allows comparison of IPA and DCM as solvents on the HGN phase. DCM has very strong dipolar character and no basic character. In contrast, IPA has very little dipolar character and moderate basic character. The basic character of IPA makes elution of pyridines (basic nitrogen compounds) possible, whereas they are very strongly retained with DCM. When IPA is used as a strong solvent instead of DCM, there is a dramatic increase in the retention of PAHs. With 25% DCM, the k value of pyrene is 4.2, and when a similar mobile phase of 20% IPA is used, the k increases 6-fold to 25.3. The retention data indicates that the dipolar character of DCM is much more effective in eluting PAHs off the HGN stationary phase. The increased retention of PAH compounds with the use of IPA does not allow for their isolation from polar compounds, but the benefit of eluting all groups outweighs this disadvantage. The same increase in retention is also observed for pyrroles and the oxygen and sulphur standards; however for the pyridine compounds, retention is greatly reduced in changing the mobile phase

from DCM to IPA. This data indicates that the nitrogen interaction with the stationary phase is dominant for pyridine-type compounds, and best disrupted by IPA.

It is also interesting to note that decreasing IPA (5% vs. 20%) causes a decrease in retention for the PAHs benzene, anthracene and pyrene (k value of pyrene changes from 25.3 to 22.9, and anthracene changes from 16.0 to 15.1). This is contrary to what we would expect from decreasing the percentage of “strong solvent”. For the same change in mobile phase, the retention of indole increases (k value increases from 11.7 to 32.7), giving more evidence that IPA mostly acts to disrupt heteroatom-stationary phase interactions.

3.3.1.2 Gas Oil Samples

A 30 minute linear gradient with 5-50% IPA in hexane was developed and optimized for the separation of PAHs and nitrogen-containing compounds. This gradient was then used to analyze different gas oil samples. Figure 3-2 shows the separation of two samples, a light gas oil (upper black trace) and its hydrotreated product (lower grey trace) on the IPA gradient. Dashed lines corresponding to the elution times of three PAHs (benzene, anthracene and pyrene), two sulphur compounds (phenyl sulfide and dibenzothiophene), two pyridines (quinoline and acridine) and two pyrroles (indole and carbazole) are shown. Figure 3-3 is the separation of a heavy gas oil (black) and its two hydrotreated products, at temperatures T1 (red) and T2 (blue), with the same model compound markers. No group-wise separation is evident in either figure.

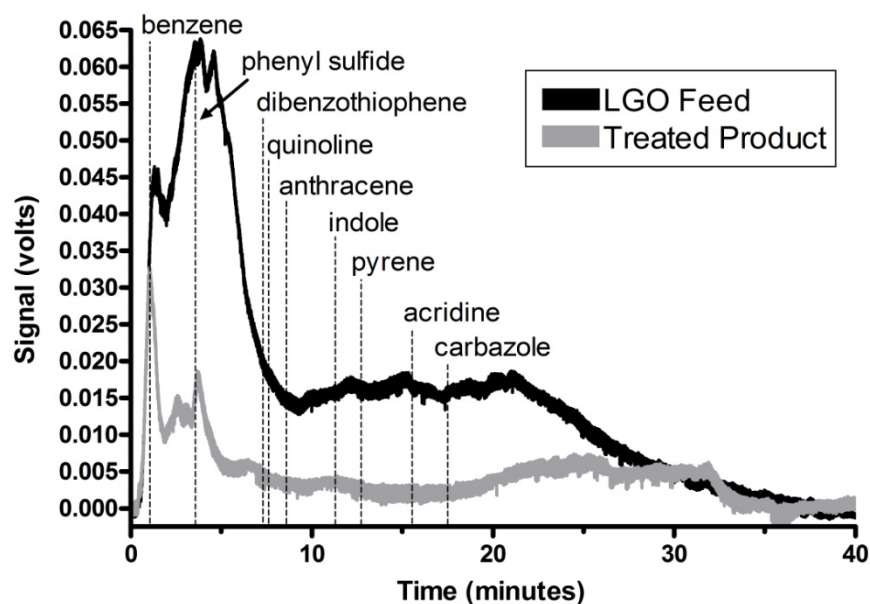


Figure 3-2. Chromatograms of a light gas oil (upper trace, black) and its first stage hydrotreated product (lower trace, grey) on the HGN column. Dashed lines indicate retention time of standards on the same gradient. Group-wise separation benchmarks are not possible due to overlap of the group-types. Conditions: linear gradient (30 min), 5-50% IPA in hexane, 15 minutes re-equilibration time following the gradient (5% IPA), $T = 35^{\circ}\text{C}$, flow rate 1.0 mL/min, detector wavelength 254 nm.

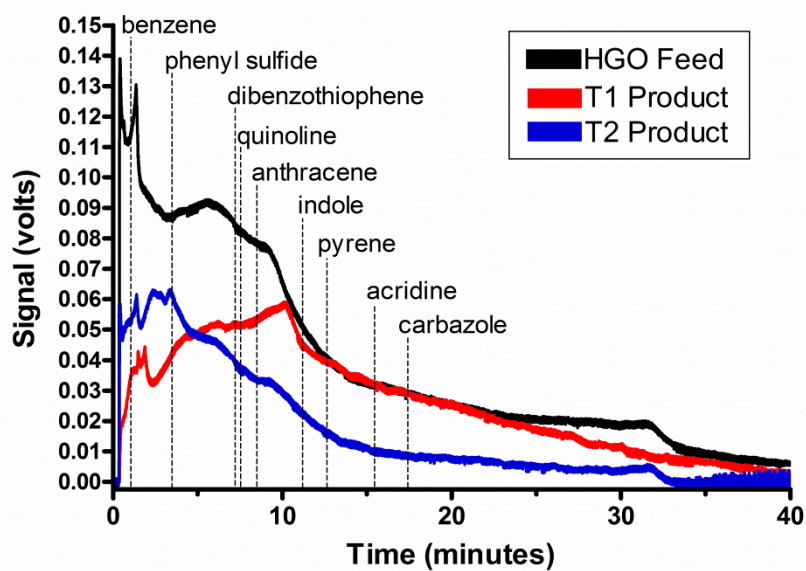


Figure 3-3. Chromatograms of a heavy gas oil (top trace, black), its hydrotreated product at T1 (red), and at T2 (blue) on the HGN column. Dashed lines indicate retention time of standards on the same gradient. Group-wise separation benchmarks are not possible due to overlap of the group-types. Conditions: linear gradient (30 min), 5-50% IPA in hexane, 15 minutes re-equilibration time following the gradient (5% IPA), $T = 35^{\circ}\text{C}$, flow rate 1.0 mL/min, detector wavelength 254 nm.

However the HGN column does spread out the compounds within the samples. With the use of a fraction collector, this provides the means to simplify the sample into fractions of varying composition. The HGN phase separates via a π - π mechanism, with significant contribution from heteroatoms in the molecule. Molecules elute roughly according to their number of rings, as well as heteroatoms present, i.e., early fractions have molecules with fewer rings and heteroatoms, and later fractions have molecules with more rings and heteroatoms. This is confirmed by the disappearance of the UV absorbance signal in the early region of the chromatogram (0-10 minutes) and a slight rise in signal at later elution times (10-20 minutes) when higher wavelengths corresponding to the absorbance of large PAHs are used for detection (Figure 3-4).

Figures 3-2 and 3-3 give a quick visual assessment of the amount of aromatic products removed by different hydrotreating processes. In the light gas oil (Figure 3-2), the majority of its compounds lie between benzene and anthracene, with low levels of nitrogen present (Table 3-2). When the light gas oil was hydrotreated almost all of the later eluting larger molecules are removed, along with most of the nitrogen and sulphur content, as would be expected [34]. When comparing light gas oils to heavy gas oils, it is instructive to note the difference in scales between Figures 3-2 and 3-3. A heavy gas oil has a higher boiling range (321-426°C) than a light gas oil (215-321°C) [35] and as such we would expect to see a greater number of larger or heteroatom-containing compounds in the heavy gas oil.

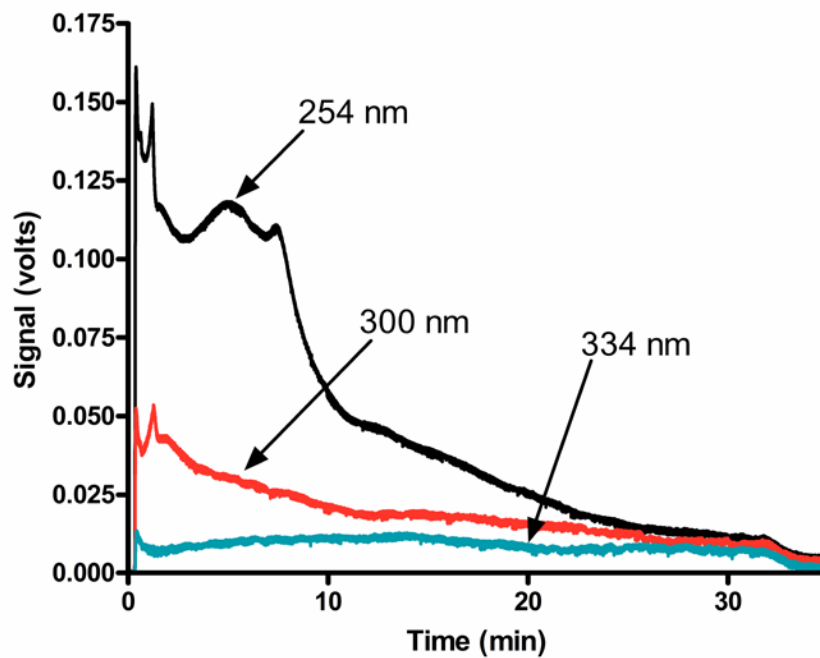


Figure 3-4. Chromatograms of a heavy gas oil on the HGN column with different detection wavelengths. Top black trace: 254 nm, middle red trace: 300 nm, lower blue trace: 334 nm. Higher wavelengths correspond to absorption maxima for larger PAH compounds. Conditions: linear gradient (30 min), 5-50% IPA in hexane, 15 minutes re-equilibration time following the gradient (5% IPA), $T = 35^{\circ}\text{C}$, flow rate 1.0 mL/min.

The heavy gas oil has a greater intensity of compounds up to the pyrene marker, indicating more large and heteroatom-containing molecules. The two different HGO hydrotreated products are interesting, as they are both removing a notable number of molecules, but their different profiles indicate that the temperature of the hydrotreating process affects the types of compounds removed. The T2 process is more effective at removing sulphur and nitrogen containing compounds (Table 3-2), while the T1 process is more effective for removing smaller and less polar compounds. Studies on similar HGO samples have also found that hydrotreating temperature can affect compound removal, with higher temperatures causing increased removal of both PAHs and heteroatom compounds [36].

Studies with the model compounds (Section 3.1.1) indicated that IPA was effective at eluting all compounds. Similarly, with IPA the HGN column could reproducibly analyze the gas oil samples. The retention of anthracene was found to change by only 1% during the course of analyzing gas oil samples. This shows that the HGN phase tolerates these heavy samples and that retention is not dramatically altered by analysis of petroleum samples. Fractionating samples on the HGN column reduces the complexity of samples for further analysis such as petroleomics [1, 37], and the chromatograms give a visual comparison of the samples compared to each other or before/after various treatment steps. These benefits are notable, despite HGN's inability to separate compounds in a group-wise fashion. Separations of three different concentrations of the HGO treated at temperature T1 on HGN showed that at concentrations of less than 50 mg/mL, we

begin to lose the features of the chromatogram, and are unable to see sufficient signal for a separation (Figure 3-5). Thus, we need higher concentrations of gas oil samples on this stationary phase to discern the separation occurring.

3.3.2 Restek Biphenyl Phase

The biphenyl phase is designed for reversed phase HPLC. However we felt that given the structural similarity to HGN (Figure 3-1A, B) it would be an interesting column to explore. Retention on the HGN column is dominantly by π - π interactions [15, 20]. The biphenyl phase retains via π - π and dispersive interactions [15] under reversed phase conditions, making it an ideal comparison.

Under quasi-normal phase conditions, the biphenyl phase showed very little retention for the model compounds tested, except for the pyridines. Table 3-4 lists retention factors for model compounds on the biphenyl phase, in a weak mobile phase of 5% DCM in hexane. The two pyridine compounds, quinoline and phenanthridine, have retention factors close to 20, while the remaining compounds are ≤ 1 . Pyridine irreversibly adsorbs onto bare silica under normal phase conditions [38], and so the pyridine retention observed may be due to interaction with the underlying silanols on the silica particles, rather than with the biphenyl phase. While these preliminary results indicate that this phase may be a good candidate for the isolation of pyridine compounds from petroleum, chromatograms of gas oil samples show only large dead-time peaks and no further separation.

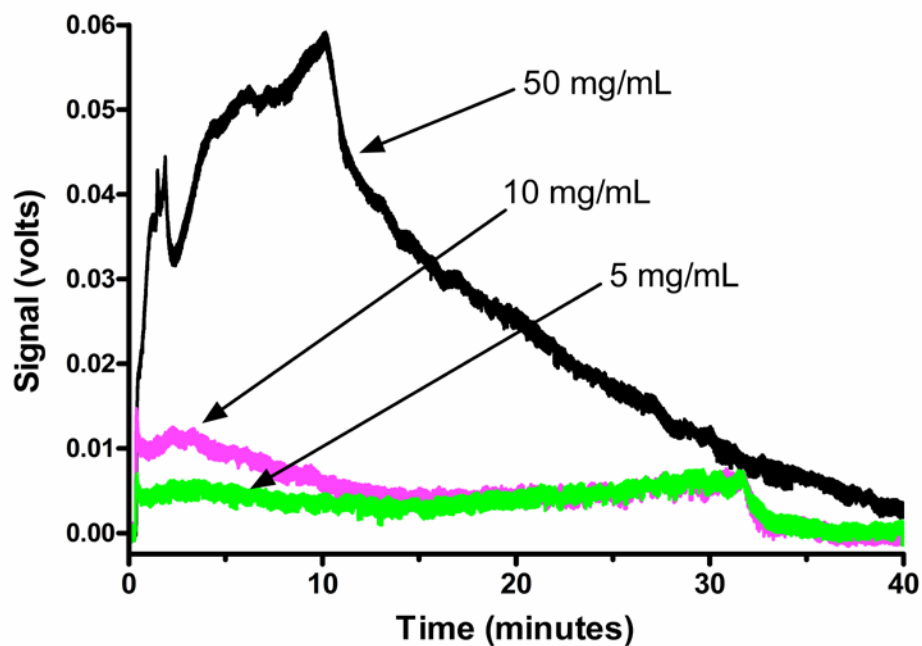


Figure 3-5. Chromatograms of a heavy gas oil treated product at temperature T1 on the HGN column at three different concentrations. Top black trace: 50 mg/mL; middle pink trace: 10 mg/mL; bottom green trace: 5 mg/mL. Conditions: linear gradient (30 minutes), 5-50% IPA in hexane, 15 minutes re-equilibration time following the gradient (5% IPA), T = 35°C, flow rate 1.0 mL/min, detector wavelength 254 nm.

Table 3-4. Retention factors of model compounds on the Restek biphenyl column.*

Compound	k
benzene	0.02
anthracene	0.2
pyrene	0.3
carbazole	1.1
indole	0.9
quinoline	23.0
phenanthridine	19.7
phenyl sulfide	0.1
2-naphthalenethiol	0.3
methyl benzoate	0.4
benzofuran	0.1
propiophenone	0.5

* The mobile phase is 5% dichloromethane in hexane.

The experiments on the biphenyl column indicate that hypercrosslinked polystyrene is unique in both its selectivity and versatility. The HGN column can be used under both reversed and quasi-normal phase conditions, while the biphenyl does not appear to exhibit quasi-normal phase retention of polar aromatics. The π - π retention on HGN is a characteristic of the phase as a whole, and not just of the aromatic rings. If the aromatic rings were the sole cause of the selectivity and retention on HGN, we likely would have seen similar trends on the biphenyl column.

3.3.3 “DNAP”: Dinitrophenyl Phase

3.3.3.1 Model Compounds

The “DNAP” phase discussed in this section is sold for the analysis of petroleum samples, and is expected to show interesting selectivity for model petroleum compounds. It also serves as a useful comparison to the non-conventional phases, HGN and biphenyl. We would like to reiterate that the “DNAP” phase discussed here is not identical in structure to the DNAP phases in the literature (Section 3.1), which may account for the different selectivity observed.

Retention of model compounds under varying concentrations of DCM in hexane was studied. As would be expected for a column designed for petroleum analysis, the “DNAP” phase does not irreversibly retain any of the model compounds. Interestingly, our experiments indicate that this phase has low retention for all model compounds not containing nitrogen. The selectivity for

nitrogen-containing compounds is beneficial for the goals of our project, but unexpected in light of the literature for previous DNAP phases. Much of the literature for the “traditional” DNAP phases uses this stationary phase with mobile phases of a linear alkane (hexane or pentane) with varying percentages of DCM to separate PAHs based on ring size [22-29]. For example, Nondek and Chvalovsky saw very similar retention for indole, carbazole, pyrene and anthracene ($k < 0.3$) using pure DCM with 0.5% (v/v) IPA to suppress tailing [39]. However the low retention may have masked selectivity differences.

Figure 3-6 graphically illustrates our isocratic retention results. The three PAHs (compounds 1-3) show low retention under all solvent conditions, with $k < 4$. When compared to the nitrogen compounds (4-8), the selectivity of the phase for nitrogen is apparent. With 25% DCM, the nitrogen-containing compounds experience retention with a k value approaching 10, and going up to almost 90 with 5% DCM. The sulphur and oxygen standards (compounds 9-12 and 13-20, respectively) exhibit similar retention behavior to the PAHs, with no $k > 10$, regardless of the mobile phase composition. Based on previous DNAP literature we expected to see the oxygen and sulphur compounds behaving similar to the nitrogen compounds, as all polar groups often co-eluted on a DNAP column [23, 25, 28, 30]. However the selective interaction of nitrogen compounds with the phase does suit our analysis perfectly – by decreasing the DCM and subsequently the mobile phase strength, we are able to resolve the nitrogen compounds from the rest of the compounds in the sample.

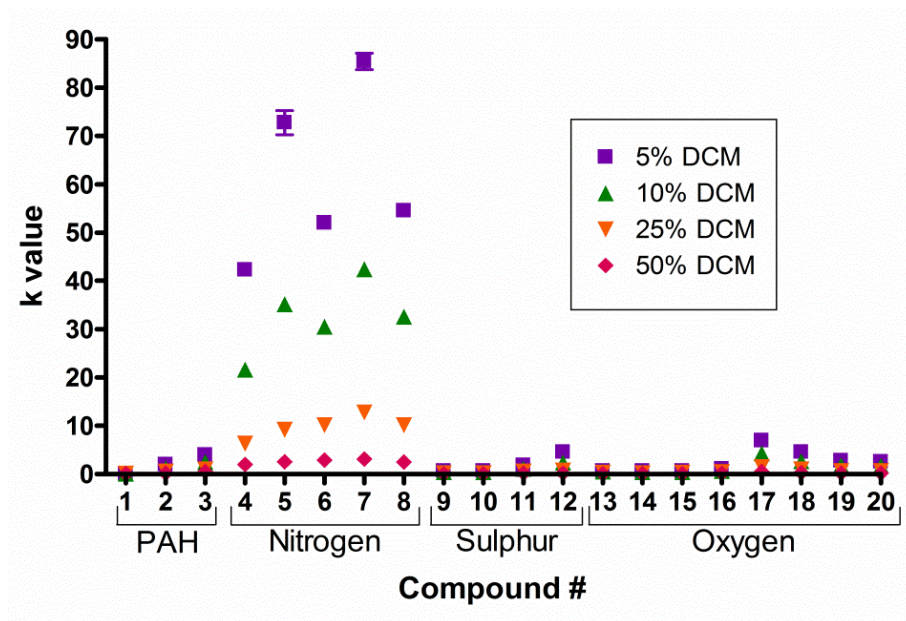


Figure 3-6. Retention factors for standard compounds on the “DNAP” column with changing solvent conditions. Compounds 1-3 are PAHs, 4-9 nitrogen compounds, 10-13 sulphur compounds, 14-21 oxygen compounds. Numbering corresponds to Table 3-1. Conditions: “DNAP” column, varying % DCM in hexane, T = 35°C, flow rate 1.0 mL/min, detection wavelength 254 nm.

Figure 3-7 shows a chromatogram of a mixture of PAHs, pyrrole and pyridine compounds, analyzed under a step gradient of 5-100% DCM in hexane on the “DNAP” column. Under the gradient there is a better separation of benzene, anthracene and pyrene (PAHs), which is more consistent with what we expected of the phase. We also get resolution of the nitrogen compounds from the PAHs. The nitrogen groups (pyrroles and pyridines) are not separated, with indole and carbazole (pyrroles) co-eluting in the same region as quinoline, acridine and phenanthridine (pyridines). This separation of nitrogen compounds from other compounds in the sample is excellent, allowing for isolation and further analysis if desired. However if one wishes to analyze oxygen or sulphur containing compounds or PAHs using this stationary phase, DCM as the strong solvent may not be the best choice.

The work done on the new “DNAP” phase demonstrates unique selectivity when compared to traditional DNAP. Traditional DNAP elutes all polar groups together [23, 25, 28, 30], whereas the new “DNAP” shows stronger retention of only the nitrogen-containing compounds. The separations demonstrated in this chapter also show that while nitrogen compounds have stronger retention than PAHs, allowing them to be separated as a group, it is not difficult to elute them off the phase with a binary solvent gradient. Traditional DNAP often required the use of a ternary solvent gradient to elute the polar fraction [25, 28, 30]. For our goals of separating nitrogen compounds, the new “DNAP” works better than traditional DNAP.

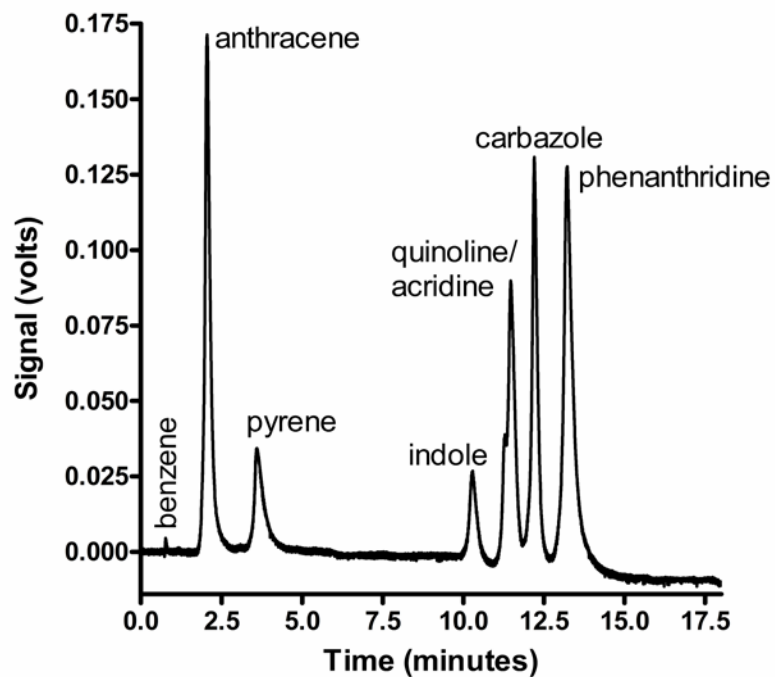


Figure 3-7. Separation of PAHs and N-containing standards on the “DNAP” phase. Conditions: step gradient, 5-100% dichloromethane in hexane, 20%/4 min steps, 15 minutes re-equilibration time following the gradient (5% DCM); T = 35°C, flow rate 1.0 mL/min, detection wavelength 254 nm.

However, if the goal is separation of PAHs, traditional DNAP would be more appropriate, as it shows more separation of PAH compounds than does the new “DNAP” [22-29]. The separation of nitrogen groups from PAHs on the new “DNAP” has not been shown anywhere else.

3.3.3.2 Gas Oil Samples

The “DNAP” column was used to analyze the same gas oil samples analyzed on the HGN column. Figure 3-8 shows an LGO and its hydrotreated product and Figure 3-9 shows a chromatogram of an HGO with its two hydrotreated products. As with Figures 3-2 and 3-3, the UV traces have been overlaid to show how the sample changes following the hydrotreating process. The chromatograms of the HGO and its products show a series of distinct peaks, which is different from the continuous elution of compounds seen on the HGN column. The HGN column also shows quite a difference between the two different refining stages of the heavy gas oils, while the two traces are nearly identical on the “DNAP” column. This speaks to the differences in retention and selectivity between these two phases.

The group-wise separation on “DNAP” allows us to separate the chromatograms into regions with and without nitrogen (shown in Figure 3-9 by dotted vertical lines). The large peak on the HGO feed around 7.5 is markedly removed with hydrotreating at both temperatures, and we have yet to determine the identity of this peak.

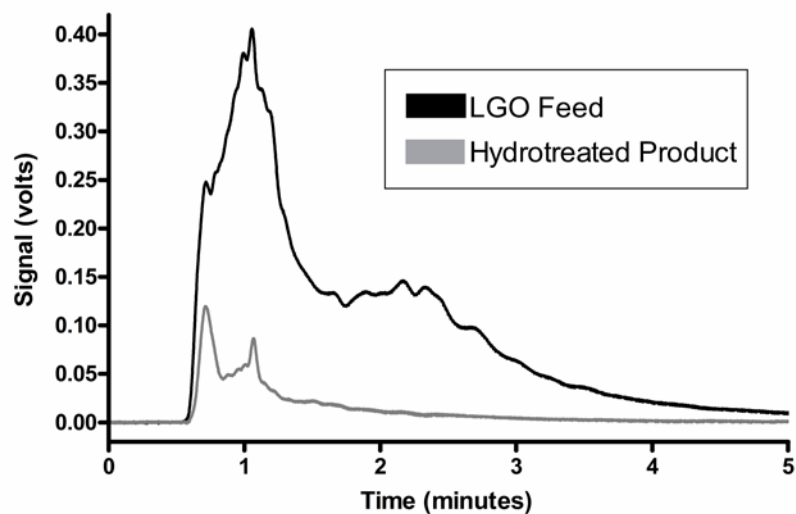


Figure 3-8. Chromatogram of a light gas oil (top trace, black) and its first stage hydrotreated product (lower trace, grey); “DNAP” column. The chromatogram has been truncated after five minutes due to a very low absorbance signal and no discernible peaks. Conditions: “DNAP” column, step gradient, 5-100% dichloromethane in hexane, 20%/4 min steps, 15 minutes re-equilibration time following the gradient (5% DCM); T = 35°C, flow rate 1.0 mL/min, detection wavelength 254 nm.

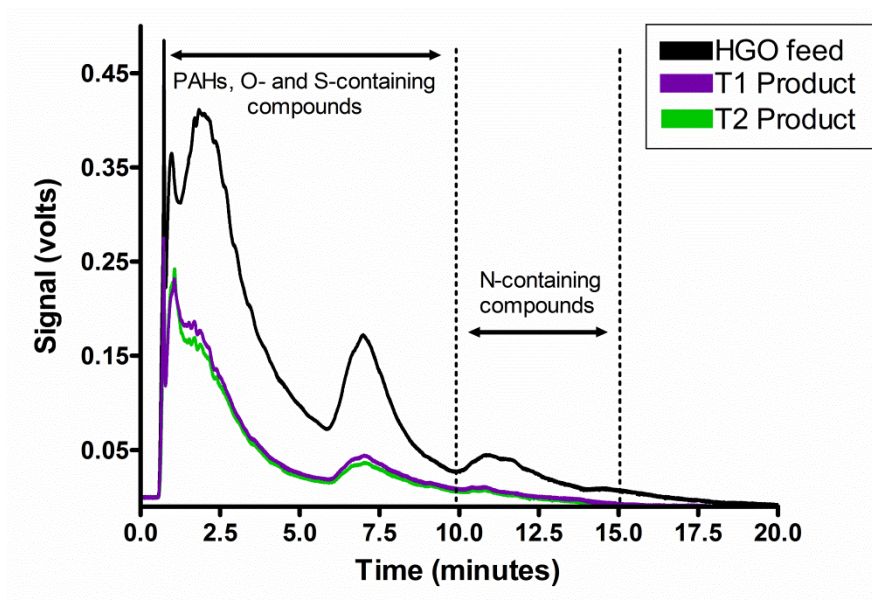


Figure 3-9. Chromatograms of a heavy gas oil (top trace, black), its hydrotreated product at T1 (purple), and at T2 (green) on the “DNAP” column. Conditions: step gradient, 5-100% dichloromethane in hexane, 20%/4 min steps, 15 minutes re-equilibration time following the gradient (5% DCM); T = 35°C, flow rate 1.0 mL/min, detection wavelength 254 nm.

Preliminary high resolution mass spectrometric (Fourier Transform Ion Cyclotron Resonance) data indicates that alkylated polar compounds contribute to this peak, and UV absorbance data shows a range in absorbance from approximately 230 to 400 nm, corresponding to multiple aromatic rings. These chromatograms also allow us to look specifically at the nitrogen compounds in a sample; the region is distinct, and there is a peak in the HGO feed between 10 and 15 minutes that is almost removed after hydrotreating. Hydrotreating is designed to do just this [34], further confirming the identity of the peak. The chromatograms of an LGO and its hydrotreated product in Figure 3-8 qualitatively show that the majority of the compounds in these types of samples are likely PAHs or non-aromatic structures that are not detected by the UV detector. There are no peaks or signal past five minutes, or in the region where we would expect to see nitrogen-containing compounds. The chromatograms allow us to quickly see that there are likely no or very low levels of nitrogen compounds in these samples. Figure 3-8 also had a number of small distinct peaks likely containing different PAHs that could be isolated for further analysis if so desired.

The “DNAP” column is also tolerant of petroleum samples. Retention of toluene (manufacturer recommended) was checked before, between and after analysis of many gas oil samples, including the heavy gas oil feed. Over the course of all analyses, the retention time of the standard peak only shifted by 1%, indicating that the gas oil samples did not significantly change the chemistry of the stationary phase during analysis. Separations of three different concentrations of the HGO treated product at temperature T1 on “DNAP” showed that the

concentration of 50 mg/mL used in this work was not overloading the column, and was sufficient to show features of the separation (Figure 3-10).

3.4 Conclusions

Three different commercially available stationary phases were characterized for the analysis of petroleum samples. The HGN column separates samples based on ring size, with a strong contribution from heteroatom content. HGN is useful for simplifying samples based on number of rings and heteroatoms for further analysis, but it cannot achieve a group-wise separation. The biphenyl stationary phase had very little retention of model petroleum compounds, retaining only pyridine-type compounds. Analysis of gas oils on this phase (not shown) showed no separation of components. The “DNAP” column has the best performance for the study of nitrogen groups, as it resolves nitrogen-containing compounds from all other compounds found in petroleum. This stationary phase meets the goals of this chapter. The limitation of the “DNAP” column is its inability to resolve pyrroles from pyridines. Recent publications using model petroleum compounds [40, 41] indicate that research groups are moving towards synthesizing their own model compounds containing a variety of alkylation and ring size. Once such compounds are commercially available, studies of the effect of alkylation and larger ring structures on retention for the “DNAP” and HGN stationary phases would be interesting.

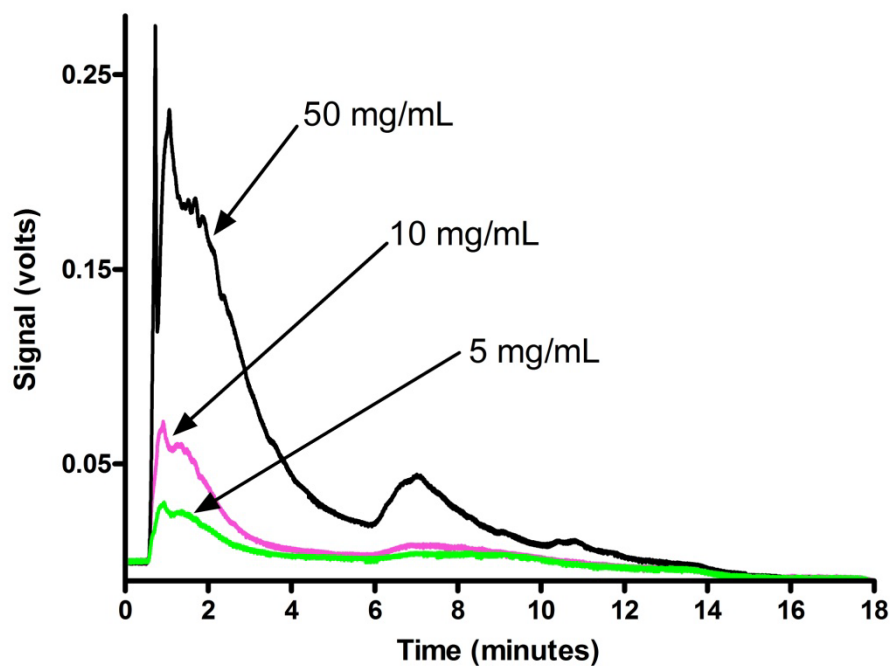


Figure 3-10. Chromatograms of a heavy gas oil treated product at temperature T1 on the “DNAP” column at three different concentrations. Top black trace: 50 mg/mL; middle pink trace: 10 mg/mL; bottom green trace: 5 mg/mL. Conditions: “DNAP” column, step gradient, 5-100% dichloromethane in hexane, 20%/4 min steps, 15 minutes re-equilibration time following the gradient (5% DCM); T = 35°C, flow rate 1.0 mL/min, detection wavelength 254 nm.

3.5 References

- [1] R.P. Rodgers, T.M. Schaub, A.G. Marshall, *Analytical Chemistry* **2005**, *77*, 20A-27A.
- [2] J. Mao, C.R. Pacheco, D.D. Traficante, W. Rosen, *Journal of Chromatography A* **1994**, *684*, 103-111.
- [3] S.K. Panda, W. Schrader, J.T. Andersson, *Journal of Chromatography A* **2006**, *1122*, 88-96.
- [4] J.R. Woods, J. Kung, G. Pleizier, L.S. Kotlyar, B.D. Sparks, J. Adjaye, K.H. Chung, *Fuel* **2004**, *83*, 1907-1914.
- [5] P.H. Arboleda, *Characterization of Gas Oil Resins Using HPLC*, M.Sc. Thesis, 2007.
- [6] V. Davankov, C.S. Sychov, M.M. Ilyin, K.O. Sochilina, *Journal of Chromatography A* **2003**, *987*, 67-75.
- [7] C.S. Sychov, M.M. Ilyin, V.A. Davankov, K.O. Sochilina, *Journal of Chromatography A* **2004**, *1030*, 17-24.
- [8] N.A. Penner, P.N. Nesterenko, M.M. Ilyin, M.P. Tsyurupa, V.A. Davankov, *Chromatographia* **1999**, *50*, 611-620.
- [9] V. Davankov, M. Tsyurupa, M. Ilyin, L. Pavlova, *Journal of Chromatography A* **2002**, *965*, 65-73.
- [10] N.A. Penner, P.N. Nesterenko, A.V. Khryashevsky, T.N. Stranadko, O.A. Shpigun, *Mendeleev Communications* **1998**, 24-27.
- [11] X. Zhang, S.H. Shen, L.Y. Fan, *Journal of Materials Science* **2007**, *42*, 7621-7629.
- [12] N.A. Penner, P.N. Nesterenko, *Analyst* **2000**, *125*, 1249-1254.

- [13] M.P. Tsyurupa, M.M. Ilyin, A.I. Andreeva, V.A. Davankov, *Fresenius Journal of Analytical Chemistry* **1995**, 352, 672-675.
- [14] C.S. Sychov, V.A. Davankov, N.A. Proskurina, A.J. Mikheeva, *LC GC Europe* **2009**, 22, 20.
- [15] Restek, Chromatography Products, 2011-2012, p.154.
- [16] M. Przybyciel, Personal Communication, 2010.
- [17] L. Nondek, R. Ponec, *Journal of Chromatography* **1984**, 294, 175-183.
- [18] C. Debouit, A. Bazire, G. Lallement, D. Daveloose, *Journal of Chromatography B* **2010**, 878, 3059-3066.
- [19] D.K. Kim, E.J. Park, J.H. Jeong, S.H. Jeon, E.J. Kim, H.J. Shim, J.I. Lim, H.S. Lee, *Archives of Pharmacal Research* **2009**, 32, 1743-1748.
- [20] R. Lake, R. Wittrig, *LC GC North America* **2006**, 74-74.
- [21] R.A. Miller, R. Reimschuessel, M.C. Carson, *Journal of Chromatography B-Analytical Technologies in the Biomedical and Life Sciences* **2007**, 852, 655-658.
- [22] J.S. Thomson, J.W. Reynolds, *Analytical Chemistry* **1984**, 56, 2434-2441.
- [23] D.M. Padlo, R.B. Subramanian, E.L. Kugler, *Fuel Processing Technology* **1996**, 49, 247-258.
- [24] L. Carbognani, *Journal of Chromatography A* **1994**, 663, 11-26.
- [25] C.S. Hsu, K. Qian, *Energy & Fuels* **1993**, 7, 268-272.
- [26] P. Ghosh, B. Chawla, P.V. Joshi, S.B. Jaffe, *Energy & Fuels* **2006**, 20, 609-619.

- [27] L. Nondek, M. Minarik, J. Malek, *Journal of Chromatography* **1979**, *178*, 427-434.
- [28] C.S. Hsu, M.A. McLean, K. Qian, T. Aczel, S.C. Blum, W.N. Olmstead, L.H. Kaplan, W.K. Robbins, W.W. Schulz, *Energy & Fuels* **1991**, *5*, 395-398.
- [29] P.L. Grizzle, J.S. Thomson, *Analytical Chemistry* **1982**, *54*, 1071-1078.
- [30] C.S. Hsu, K.N. Qian, W.K. Robbins, *HRC-Journal of High Resolution Chromatography* **1994**, *17*, 271-276.
- [31] Z. Liang, C.S. Hsu, *Energy & Fuels* **1998**, *12*, 637-643.
- [32] N.E. Oro, C.A. Lucy, *Journal of Chromatography A* **2010**, *1217*, 6178-6185.
- [33] L.R. Snyder, P.W. Carr, S.C. Rutan, *Journal of Chromatography A* **1993**, *656*, 537-547.
- [34] J.G. Speight, *The Chemistry and Technology of Petroleum*, 4th ed., CRC Press, 2007.
- [35] J.H. Gary, G.E. Handwerk, *Petroleum Refining: Technology and Economics*, 5th ed., CRC Press, 2007.
- [36] M. Mapiour, V. Sundaramurthy, A.K. Dalai, J. Adjaye, *Fuel* **2010**, *89*, 2536-2543.
- [37] A.G. Marshall, R.P. Rodgers, *Accounts of Chemical Research* **2004**, *37*, 53-59.
- [38] R.E. Paproski, C. Liang, C.A. Lucy, *Energy & Fuels* **2011**, *25*, 4469-4478.
- [39] L. Nondek, V. Chvalovsky, *Journal of Chromatography* **1984**, *312*, 303-312.
- [40] M.R. Gray, A.H. Alshareef, K. Azyat, R.R. Tykwinski, *Energy & Fuels* **2010**, *24*, 3998-4004.

[41] H. Sabbah, A.L. Morrow, A.E. Pomerantz, O.C. Mullins, X.L. Tan, M.R. Gray, K. Azyal, R.R. Tykwinski, R.N. Zare, *Energy & Fuels* **2010**, *24*, 3589-3594.

CHAPTER FOUR. Sample Handling and Contamination Encountered When Coupling Offline High Performance Liquid Chromatography Fraction Collection of Petroleum Samples to Fourier Transform Ion Cyclotron Resonance Mass Spectrometry*

4.1 Introduction

High performance liquid chromatography (HPLC) has the ability to separate compound classes found in petroleum samples, but is unable to fully determine chemical composition of the samples. Petroleomics is a field of science that uses the chemical composition of petroleum samples to predict their behavior [1]. There are a number of different methods being pursued to determine this chemical composition, including ion mobility mass spectrometry [2, 3], advanced distillation curve methods [4], and small angle scattering [5]. One of the most active research areas in petroleomics is using high resolution Fourier Transform Ion Cyclotron Resonance Mass Spectrometry (FT-ICR MS) to assign chemical composition to petroleum samples [1, 6-8]. The majority of the literature published thus far using FT-ICR MS for petroleomics uses samples that have usually been subjected to open column separation or nitrogen-concentration procedures [9-15], but there are very few papers that use high performance separation techniques prior to MS analysis. In Chapters 2 and 3, the focus was on HPLC for the separation of nitrogen group-types in petroleum, with little discussion of follow-up analyses. Fractionating a sample using HPLC and then

* A version of this chapter has been submitted for publication. Oro N.E., Whittal R.M., Lucy C.A.; *Analytica Chimica Acta* **2012**.

doing petroleomic analysis can determine chemical classes in chromatographic peak regions and can also reduce the complexity of data in the subsequent analysis.

Online LC-MS is common and very popular, and a Web of Science search (January 2012) for the topic “LC-MS” returns over 22 000 results. In the field of petroleomics, there has been only one published report of MS analysis of HPLC fractions [16]. The authors of this paper demonstrated successful analysis of HPLC fractions from the separation of a coker gas oil, but omitted any detailed sample preparation procedures.

Online LC-MS of petroleum samples is challenging due to incompatibility of normal phase HPLC solvents with the MS interface. Fraction collection followed by offline MS analysis is more robust and flexible, but it increases the sample preparation time and possibility of sample loss [17], and dilutes the sample. When the sample concentration becomes low, contaminants and interferences become more prominent, and may mask sample peaks of interest. FT-ICR MS is popular because of its high resolution and low detection limits [18], but this also poses a problem because many low concentration interferences can be seen in the mass spectra. This chapter focuses on the minimization and elimination of contaminants observed in the petroleomic analysis of normal phase HPLC fractions of gas oil samples.

In 2008, a highly pragmatic and practical review article was published in *Analytica Chimica Acta* discussing common contaminants in mass spectra [19]. Included in the supplemental data were tables describing masses and compound

identities, allowing researchers to use these tables to identify interferences in their own work. This review fits into a larger body of literature in which research groups are endeavouring to identify and eliminate sources of contamination in their mass spectra. Discovering the identity of a problem peak is non-trivial, with often an entire application note or paper dedicated to one contaminant [20-29]. In many cases, the removal of contamination peaks is highly desirable, as they can obscure the peaks of interest or prevent the analysis from being done at all [22, 24, 26, 27].

Contamination can come from many different sources in the laboratory, with the source only becoming apparent after some scientific detective work; knowing where the contamination peaks come from is essential for successful removal of the contaminant. The presence of soap on laboratory glassware or in an instrument has become a common interference [19, 22], as has the presence of plasticizers [26, 27, 30-33]. Something as simple as handling samples or containers with bare hands can introduce quaternary ammonium compounds to a sample, as they are common additives in hand lotions and laundry detergents [21]. Tubing [27, 28, 30, 34], rubber stoppers [29], nylon filters [25, 35], and chemicals in the ambient laboratory air [23] have also been identified as introducing contamination. All of these examples illustrate how important it is to be diligent and careful during method development, and especially so when collecting offline HPLC fractions with low sample concentrations. The majority of the published literature discusses contamination in positive mode electrospray [20-27, 29, 31-

33], however contamination is still present in negative mode electrospray [19, 36, 37], and both are important for petroleomics.

This chapter discusses the methods developed to couple offline HPLC fraction collection to FT-ICR MS, and describes the interferences and contaminants encountered in this process. The focus is on contamination issues that arise during sample handling, and on how to enhance the signal of sample peaks of interest. No discussion is made of possible hardware or software solutions to eliminating contamination peaks; these types of solutions are beyond the scope of this project. Contaminant peaks are described for both positive and negative mode electrospray ionization (ESI). Three new positive contamination peaks not previously published are described, with ion mass, formula, possible sources and removal. The work presented in this chapter is unique to petroleomics and the use of offline HPLC fraction collection, but is broadly applicable to any analysis using FT-ICR MS where there is low sample concentration or multiple steps of sample handling.

4.2 Experimental

4.2.1 Apparatus

All HPLC experiments were performed on the Varian ProStar HPLC system (Varian, Palo Alto, CA, USA) described in Section 2.2.1. The HPLC had a Varian ProStar 701 Fraction Collector installed as part of the system to collect the column effluent as offline fractions for MS analysis. Details of the fraction collection can be found in Section 4.2.3.

MS analysis was done on a Bruker Apex-Qe 9.4 T Fourier Transform Ion Cyclotron Resonance Mass Spectrometer (Bruker Daltonics, Bremen, Germany), and data analysis was done with Bruker's DataAnalysis 4.0 SP 2 software. The MS was equipped with a quadrupole mass filter, a hexapole collision cell, an FT-ICR infinity cell and a 9.4 T/110 mm bore magnet. Sample solutions were infused by an electrospray source at 120 μ L/h using a syringe pump (Cole Parmer, Vernon Hills, IL) and glass syringe (Hamilton Company, Reno, NV). The MS was operated with sidekick trapping and the apodization used was sine bell multiplication. Acquisition was performed in broadband detection mode. The instrument parameters for positive and negative mode are listed in Table 4-1.

4.2.2 Chemicals

Optima grade dichloromethane (DCM), toluene and hexanes and GC Resolv grade methanol (MeOH) were used (Fisher Chemicals, Fairlawn, NJ, USA). Chromatographic separations were done on the HC-Tol column described in Section 2.2.2 unless otherwise noted. FT-ICR MS parameters were optimized using a fraction from a separation of the HGO T1 product listed in Table 3-2 on the HC-Tol column. The HGO sample was prepared as described in Section 3.2.2, at concentrations ranging from 0.05 – 0.5 g/mL and stored in glass vials.

Table 4-1. FT-ICR MS instrument parameters for positive and negative mode electrospray.

Parameter	(-) Mode	(+) Mode
Acquisition Mass Control		
Acquisition Size (points)	4M	2M
Low mass (m/z)	144.37	187.67
High mass (m/z)	2000.00	2000.00
Transient length (s)	2.0972	1.3631
Accumulation		
Number of spectra averaged	16	12
Source accumulation (s)	0.01	0.01
Collision cell accumulation (s)	1.0	1.0
TOF (s)	0.0012	0.0010
ESI Spray Chamber		
Capillary (V)	3200	4200
Spray shield (V)	2700	3700
Nebulizer gas flow (L/min)	1.5	1.6
Dry gas flow (L/min)	3.0	5.0
Dry temperature (°C)	150	180
Source Optics		
Capillary exit (V)	-340	300
Deflector plate (V)	-250.0	250.0
Funnel 1 (V)	-190	150
Skimmer 1 (V)	-20.0	20.0
Funnel 2 (V)	-7.6	7.6
Skimmer 2 (V)	-4.5	5.3
Hex DC (V)	-3.9	4.0
Trap (V)	-20	20
Extract (V)	10	-10
RF Control		
Funnel RF (V)	160	160
Hexapole RF amplitude (Vpp)	370	360
Hexapole frequency (MHz)	5.0	5.0

Table 4-1. Continued FT-ICR MS instrument parameters.

Parameter	(-) Mode	(+) Mode
Qh Optics		
Focus lens (V)	89	-80
Entrance lens (V)	2.0	2.0
Pre-filter DC bias (V)	0.0	0.0
DC bias (V)	0.0	0.0
Post-filter DC bias (V)	0.0	0.0
Entrance lens trap (V)	-4.5	4.8
Entrance lens extract (V)	-20	20
Collision voltage (V)	1.5	-1.0
DC extract bias (V)	-1.4	1.5
Exit lens trap (V)	-20.0	20.0
Exit lens extract (V)	10.0	-10.0
Qh Gas Control		
Collision gas flow (L/s)	0.51	0.61
Collision gas flush time (min)	1.0	1.0
ICR Transfer		
Accelerator 1 (V)	35	-30
Accelerator 2 (V)	0.0	0.0
Accelerator 3 (V)	0.0	0.0
Vertical Beam Steer 1 (V)	-2.5	5.0
Vertical Beam Steer 2 (V)	0.0	0.0
Horizontal Beam Steer 1 (V)	-15.5	20.5
Horizontal Beam Steer 2 (V)	0.0	0.0
Focusing lens 1 (V)	140	-150
Focusing lens 2 (V)	-50	100
Focusing lens 3 (V)	-100	-10
Analyzer		
Sidekick (V)	5.0	-3.0
Sidekick offset (V)	0.400	-0.750
Excitation amp (dB)	12.00	8.00
Front trap plate (V)	-0.650	0.800
Back trap plate (V)	-0.950	0.700
Analyzer entrance (V)	3.00	-5.00

The MS was externally calibrated in positive mode with a solution of four quaternary amines (hexadecyltrimethylammonium bromide, didodecyl-dimethylammonium bromide, dihexadecyldimethylammonium bromide and dimethyldioctadecylammonium bromide; Sigma-Aldrich, St. Louis, MO) at ~ 0.1 μM . External calibration was performed in negative mode with a mixture of C_{17} - C_{26} saturated fatty acids (heptadecanoic acid, Ultra Scientific, North Kingstown, RI; hexacosanoic acid, Sigma-Aldrich, St. Louis, MO) at ~ 10 μM . The presence of palmitic and stearic acid as ubiquitous ions was also exploited for calibration purposes in negative ion mode. Both calibration solutions were prepared in 3:1 methanol:toluene. Formic acid (88%, Fisher Chemicals, Fairlawn, NJ, USA) was added to positive mode samples (5.7 μL in 1 mL of sample) and ammonium hydroxide (28%, Sigma-Aldrich, St. Louis, MO) was added to negative mode samples (10 μL in 1 mL of sample) to enhance de/protonation and increase signal [38]. The HGO analyzed directly on the FT-ICR MS was prepared by dissolving ~10-20 mg in 3 mL of toluene and then further diluted with 17 mL of methanol. Formic acid was added to samples analyzed in positive mode and ammonium hydroxide was added to samples that were analyzed in negative mode.

4.2.3 Fraction Collection and Sample Preparation

Fractions from the HPLC were collected and analyzed offline on the FT-ICR MS. Chromatograms were pre-screened for peaks of interest and the fraction collector was programmed using Varian's Star Chromatography Workstation software, version 6.20, to collect fractions based on time points at the beginning

and ends of the desired peaks. Effluent was collected in labelled glass test tubes and manually pipetted into ½ dram glass sample vials with Teflon-lined caps. The vials containing the fractions were then placed in a Savant SpeedVac Plus Concentrator (Model SC110A, Thermo Fisher Scientific, Waltham, MA) and the solvent was removed under a cold vacuum at ~0.1 Torr. Following solvent removal, 1 mL of 3:1 methanol:toluene was added to the vials for redissolution, and either formic acid or ammonium hydroxide was added for positive ion or negative ion analysis, respectively. The solvent and ionization aids were added to the vials using Eppendorf pipettes and standard pipette tips (Fisher Scientific, Nepean, ON). All storage materials used were glass.

4.3 Results and Discussion

When collecting offline HPLC fractions of a petroleum sample, a significant amount of dilution occurs. The original sample must be diluted so that it does not overload the HPLC column. The sample is then diluted via band broadening occurring during the HPLC separation. The resulting fraction collected from the HPLC system may have only trace concentrations of compounds of interest. The key to successful analysis is two-fold; the concentration of the sample must be high enough to overcome contaminant peaks (Section 4.3.1), and the presence of interfering ions must be minimized (Section 4.3.2). When trying to eliminate interferences, one must consider the entire path of the sample, from initial collection to final MS analysis. Any material that the sample comes into contact with has the possibility to introduce interfering ions.

4.3.1 Sample Concentration

4.3.1.1 Sample Screening and Fraction Selection

The majority of the work in this chapter was done using a hydrotreated heavy gas oil (HGO, Section 4.2.2). The HPLC columns used to optimize our experiments were a custom synthesized HC-Tol hypercrosslinked polystyrene stationary phase (Chapter 2), and a commercially available “DNAP” stationary phase (Chapter 3). These two columns were selected on the basis of our previous work indicating their potential for the separation of nitrogen group-types found in petroleum samples [39, 40]. Prior to HPLC fractionation, the HGO was diluted and directly analyzed by FT-ICR MS. Figures 4-1 and 4-2 show positive and negative mode ESI mass spectra of the HGO. The distribution of peaks goes to a higher m/z value in the positive ion spectrum than negative mode (m/z 220-600 vs. 200-450), which is unexplained but consistent with other published literature for high resolution mass spectra of gas oils [41].

Both positive and negative mode spectra indicate the presence of a large number of nitrogen-containing peaks in the HGO sample (~1050 in positive mode and ~420 in negative mode). Normal phase HPLC was performed on the HC-Tol column discussed in Chapter 2. Work in Chapter 2 indicated that pyrroles elute between 5.8 and 8 minutes and so this region was selected for fraction collection and MS analysis (Section 2.3.4). Figure 4-3 shows a chromatogram of the HGO on the HC-Tol column, with dotted lines indicating the fraction collected. These first steps are necessary to decide on a region for fraction collection, and to confirm the presence of species that will ionize by ESI in the sample.

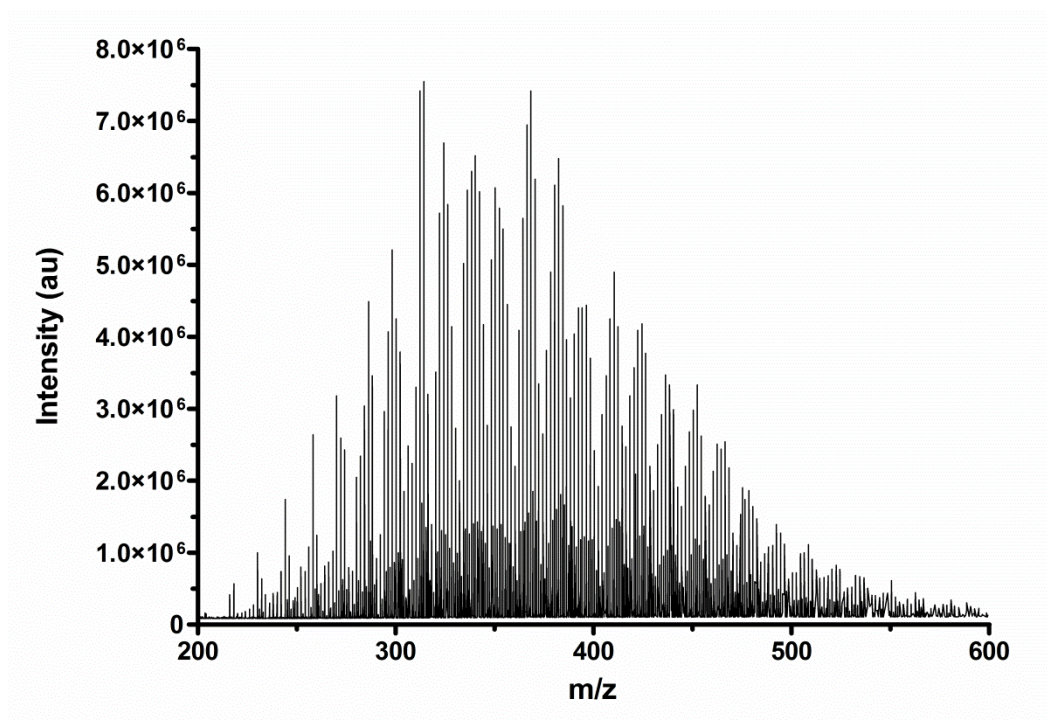


Figure 4-1. Positive ion mass spectrum of the hydrotreated heavy gas oil.

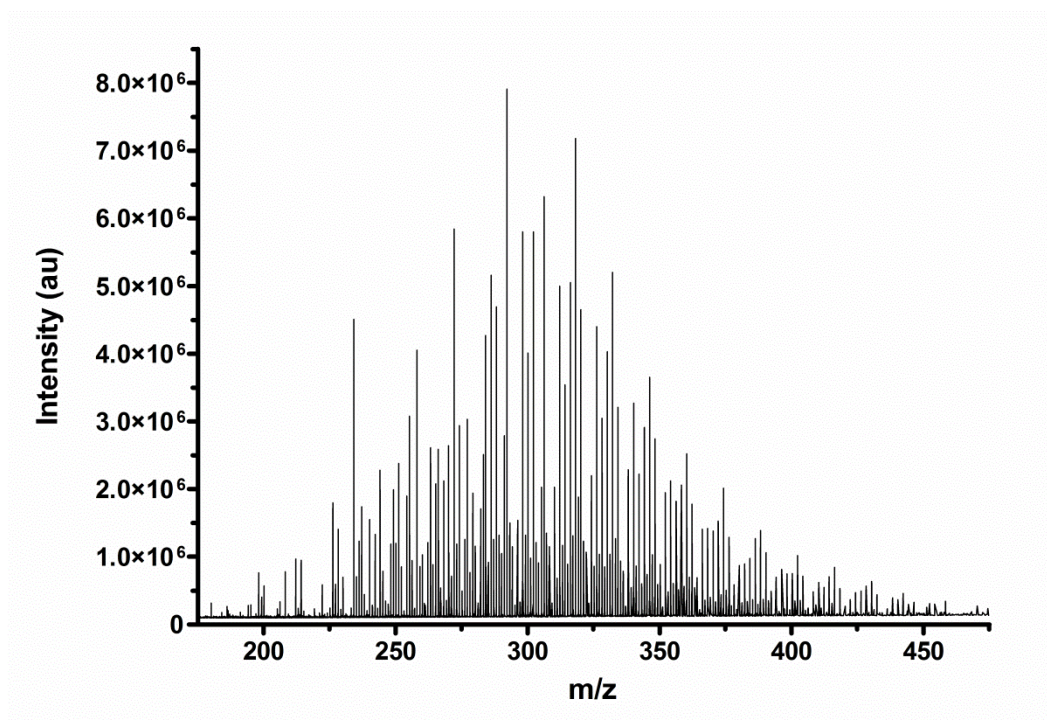


Figure 4-2. Negative ion mass spectrum of the hydrotreated heavy gas oil.

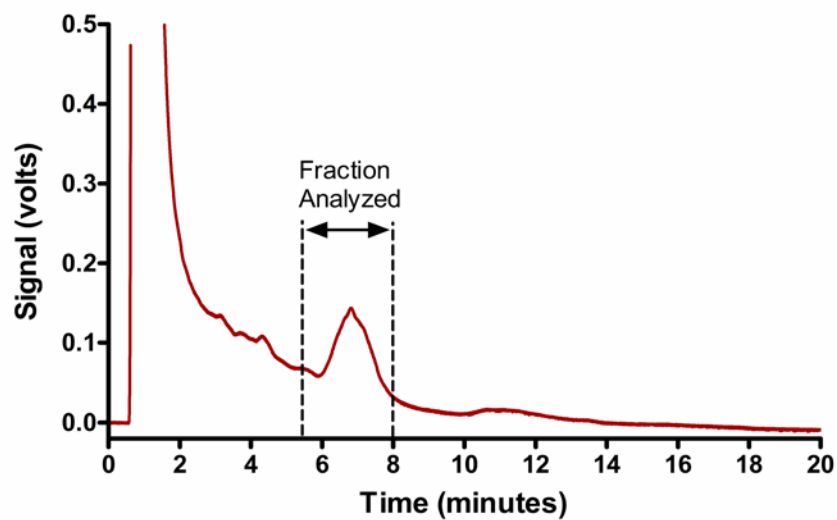


Figure 4-3. Chromatogram of the treated HGO on HC-Tol, with dotted lines showing the area collected for MS analysis. Step gradient program 5-100% dichloromethane in hexane, 20%/4 minute steps, 15 minute re-equilibration time; T = 35°C, flow rate 1.0 mL/min, detection wavelength 254 nm, 5.0 x 0.46 cm column, 5.0 μ m particles.

4.3.1.2 Sample Preparation

When preparing a sample to be injected into the HPLC, one needs to consider the initial concentration and the impact that concentration will have on the MS analysis. Ideally the concentration should be as high as possible. Over the concentration range of 0.05 – 0.5 g/mL of HGO we found that the higher initial concentration produced stronger signal intensity in the MS analysis. However one also has to be conscious of overloading the HPLC column with a too-high sample concentration [42]; it may take some time to find the correct balance. Gas oil samples of 0.5 g/mL gave excellent MS signal without overloading the HPLC column. The concentration can also be lowered to 0.1 g/mL if the volume of solvent used to re-dissolve the fraction for MS analysis is reduced accordingly.

To maximize the MS signal, the HPLC fractions need to be concentrated by evaporating the solvent. A vacuum evaporator was used to remove all of the mobile phase from the fractions, and the dry fractions were re-dissolved in a solvent mixture suitable for the ESI interface. MS analysis of an unfractionated HGO sample before and after evaporation indicates that the evaporation step changes the distribution of compounds in the sample, increasing the intensity of higher mass ions. There was no loss of target nitrogen compounds, and the solvent removal step concentrated the higher mass compounds (m/z 600 or greater) in the sample, making them visible in the post-evaporation spectrum where they were not visible in the pre-evaporation spectrum. The pre- and post-evaporation positive mode spectra are shown in Figures 4-4 and 4-5.

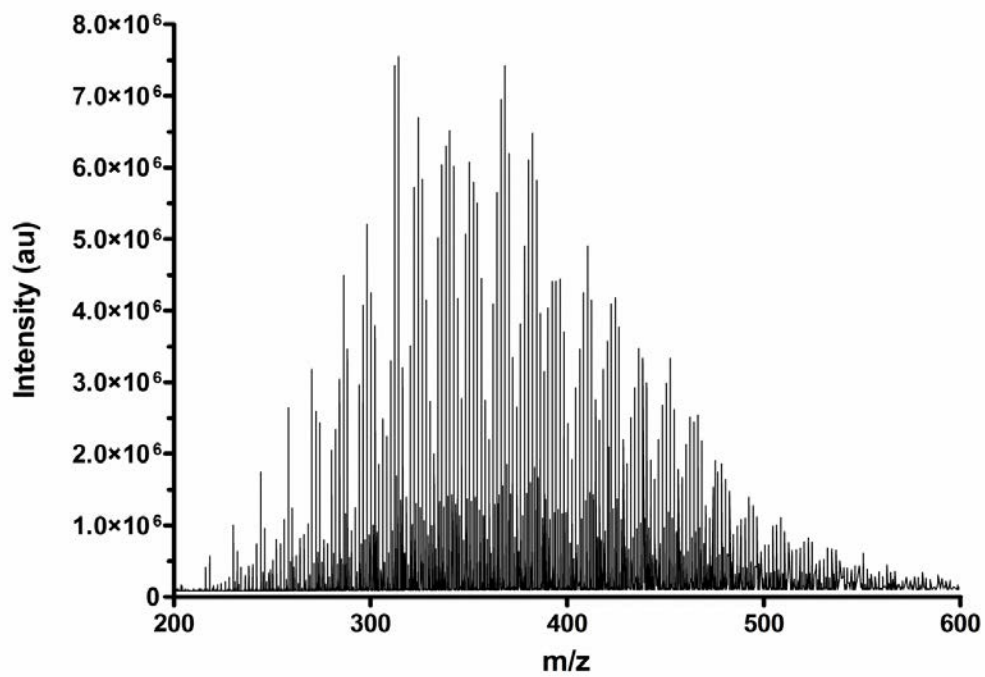


Figure 4-4. Positive ion mass spectrum of the HGO sample prior to the evaporation step.

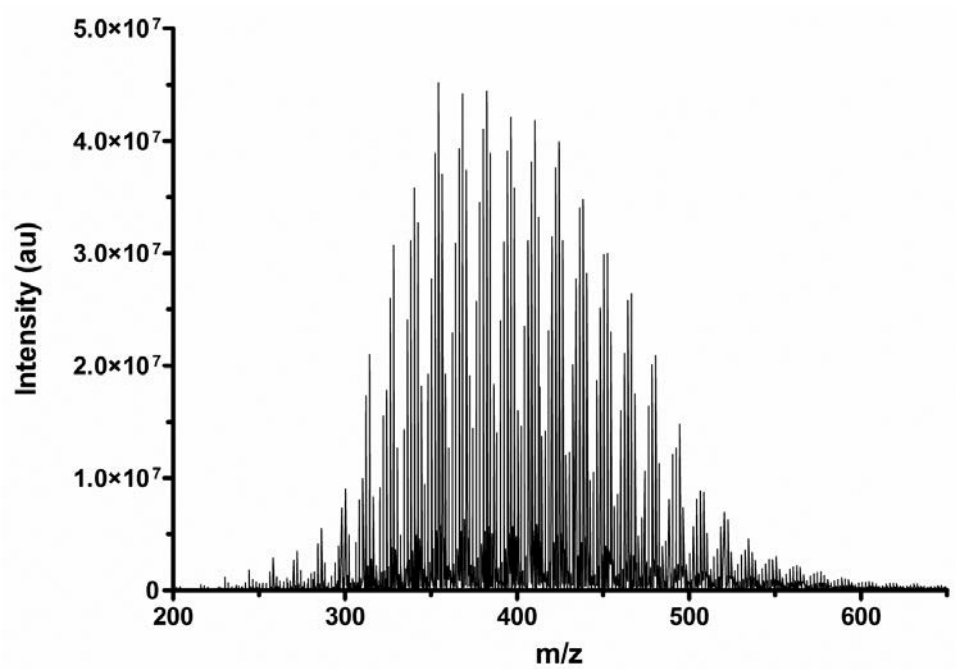
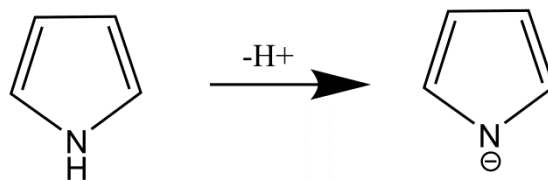


Figure 4-5. Positive ion mass spectrum of the HGO sample following the evaporation/solvent removal step.

The work done by Alan Marshall and Ryan Rodgers in the field of petroleomics has demonstrated the need for the addition of a strong acid or base to samples to enhance signal, and we have found this to be very important as well [38]. Pyrroles deprotonate on the nitrogen in the five-membered ring, and are detected in negative mode ESI. Pyridines protonate on the nitrogen in the six-membered ring to create a positive charge and are detected in positive mode ESI. Figure 4-6 illustrates this process. The addition of strong base or acid respectively to samples is essential because it increases the signal intensity of peaks of interest by approximately 100%. Without the presence of strong acid or base, we were unable to see any peaks of interest in many of the fractions collected. The increase of signal intensity can be observed in Figure 4-7, which illustrates the positive ion spectra of an HPLC fraction before and after the addition of formic acid.

In addition to the previously described steps for increasing concentration, collecting multiple subsequent HPLC runs of the same fraction was done to see if it would provide an increase in signal. Figure 4-8 shows three stacked mass spectra of the same fraction; the top spectrum is of one collected HPLC run, the middle is three combined runs, and the bottom is five combined runs. Mass spectra produced from combined HPLC runs have increased signal intensity, but ultimately the same number of peaks were visible. It was decided that the increased intensity was not worth the extra time required to collect and concentrate the extra fractions.

Deprotonation of pyrroles



Protonation of pyridines

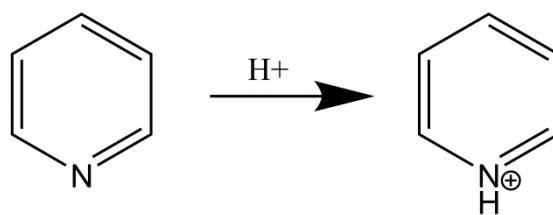


Figure 4-6: Charge creation processes in ESI for nitrogen-containing species.

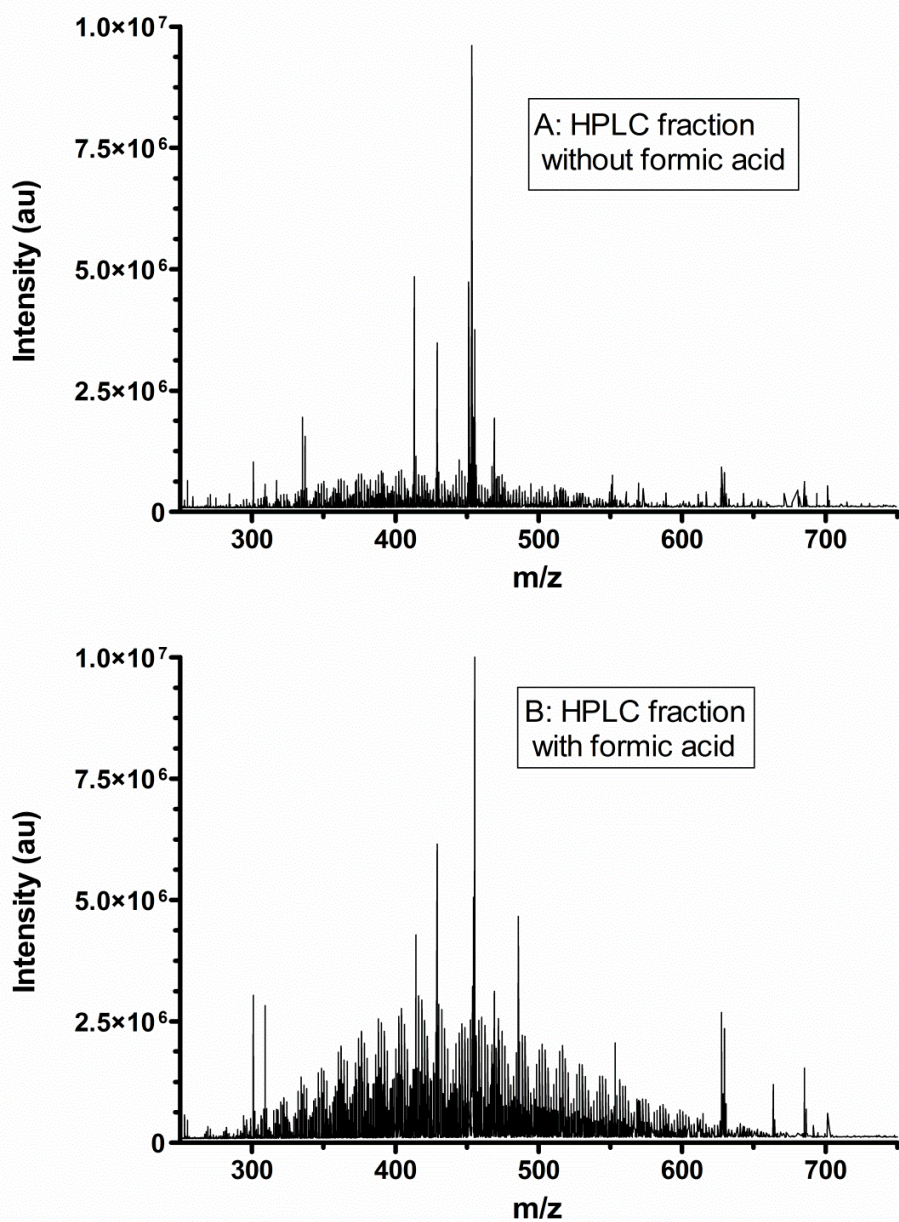


Figure 4-7. Positive mode mass spectrum of an HPLC fraction, before (A) and after (B) adding formic acid to aid in ionization.

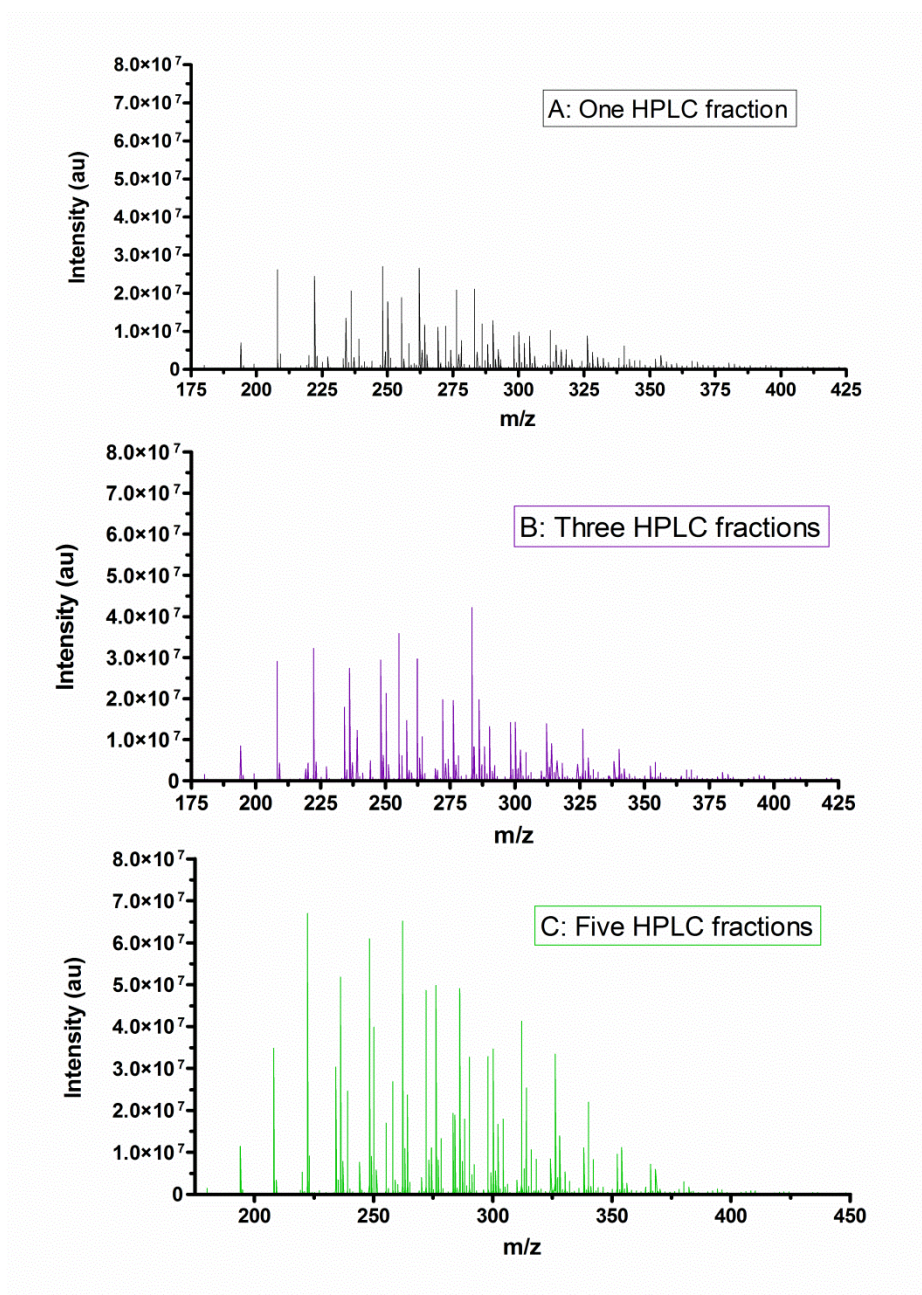


Figure 4-8. Negative mode mass spectra of an HPLC fraction from the HGO separation. The top spectrum is one HPLC run, the middle is three combined runs, and the bottom is five combined runs. The spectra are the same except for the intensity of peaks; adding multiple HPLC fractions increases intensity but is not necessary to analyze the fraction.

4.3.2 Contaminants and Interferences

Contaminant peaks can appear in a mass spectrum from many sources, some of which are expected and some of which are not. The methods described in Section 4.3.1 are more specific to offline fraction collection, whereas this section is more general and describes issues that arise during sample handling. The examples given are in the context of petroleomics and offline fraction collection, but the sources of contaminants can be found in any laboratory or analyses. They are especially problematic for cases when samples are dilute.

4.3.2.1 Soaps and Detergents

It is common laboratory practice to wash glassware with soap and it is not surprising that soap residue may be found on glassware used to prepare samples. Soap residue can appear as contamination in both MS and HPLC work [19, 22, 43]. In cases where glassware was not fully rinsed after cleaning with soap, we found that the peaks resulting from soap were strong and obscured our analysis. To eliminate this problem, new glassware was purchased specially for MS analysis and kept separate from communal lab glassware. Prior to use, and between samples, the glassware was washed with three rinses of dichloromethane, followed by three rinses with a 3:1 mixture of methanol:toluene. The glassware was left to dry on a clean paper towel in a fumehood overnight, and then baked in an oven at 100°C for eight hours. When glassware was cleaned in this manner, no soap peaks were present in the mass spectra.

In our experience new HPLC systems can be shipped with residual soap in their lines, which result in strong contaminant signals in the MS spectra. The HPLC required an overnight wash with water to remove this contamination. Figure 4-9 is a positive ion mass spectrum of an HPLC fraction from a system with both soap and plasticizer contamination. The tall peaks labelled with an * have been identified as contaminants, and are summarized in Table 4-2. Contamination resulting from soap presents as a series of peaks differing by 44.03 mass units (repeating unit of polyethylene glycol) [19]. In this case, the starred peaks between m/z 537 and m/z 757 can all be attributed to soap. The low intensity series of peaks between m/z 300-600 in Figure 4-9 are the analytes of interest, but the high relative intensity of the soap and other contaminants makes it difficult to carry out proper data analysis. The peaks at m/z 453 and 485 are contamination peaks resulting from iron oxide clustering with formate ions; they will be discussed further in Section 4.3.2.4.

4.3.2.2 Molecular Sieves

In normal phase HPLC, it is common to dry solvents with molecular sieves, as any water dissolved in organic solvents can strongly adsorb onto the polar stationary phases used and negatively affect reproducibility [42]. Molecular sieves are composed of salts containing potassium, sodium, aluminum and silica [44]. When molecular sieves are used to dry a solvent, the salts dissolve into the solvent and ionize strongly in positive mode ESI. The peaks caused by these salts overwhelm the spectra.

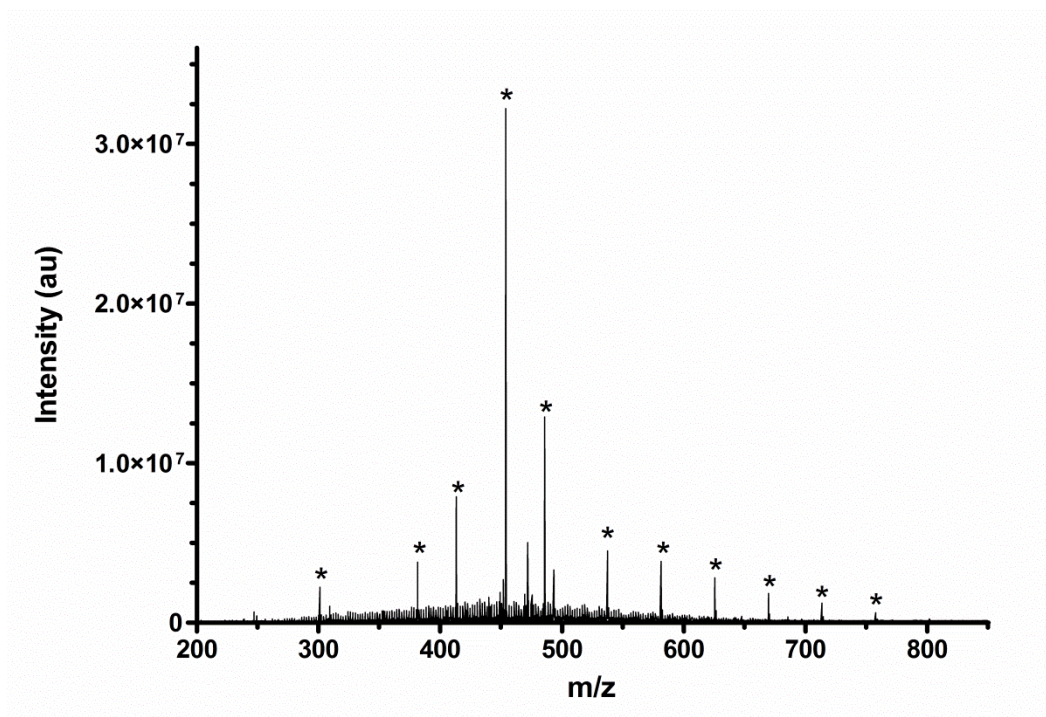


Figure 4-9. Positive mode spectrum of an HPLC fraction from a commercial column (“DNAP”, Section 3.2.2) where soap and plasticizer contamination was present. The asterisks mark peaks that have been identified as contamination. Their masses and sources are listed in Table 4-2.

Table 4-2. Mass values and sources for positive contaminant peaks identified in Figure 4-9. The peak assignments for the plasticizer and detergent were made based on the supplemental tables from reference [19].

Observed m/z	Mono-isotopic ion mass (singly charged)	Formula	Source
301.14153	301.14103	$C_{16}H_{22}O_4Na$	Dibutyl phthalate, plasticizer
381.2984	381.29753	$C_{21}H_{42}O_4Na$	Stearoylglycerol*
413.26717	413.26623	$C_{24}H_{38}O_4Na$	Diisooctyl phthalate, plasticizer
453.78601	453.78512	$(HCO_2)_6Fe_3O$	Iron (III) oxide – formate cluster
485.81205	485.81134	$(HCO_2)_6(CH_3OH)Fe_3O$	MeOH adduct of 453 ion
537.34199	537.33979	$(C_{14}H_{22}O)(C_2H_4O)_7Na$	Triton detergent
581.36734	581.36601	$(C_{14}H_{22}O)(C_2H_4O)_8Na$	Triton detergent
625.39494	625.39222	$(C_{14}H_{22}O)(C_2H_4O)_9Na$	Triton detergent
669.42136	669.41844	$(C_{14}H_{22}O)(C_2H_4O)_{10}Na$	Triton detergent
713.44463	713.44465	$(C_{14}H_{22}O)(C_2H_4O)_{11}Na$	Triton detergent
757.47071	757.47087	$(C_{14}H_{22}O)(C_2H_4O)_{12}Na$	Triton detergent

*See note with Table 4-3.

Figure 4-10A is a positive mode mass spectrum of methanol that has been dried with molecular sieves. A mass spectrum of fresh methanol that has not been dried with sieves is shown in Figure 4-10B, illustrating how well the salts ionize in Figure 4-10A. If solvents dried with molecular sieves were used in the HPLC, a two-hour rinse of the HPLC with clean mobile phase (50/50 DCM/hexane) was necessary. HPLC samples were also diluted in solvents that were not treated with molecular sieves. These steps removed all of the molecular sieve salt peaks from the mass spectra.

4.3.2.3 Plastic

Plasticizers are very common and persistent contaminant peaks in positive mode ESI [26, 27, 30-33]. The interferences caused by plasticizers have been reduced by using Teflon or glass for storage and transport whenever possible. The petroleum samples we receive are shipped to us in plastic containers and are stored in these containers for an undetermined amount of time, allowing ample time for plasticizers to dissolve into the sample. However, analysis of blanks indicates that the plastic contamination is introduced during the separation and fraction collection steps. The autosampler and fraction collector modules of our HPLC system also contain interior plastic lines. A number of the plastics used in these modules are proprietary, making it very difficult to determine the types of plastic the sample may come into contact with in the HPLC system.

For these reasons we have decided not to pursue the complete elimination of plasticizer peaks in our spectra at this time. To reduce contamination, we use Teflon or glass for sample storage and ensure that caps on vials are Teflon-lined.

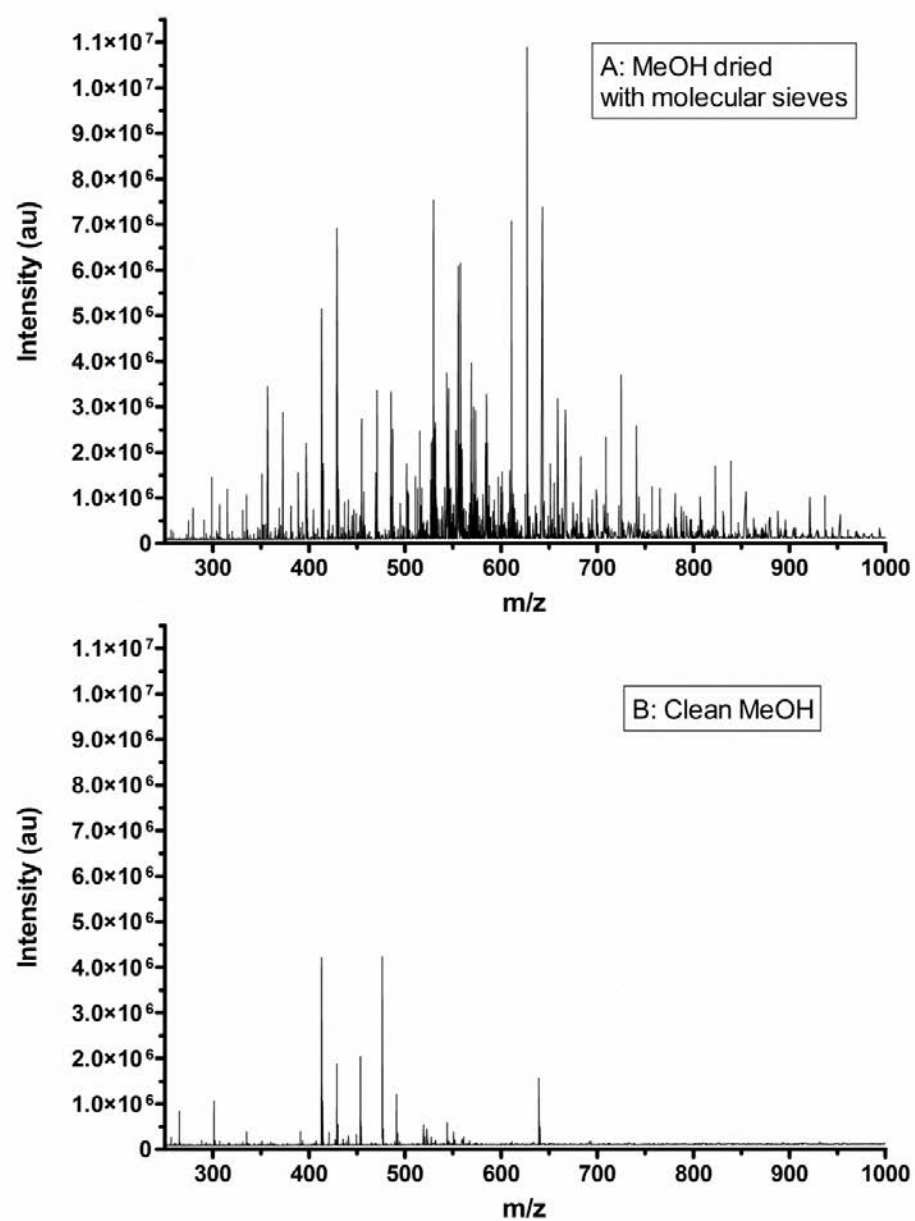


Figure 4-10. Positive mode mass spectrum of (A) methanol dried over molecular sieves and (B) clean methanol that was not dried using sieves.

Table 4-3 lists the contamination peaks present in the positive ion spectra, and two plasticizer peaks are among them. In the future, it may be worthwhile to do an in-depth investigation to determine the exact source of these peaks in an effort to eliminate them.

4.3.2.4 Identified Interferences

The steps described in this chapter have greatly improved the quality of data and made analysis of fractions by MS possible. There have been a number of contaminant peaks in both positive and negative mode that have been identified by not completely eliminated. Table 4-4 lists the four dominant interfering peaks that are still present in the negative ion mass spectra. All four appear to be fatty acids, two of which (m/z 255 and 283) have been identified as the anions of palmitic acid and stearic acid [19]. The peak at m/z 269 is a C_{17} fatty acid (heptadecanoic acid) that is present in our calibration solution and is likely present in our HPLC fractions due to carryover. The m/z 199 peak has a molecular formula consistent with a fatty acid, but without further MS/MS studies, the exact branching and structure cannot be assigned conclusively. If it is similarly saturated to palmitic and stearic acid, the peak is likely from lauric acid. Saturated fatty acids are very common in the environment and are used in soaps and cosmetics [45]; thus their presence is not surprising. The intensity of analyte ions in the HPLC fractions has been high enough that these negative ions have not been found to cause any problems with analysis of the data.

Table 4-3. Positive ion contamination peaks observed in HPLC fractions analyzed. The m/z 413 and 421 peaks were identified using reference [19].

Observed m/z	Mono-isotopic ion mass (singly charged)	Formula	Source
353.26590	353.26623	C ₁₉ H ₃₈ O ₄ Na	Palmitoylglycerol*
381.29709	381.29753	C ₂₁ H ₄₂ O ₄ Na	Stearoylglycerol*
413.26589	413.26623	C ₂₄ H ₃₈ O ₄ Na	Diisooctyl phthalate (plasticizer)
421.23351	421.23	C ₂₀ H ₃₈ O ₇ P	Tris(2-butoxyethyl) phosphate (plasticizer)
439.80605	439.80639	(HCO ₂) ₆ Fe ₃ H ₂	Iron hydride formate cluster
453.78497	453.78512	(HCO ₂) ₆ Fe ₃ O	Iron oxide formate cluster
471.79550	471.79569	(HCO ₂) ₆ (H ₂ O)Fe ₃ O	H ₂ O adduct of 453 ion
485.81138	485.81134	(HCO ₂) ₆ (CH ₃ OH)Fe ₃ O	MeOH adduct of 453 ion

*Tentative assignment, based on elemental composition and the known presence of stearic and palmitic acid in the samples.

Table 4-4. Negative ion contamination peaks observed in HPLC fractions analyzed. Peak assignments for palmitic acid and stearic acid were made using reference [19].

Observed m/z	Mono-isotopic ion mass (singly charged)	Formula	Source
199.17034	199.17035	$C_{12}H_{23}O_2$	Unknown
255.23300	255.23295	$C_{16}H_{32}O_2$	Palmitic acid (carboxylate anion) C16:0
269.24871	269.2486	$C_{17}H_{33}O_2$	Heptadecanoic acid (carboxylate anion) C17:0
283.26435	283.26425	$C_{18}H_{36}O_2$	Stearic acid (carboxylate anion) C18:0

Table 4-3 has a similar list of contaminant ions found in the spectra for positive mode. The formulae found for the peaks at 353 and 381 are $C_{19}H_{38}O_4 + Na$ and $C_{21}H_{42}O_4 + Na$, respectively and are tentatively assigned to the compounds palmitoylglycerol and stearyl glycerol. These compounds have not previously been reported as contaminant peaks. The intensity of these two peaks was low compared to sample peaks, and was not found to cause interference in data analysis. The peaks at m/z 413 and 421 belong to plasticizers, as discussed in Section 4.3.2.3.

The peaks at m/z 439.8, 453.8, 471.8 and 485.8 belong to a family of contamination not discussed in any previous publications. The peak at m/z 453.8 was very intense in many of the fractions, in some cases obscuring proper data analysis (Figure 4-11A). Analysis of blanks from the HPLC system indicated that the 0.8 mass defect peaks were only present after the addition of formic acid to the sample vials. Attempts to isolate the m/z 453.8 peak for MS/MS analysis were unsuccessful, suggesting an unstable cluster peak. When the skimmer voltage was adjusted to break apart this peak in source, three new peaks appeared at m/z 318.8, 363.8 and 408.8. The mass difference between these peaks is 45, consistent with addition of formate ions. The observed isotope pattern of the m/z 453.8 peak was consistent with a compound containing multiple iron atoms; the observed and theoretical isotope patterns for this peak are shown in Figure 4-12. This, along with the knowledge that formate is somehow causing the peak, led to the assignment of the m/z 318.8 peak as $(HCO_2)_3Fe_3O$.

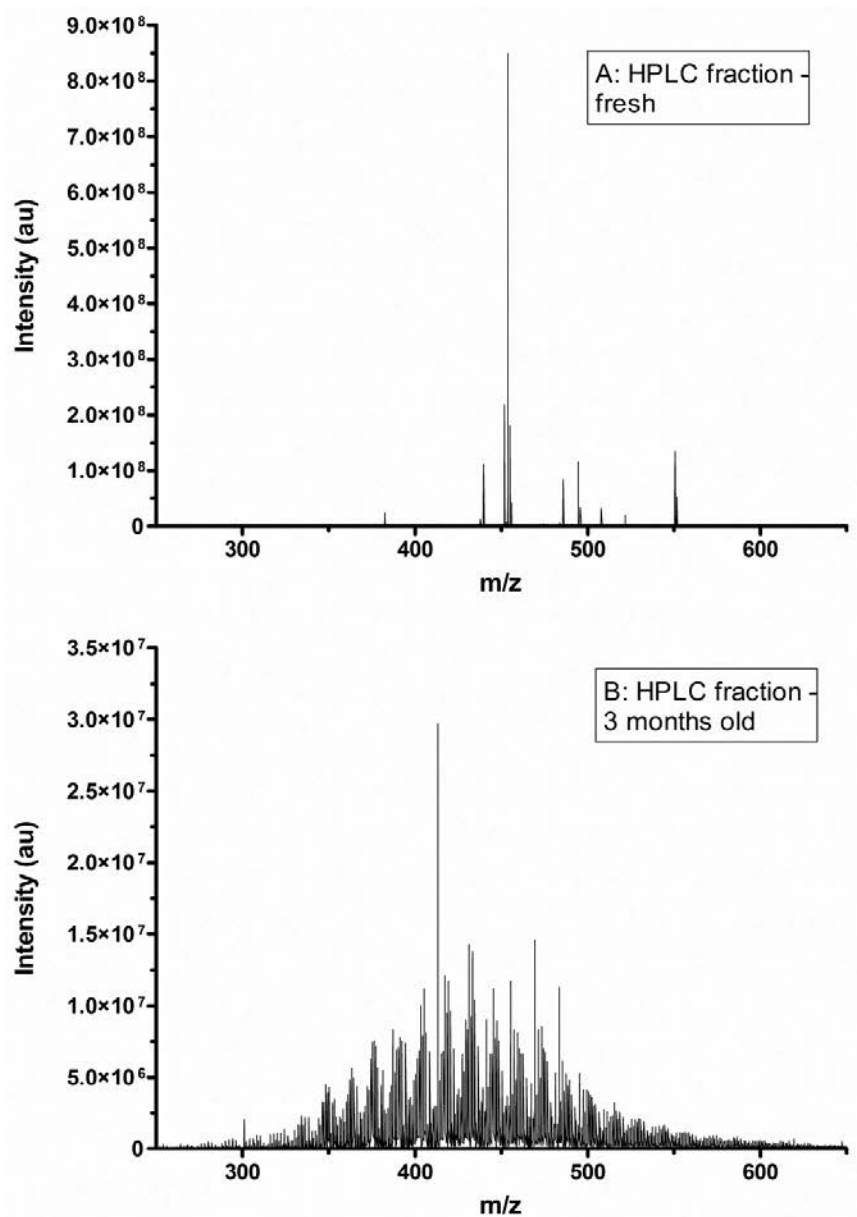


Figure 4-11. Positive mode spectra of an HPLC fraction from a commercial column (“DNAP”, Section 3.2.2). Spectrum A contains the iron-formate cluster contamination, and was analyzed within one day of preparing the fraction. Spectrum B is the same sample vial analyzed after three months of storage; the clusters have broken up and are no longer present.

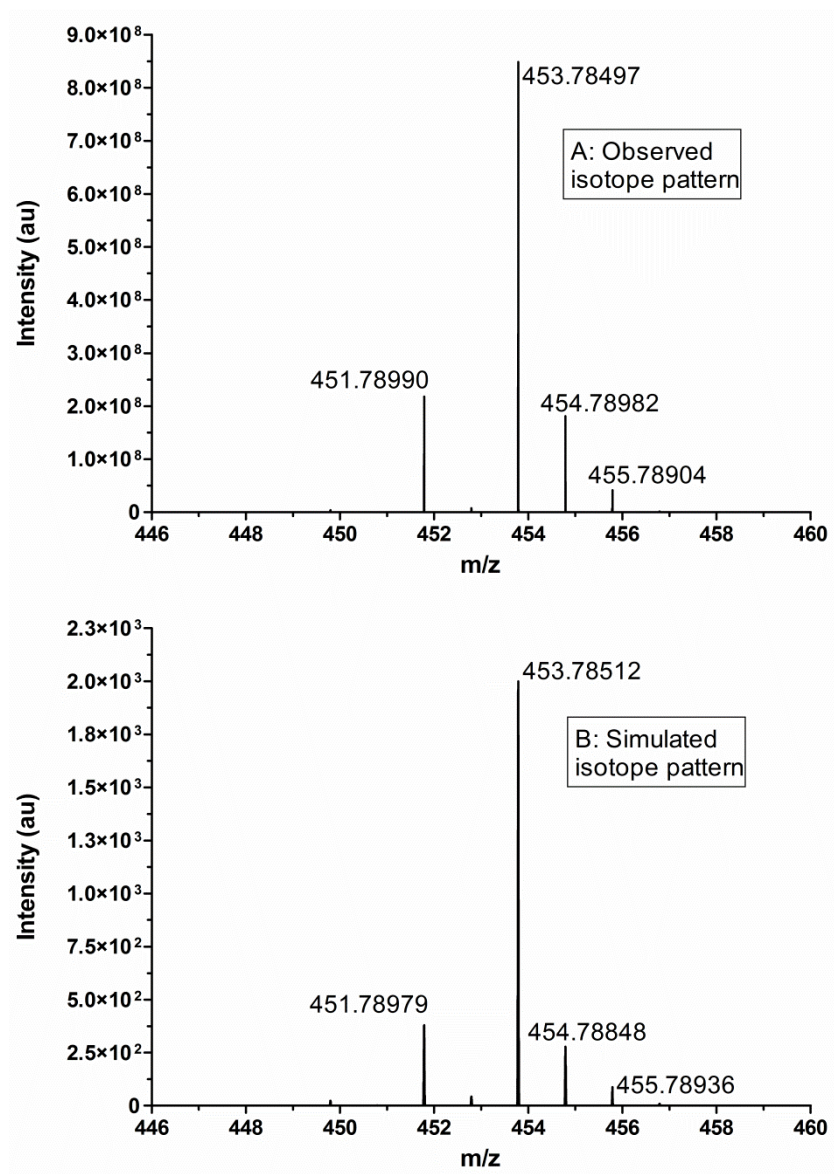


Figure 4-12. A: Observed isotope pattern for the iron-formate cluster peak at m/z 453.8. B: Simulated isotope pattern for $(\text{HCO}_2)_6\text{Fe}_3\text{O}$.

This assignment allowed the deduction that the m/z 453.8 peak is a cluster with three additional formate ions: $(\text{HCO}_2)_6\text{Fe}_3\text{O}$. In addition, the corresponding acetic acid-iron cluster peak, $(\text{CH}_3\text{CO}_2)_6\text{FeO}$, has been reported [19, 30, 34, 46]. The peak at m/z 439.8 was identified as an iron hydride cluster containing six formate ions $((\text{HCO}_2)_6\text{Fe}_3\text{H}_2)$. The peak at m/z 471.8 is the water adduct of the m/z 453.8 peak. The water is likely from the formic acid added to the samples. The m/z 485.8 peak is the methanol adduct of the peak at m/z 453.8. The most intense peak was at m/z 453.8, and the measured mass for this peak was m/z 453.78497, corresponding to an absolute error of 0.3 ppm compared to the calculated m/z of 453.78512. Similarly, the measured masses for the other three iron formate peaks were m/z 439.80605, 471.79550 and 485.81138. The absolute errors on these peaks are 0.8, 0.4 and 0.08 ppm, respectively. The low errors and observed isotope pattern give strong confidence in the assignment of the peaks.

The iron in these clusters is likely from the stainless steel tubing present in the normal phase HPLC system. The use of stainless steel is unavoidable due to the use of harsh solvents such as dichloromethane. The absence of these cluster peaks in unfractionated samples and presence in HPLC blanks also indicates that they are introduced during the fractionation process. However, we found that these clusters are not stable in solution, and disappear completely over time. Figure 4-11 shows the same sample vial of a fraction analyzed three months apart; the top spectrum is obscured by cluster peaks (A), while the bottom spectrum does not experience any interference (B). Increasing the skimmer voltage to break up the clusters in source effectively removes all of the cluster peaks

reported in Table 4-3, but does cause the appearance of non-clustered peaks at m/z 318.8, 363.8 and 408.8. The intensity of these three new peaks is low compared to the sample and they do not interfere with sample analysis. These clusters may be unique to normal phase HPLC systems and offline fraction collection, due to the use of stainless steel tubing in normal phase. The common use of PEEK tubing in reversed phase HPLC would not introduce iron into the samples. There are also no reports of these clusters in reversed phase LC-MS experiments. Fortunately, their lack of stability means that a user performing these experiments can adjust the MS parameters to break up the clusters, resulting in greatly improved data quality.

4.4 Conclusions

Successfully performing offline fraction collection on an HPLC system and using high resolution MS to analyze the fractions requires care and attention when handling and preparing samples. It is important to maintain a sufficient concentration of analyte compounds throughout many dilution steps, while taking precautions to minimize contamination from common sources such as soap, plastics, and salts. Most of the contaminants discussed in this chapter are not unique to petroleomics. This chapter discussed how to minimize interferences from these sources, and also identified a previously unreported source of iron-formate contamination, likely originating from the stainless steel present in a normal phase HPLC system. As more scientists become aware of contamination in MS, the body of literature continues to grow, providing researchers with the

tools to more easily and efficiently identify and eliminate problems in their own analyses.

4.5 References

- [1] R.P. Rodgers, T.M. Schaub, A.G. Marshall, *Analytical Chemistry* **2005**, *77*, 20A-27A.

- [2] A. Ahmed, Y.J. Cho, M. No, J. Koh, N. Tomczyk, K. Giles, J.S. Yoo, S. Kim, *Analytical Chemistry* **2011**, *83*, 77-83.

- [3] Z. Li, S.J. Valentine, D.E. Clemmer, *Journal of the American Society for Mass Spectrometry* **2011**, *22*, 817-827.

- [4] T.J. Bruno, L.S. Ott, T.M. Lovestead, M.L. Huber, *Chemical Engineering & Technology* **2010**, *33*, 363-376.

- [5] E.Y. Sheu, *Journal of Physics: Condensed Matter* **2006**, *18*, S2485–S2498.

- [6] A.G. Marshall, R.P. Rodgers, *Proceedings of the National Academy of Sciences* **2008**, *105*, 18090–18095.

- [7] C.S. Hsu, C.L. Hendrickson, R.P. Rodgers, A.M. McKenna, A.G. Marshall, *Journal of Mass Spectrometry* **2011**, *46*, 337–343.

- [8] O.C. Mullins, E.Y. Sheu, A. Hammami, A.G. Marshall, *Ashphaltenes, Heavy Oils and Petroleomics*, 1st ed., Springer Science, New York, 2007.

- [9] J. Fu, G.C. Klein, D.F. Smith, S. Kim, R.P. Rodgers, C.L. Hendrickson, A.G. Marshall, *Energy & Fuels* **2006**, *20*, 1235-1241.

- [10] T. Kekalainen, J.M.H. Pakarinen, K. Wickstrom, P. Vainiotalo, *Energy & Fuels* **2009**, *23*, 6055-6061.

- [11] G.C. Klein, R.P. Rodgers, A.G. Marshall, *Fuel* **2006**, *85*, 2071-2080.

- [12] D.F. Smith, P. Rahimi, A. Teclemariam, R.P. Rodgers, A.G. Marshall, *Energy & Fuels* **2008**, *22*, 3118-3125.
- [13] L.A. Stanford, S. Kim, R.P. Rodgers, A.G. Marshall, *Energy & Fuels* **2006**, *20*, 1664-1673.
- [14] Z. Wu, R.P. Rodgers, A.G. Marshall, J.J. Strohm, C. Song, *Energy & Fuels* **2005**, *19*, 1072-1077.
- [15] Y. Zhang, C. Xu, Q. Shi, S. Zhao, K.H. Chung, D. Hou, *Energy & Fuels* **2010**, *24*, 6321-6326.
- [16] X. Zhu, Q. Shi, Y. Zhang, N. Pan, C. Xu, K.H. Chung, S. Zhao, *Energy & Fuels* **2011**, *25*, 281-287.
- [17] X. Tian, R. Zhao, N. Tolic, R.J. Moore, D.L. Stenoien, E.W. Robinson, R.D. Smith, L. Pasa-Tolic, *Proteomics* **2010**, *10*, 3610-3620.
- [18] T.M. Schaub, C.L. Hendrickson, S. Horning, J.P. Quinn, M.W. Senko, A.G. Marshall, *Analytical Chemistry* **2008**, *80*, 3985-3990.
- [19] B.O. Keller, J. Sui, A.B. Young, R.M. Whittal, *Analytica Chimica Acta* **2008**, *627*, 71-81.
- [20] C.R. Gibson, C.M. Brown, *Journal of the American Society for Mass Spectrometry* **2003**, *14*, 1247-1249.
- [21] M.L. Manier, D.S. Cornett, D.L. Hachey, R.M. Caprioli, *Journal of the American Society for Mass Spectrometry* **2008**, *19*, 666-670.
- [22] R.W. Purves, W. Gabryelski, L. Li, *Review of Scientific Instruments* **1997**, *68*, 3252-3253.
- [23] A. Schlosser, R. Volkmer-Engert, *Journal of Mass Spectrometry* **2003**, *38*, 523-525.
- [24] A. Shukla, R. Zhang, D.J. Orton, R. Zhao, T.R.W. Clauss, R. Moore, R.D. Smith, *Rapid Communications in Mass Spectrometry* **2011**, *25*, 1452-1456.

- [25] J.C. Tran, A.A. Doucette, *Journal of the American Society for Mass Spectrometry* **2006**, *17*, 652-656.
- [26] K.M. Verge, G.R. Agnes, *Journal of the American Society for Mass Spectrometry* **2002**, *13*, 901-905.
- [27] Y.Q. Xia, S. Patel, R. Bakhtiar, R.B. Franklin, G.A. Doss, *Journal of the American Society for Mass Spectrometry* **2005**, *16*, 417-421.
- [28] Y. Yu, M.L. Alexander, V. Perraud, E.A. Bruns, S.N. Johnson, M.J. Ezell, B.J. Finlayson-Pitts, *Atmospheric Environment* **2009**, *43*, 2836-2839.
- [29] X.K. Zhang, R.C. Dutky, H.M. Fales, *Analytical Chemistry* **1996**, *68*, 3288-3289.
- [30] Waters, available online at http://www.waters.com/webassets/cms/support/docs/bkgrnd_ion_mster_list.pdf, accessed on January 15, 2012.
- [31] New Objective Technical Note PV-3: Common Background Ions for Electrospray, 2007.
- [32] X.H. Guo, A.P. Bruins, T.R. Covey, *Rapid Communications in Mass Spectrometry* **2006**, *20*, 3145-3150.
- [33] B. Aebi, J.D. Henion, *Rapid Communications in Mass Spectrometry* **1996**, *10*, 947-951.
- [34] B. Mahn, LC/MS Contaminant Peaks, March 21, 2006, Thermo Corporation, available online at <http://www.abrf.org/index.cfm/list/msg/66994>, accessed January 5, 2012.
- [35] P. Onnerfjord, LC/MS Peak at 679.5, available online at www.abrf.org/index.cfm/list/msg/58765, March 16, 2004.
- [36] M. Trotzmuller, X.H. Guo, A. Fauland, H. Kofeler, E. Lankmayr, *Journal of Mass Spectrometry* **2011**, *46*, 553-560.

- [37] H. Tong, D. Bell, K. Tabei, M.M. Siegel, *Journal of the American Society for Mass Spectrometry* **1999**, *10*, 1174-1187.
- [38] D.F. Smith, G.C. Klein, A.T. Yen, M.P. Squicciarini, R.P. Rodgers, A.G. Marshall, *Energy & Fuels* **2008**, *22*, 3112–3117.
- [39] N.E. Oro, C.A. Lucy, *Journal of Chromatography A* **2010**, *1217*, 6178-6185.
- [40] N.E. Oro, C.A. Lucy, *Journal of Chromatography A* **2011**, *1218*, 7788-7795.
- [41] T. Kekalainen, J.M.H. Pakarinen, K. Wickstrom, P. Vainiotalo, *Energy & Fuels* **2009**, *23*, 6055–6061.
- [42] L.R.K. Snyder, J.J.; Dolan, J.W., *Introduction to Modern Liquid Chromatography*, 3rd ed., Wiley, Hoboken, New Jersey, 2010.
- [43] D.E. Hughes, A.M. Bramer, *Journal of Chromatography* **1987**, *408*, 296-302.
- [44] Sigma-Aldrich, Molecular Sieve UOP Type 3Å Product Information, available online at http://www.sigmaaldrich.com/catalog/ProductDetail.do?lang=en&N4=208582|SIAL&N5=SEARCH_CONCAT_PNO|BRAND_KEY&F=SPEC, accessed on January 4, 2012.
- [45] Fatty Acids/Esters, available online at <http://www.chromatography-online.org/directory/analtcat-12/page.html>, accessed January 15, 2012.
- [46] C.F. Ijames, R.C. Dutky, H.M. Fales, *Journal of the American Society for Mass Spectrometry* **1995**, *6*, 1226-1231.

CHAPTER FIVE. Analysis of Nitrogen Content in Distillate Cut Gas Oils and Treated Heavy Gas Oils Using Normal Phase HPLC, Fraction Collection and Petroleomic FT-ICR MS Data

5.1 Introduction

The removal of nitrogen containing compounds from petroleum is an important and non-trivial issue. It is necessary to remove as much nitrogen as possible from petroleum to improve the quality of the product and reduce pollution. A key first step to obtaining better removal of nitrogen compounds is the determination of the group type and structure of the compounds remaining after nitrogen removal treatment. The complexity of these samples presents an interesting challenge to analytical chemists to develop methods to study nitrogen species in a sea of other compounds. This chapter is the culmination of the knowledge gained in Chapters 2, 3 and 4, bringing together normal phase high performance liquid chromatography (HPLC) methods for the separation of nitrogen compounds with offline fraction collection and petroleomic analysis of HPLC fractions.

An important step in the upgrading of heavy oil is hydrotreating, a process where the crude is reacted over a catalyst to remove heteroatoms such as nitrogen and sulphur, as well as metals [1, 2]. Removal of nitrogen takes place via a two-step process, in which the aromatic rings are first saturated, followed by C-N bond breakage [1, 3, 4]. Nitrogen species present in the crude feed can deactivate the catalysts and reduce the efficiency of further nitrogen removal [5, 6]. For this

reason, it is important to study new catalysts to achieve the highest level of nitrogen removal possible. In addition to hydrotreating, adsorptive processes are being explored. Adsorptive denitrogenation involves the treatment of feeds with an adsorbant to remove nitrogen compounds prior to hydrotreating, in an effort to remove poisoning compounds and increase the efficiency of hydrotreating [7-9].

Petroleomics is the study of the chemical composition of petroleum samples, with the goal of using the structure and type of the individual compounds to predict the behavior of the sample in different processing and upgrading steps [10-12]. Fourier Transform Ion Cyclotron Resonance Mass Spectrometry (FT-ICR MS) is a high resolution technique [12, 13], capable of resolving ion signals only 0.0034 Da apart [10] and of resolving over 10 000 chemically distinct species in a sample [14, 15]. For these reasons, FT-ICR MS has been the technique of choice for MS analysis of petroleum samples. In recent years the technology has advanced to the point that scientists are able to use petroleomic data to tackle interesting and relevant problems facing the oil and gas industry. Some of these studies include the analysis of acids [16-23], sulphur compounds [24-26], and asphaltenes [27-30], the boundaries of hydrocarbon size [31], and even the determination of the source of unusual color in crude oil [32].

FT-ICR MS has been used to carry out studies of nitrogen compounds in petroleum as well. One prevalent goal has been to use petroleomic data to determine the “class” (heteroatom content) and “type” (number of double bond equivalents, DBE) of nitrogen compounds in petroleum samples [33]. This information can then be used to compare nitrogen content of samples before and

after hydrotreating with the goal of identifying resistant species and designing better catalysts [34-37]. Similarly, work has been done to characterize the nitrogen content in different distillate fractions of petroleum samples to determine how molecules are separated according to temperature in the distillation process [38, 39]. Other work that is less related to this chapter includes the study of nitrogen compounds in fractions (saturates, aromatics, resins, asphaltenes) obtained from open column fractionation of samples [40], and the study of nitrogen in coker gas oils in relation to their effect on catalytic cracking [41, 42].

While open column preparation is very common prior to analytical analysis of petroleum samples, there is little published work regarding HPLC separation prior to FT-ICR MS analysis. In 2011, Zhu et al. analyzed HPLC fractions of a coker heavy gas oil by positive mode FT-ICR MS [43]. This work shows that analysis of offline HPLC fractions is possible. However there are no details given of sample preparation for the HPLC fractions, making it difficult to reproduce their work. The sample also underwent an open column separation prior to HPLC analysis, and passed through two analytical columns in series. The authors claim their column set up separates the sample by polarity, but no indication is given to whether or not their procedure will work for anything other than the coker heavy gas oil.

The ideal HPLC column for the separation of samples prior to fraction collection and MS analysis would be one that separates nitrogen compounds by group type (pyrroles and pyridines). This separation would allow one to analyze different peaks for different group types. In Chapter 2, the custom synthesized

stationary phase HC-Tol (hypercrosslinked polystyrene) was studied for its capabilities to perform a nitrogen group-type separation [44]. HC-Tol provided excellent separation of nitrogen standards, with separate elution regions for polycyclic aromatic hydrocarbons (PAHs), pyrroles and pyridines (Section 2.3.4). Chapter 3 studied the commercial dinitrophenyl “DNAP” column for the same nitrogen group-type separation, and found that pyrroles and pyridines were not separated from each other, but that the nitrogen containing standards were separated from PAHs, sulphur and oxygen standards (Section 3.3.3) [45].

This chapter examines both “DNAP” and HC-Tol for their separations of a set of heavy and light gas oil distillation cuts, as well as a heavy gas oil and the products resulting from three different types of nitrogen removal treatments. The goal was to use the MS data to identify the types of compounds in chromatographic regions to allow a user to use the chromatographic separations to analyze nitrogen content in samples following distillation or nitrogen removal. Based on preliminary studies, the “DNAP” column was selected for in-depth MS analysis of four peak regions. Separations of the gas oils on HC-Tol and “DNAP” are shown, along with the nitrogen compounds identified by positive and negative mode electrospray ionization MS in the four regions of the “DNAP” chromatogram. The chromatograms are used to qualitatively compare nitrogen content between samples. The fraction data is discussed in terms of carbon number and DBE of the nitrogen compounds, and is used to generalize the types and intensities of nitrogen compounds found in each “DNAP” peak region. The fraction data is also compared to data collected on unfractionated samples in a

case study to judge the suitability of using the fraction data for making gross generalizations about the samples analyzed.

5.2 Experimental

5.2.1 Apparatus

All HPLC experiments were performed on the Varian ProStar HPLC system (Varian, Palo Alto, CA, USA) described in Section 2.2.1. Column effluent was collected as offline fractions for MS analysis using a Varian ProStar 701 Fraction Collector. Fractions were collected and prepared for MS analysis as described in Section 4.2.3.

MS analysis was done on a Bruker Apex-Qe 9.4 T Fourier Transform Ion Cyclotron Mass Spectrometer (Bruker Daltonics, Bremen, Germany), and all experimental conditions were as described in Section 4.2.1 and Table 4-1. Analysis of the MS data was done using Bruker's DataAnalysis 4.0 SP 2 software and Sierra Analytics Composer Software, version 1.0.2 (Sierra Analytics, Modesto, CA, USA). A detailed discussion of the MS data analysis can be found in Section 5.2.3.

5.2.2 Chemicals

Optima grade dichloromethane (DCM), toluene and hexanes and GC Resolv grade methanol (MeOH) were used (Fisher Chemicals, Fairlawn, NJ, USA). Chromatographic separations were done on the HC-Tol column described

in Section 2.2.2 and the “DNAP” column described in Section 3.2.2. FT-MS parameters were optimized as described in Section 4.2.2.

The MS was externally calibrated in positive mode with a solution of four quaternary amines, and externally calibrated in negative mode with a mixture of C₁₇-C₂₆ saturated fatty acids. Formic acid and ammonium hydroxide were added to samples to promote ionization, as detailed in Section 4.2.2.

Syncrude Canada (Edmonton, AB, Canada) provided gas oil samples for analysis. Two sets of samples were analyzed. The first set of samples were distillate cuts of both treated and untreated light gas oils (LGOs) and heavy gas oils (HGOs); this sample set is referred to as “distillates”, and the sample labelling and details are in Tables 5-1 and 5-2. The second set of samples are an HGO feed and 30 different products resulting from different nitrogen-removal processes or treatments. These samples are referred to as the “catalyst” samples, and their details and labelling are in Table 5-3. For HPLC analysis, all samples were prepared at 0.1 g/mL, in 50/50 v/v% dichloromethane/hexane, to permit full dissolution. The HGO feed and treated products analyzed directly on the FT-ICR MS were prepared by dissolving ~10-20 mg in 3 mL of toluene followed by further dilution with 17 mL of methanol. Formic acid and ammonium hydroxide were added to enhance ionization (Section 4.2.2).

5.2.3 Mass Spectrum Data Analysis

The MS data from the collected fractions were analyzed with both Bruker’s DataAnalysis software and Sierra Analytics’ Composer software.

Table 5-1. Sample information for light gas oil distillate cut samples.

Sample	Description	Density (g/mL)	Avg wt% C	Avg wt% H	S (ppm)	N (ppm)	Simulated Distillation Results (°C)		
							5% mass	50% mass	95% mass
LGO Feed	Untreated LGO	0.91	85.6	11.4	24400	1330	202.5	313.5	438.5
LGO 177-343C	Untreated LGO 177-343°C cut	0.89	85.7	11.7	22400	852	205	285.5	340.5
LGO 343C+	Untreated LGO 343°C+ cut	0.96	84.9	11.0	31400	2150	356	393	502
LGO-1 177-343C	First stage treated LGO 177-343°C cut	0.86	86.9	12.8	89	4.3	194.5	276.5	338
LGO-1 343C+	First stage treated LGO 343°C+ cut	0.90	87.2	12.8	680	89.6	357.5	392.5	488.5
LGO-2 177-343C	Final product treated LGO 177- 343°C cut	0.84	86.3	13.9	2.2	0.2	189.5	267.5	334.5
LGO-2 343C+	Final product treated LGO 343°C+ cut	0.87	85.8	13.6	2.3	5.8	356.5	388.5	478

Table 5-2. Sample information for heavy gas oil distillate cut samples.

Sample	Description	Density (g/mL)	Avg wt% C	Avg wt% H	S (ppm)	N (ppm)	Simulated Distillation Results (°C)		
							5% mass	50% mass	95% mass
HGO 343-524C	Untreated HGO 343-524°C cut	0.99	84.5	10.3	20100	1700	346.5	437	515.5
HGO 524C+	Untreated HGO 524°C+ cut	1.02	84.3	9.7	41400	5380	493.5	565	735
HGO-T1	Treated HGO at T1	0.94	87.4	11.4	4700	2170	280.5	423	534.5
HGO-T1 IBP-343C	T1 HGO IBP- 343°C cut	0.90	88.3	11.8	1600	1010	194.5	308	382.5
HGO-T1 343-524C	T1 HGO 343- 524°C cut	0.94	88.1	11.8	5290	2400	342	421.5	508
HGO-T1 524C+	T1 HGO 524°C+ cut	0.95	87.8	11.9	5250	2830	508.5	551	598.5
HGO-T2	Treated HGO at T2	0.93	87.4	11.7	2960	1780	256.5	417	530.5
HGO-T2 IBP-343C	T2 HGO IBP- 343°C cut	0.89	88.4	12.1	822	629	176	299	368.5
HGO-T2 343-524C	T2 HGO 343- 524°C cut	0.94	88.1	11.8	3140	1950	342.5	423.5	511
HGO-T2 524C+	T2 HGO 524°C+ cut	0.95	87.9	12.1	3230	2300	507	547	597.5

Table 5-3. Sample information for the catalyst sample set.*

Sample	Description	S (ppm)	N (ppm)
Feed	HGO parent feed	42250	3771
Adsorptive denitrogenation			
HGO-TA	Treated feed at T _A	2064	1365
HGO-TB	Treated feed at T _B	1376	1137
HGO-TC	Treated feed at T _C	599	836
ADN-1	Product from adsorption process 1	42150	2656
ADN-2	Product from adsorption process 2	45410	3330
ADN-1-TA	Adsorption product 1 treated at T _A	2059	1173
ADN-1-TB	Adsorption product 1 treated at T _B	1323	949
ADN-1-TC	Adsorption product 1 treated at T _C	717	624
ADN-2-TA	Adsorption product 2 treated at T _A	1559	888
ADN-2-TB	Adsorption product 2 treated at T _B	1000	755
ADN-2-TC	Adsorption product 2 treated at T _C	424	549
Fixed bed reactor			
Ref-B1	Ref. catalyst treated feed, bed section 1	22670	3411
Ref-B2	Ref. catalyst treated feed, bed section 2	11740	3130
Ref-B3	Ref. catalyst treated feed, bed section 3, T1	5165	2055
Ref-B4	Ref. catalyst treated feed, bed section 3, T2	3175	1682
Ref-B5	Ref. catalyst treated feed, bed section 3, T3	1930	1402
Exp-B1	Exp. catalyst treated feed, bed section 1	20730	3410
Exp-B2	Exp. catalyst treated feed, bed section 2	9163	2855
Exp-B3	Exp. catalyst treated feed, bed section 3, T1	3522	2077
Exp-B4	Exp. catalyst treated feed, bed section 3, T2	2490	1806
Exp-B5	Exp. catalyst treated feed, bed section 3, T3	1450	1592
Different catalyst systems			
RefCat-TI	Ref. catalyst treated feed, T _I	28420	1641
RefCat-TII	Ref. catalyst treated feed, T _{II}	15690	1379
RefCat-TIII	Ref. catalyst treated feed, T _{III}	12850	1376
Cat1-TI	Catalyst 1 treated feed, T _I	26320	1891
Cat1-TII	Catalyst 1 treated feed, T _{II}	29730	1846
Cat1-TIII	Catalyst 1 treated feed, T _{III}	787	1229
Cat2-TI	Catalyst 2 treated feed, T _I	34640	1689
Cat2-TII	Catalyst 2 treated feed, T _{II}	16660	1277
Cat2-TIII	Catalyst 2 treated feed, T _{III}	11690	1177

*T indicates temperatures at which the treatment processes were performed. Information provided by Syncrude Canada.

The Composer software is based on the petroleomics work of Ryan Rodgers and Alan Marshall [46]. The program assigns compositions to the peaks in a spectrum and also allows the display of the data by heteroatom class and double bond equivalent type in formats such as bar graphs, dot plots and contour plots.

Prior to analysis, the spectra were internally recalibrated in DataAnalysis to improve mass accuracy. Uncalibrated positive ion spectra had unacceptable mass errors of approximately 2-5 ppm. Internal calibration corrected this. The mass errors were low (< 0.5 ppm) for the negative ion spectra, but recalibration was performed for consistency. Each spectrum was internally calibrated with a N-series of high intensity found in the spectrum, with a minimum of eight compounds in the calibration file. The N-series for each file were chosen based on highest intensity and also largest mass range. Recalibration was considered successful if mass errors were reduced to below 1 ppm. The mass values and peak assignments from DataAnalysis were used to check the assignments made in Composer. Approximately 5-10 peaks were checked to make sure the assignment in Composer agreed with the suggested formula given by DataAnalysis. Isotopic peaks were not included in the analysis.

The Composer software is designed to analyze and process mass spectra of unfractionated and concentrated petroleum samples. The low intensity of analyte peaks in many spectra from fractionated samples can result in the software either ignoring or mis-assigning a peak. Careful adjustment of the parameter files is required to correctly assign peaks. These parameters are detailed in five different sections, and the descriptions will be ordered in the same way. The parameters

are described in detail to enable future users of the software to troubleshoot and modify their own parameter files. Each mass spectrum needs its own parameter file, and the parameter files should be saved before exiting the program.

5.2.3.1 Composer Parameters

Processing: the default for *Intensity Calculation* is peak height, and was sufficient for the analysis of fractions. The value for *Peak detection/scan law* determines how the software assigns peaks from the raw data imported. When the width is too narrow, the software can assign three to five peaks inside one “real” peak. A value of 0.004 Da or greater was sufficient to correctly assign peaks, but this was checked for every file.

Recalibration: One step of calibration is necessary to improve the mass accuracy of the assignments. Without a correct recalibration, the mass errors were unreasonably high on peak assignments (greater than 2 ppm). Finding the best series to calibrate with can be the most time consuming part of analyzing the data in Composer, and a bad recalibration will often be the problem if the peak assignments are incorrect. To recalibrate, an *External peak list* was used, adapting the internal calibration files used to recalibrate in DataAnalysis, changing them into the text format appropriate for Composer (see Composer User Manual for format specific to version being used). For matching policy, increase the *Tolerance window* to a value of at least 5.00 ppm; this is the amount of error the program will tolerate when matching calibration values to peaks in the spectrum. The *Intensity threshold* needs to be markedly decreased from the

default value; it needs to be low enough to detect the peaks of interest, but if it is too low the software will attempt to calibrate on baseline noise. A value of 0.5% was a good starting point for optimizing recalibration. The minimum and maximum m/z are adjusted depending on the peaks in the spectrum. The default setting is also *Match maximum intensity in window*, and will revert to this every time the software is reopened. Selecting *Match closest m/z to theoretical* gave much better results. Under Calibration polynomial, the defaults of *Optimize polynomial order* and *Optimize matches for best fit* were left selected.

Excluded m/z : this option can be used to ignore any known contamination peaks in a spectrum. The contamination peaks commonly encountered during the analysis of fractions are discussed in detail in Chapter 4. Excluded m/z values need to be specified for each data file individually. *Match tolerance* was set to 5.00 ppm.

Composition: for positive mode, set *Adducts* to read H,Na and for negative mode, the *Adducts* should read H. The default values for *DBE limits* (-0.5 and 40.0) can remain as they are. The charge state is set as Positive or Negative, depending on the data file, with Min and Max both reading 1 for ESI. Under Composition matching mode, *Compute homologous series* was selected, with a CH₂ repeat. The *De novo cutoff* was typically left at 500 Da, but could be increased to higher values if the majority of the peaks in the spectrum were above 500 Da. The Composition matching constraints were adjusted based on the particular data file. The m/z constraints are matched to the peaks in the spectrum, the *m/z match tolerance* was set to 2 ppm and *Min relative abundance* was

optimized starting at 0.5%; this percentage can be decreased for low intensity peaks. The box for *Allow radical cations* is unchecked for ESI, and *Remove isolated assignments* was checked. The minimum atom count for N, O and S was reduced from 3 to 2 to prevent incorrect peak assignments.

Response factors: no work was done to determine response factors, and this was left unedited.

5.2.3.2 Composer Viewing Options

Processing is the viewing option needed to determine if the software has selected peaks properly. Zoom into individual peaks in the Spectra tab to ensure that the software is only assigning one peak to each real peak. The Recalibration tab will indicate if the recalibration procedure was successful; the window should contain peak matches with ppm errors of less than 1. If the windows in this tab are blank, the recalibration was unsuccessful and the parameters need to be adjusted.

Assignments: peak assignments will appear in a window on the left, with the spectra on the right. If the assignments are done correctly, the Unassigned Spectrum on the bottom pane should contain a minimum number of peaks. For the HPLC fractions, the most dominant class assignment should be N with an H adduct or loss. The Tables tab will display the peak assignments by class. Correct assignments will have errors of 1 ppm or less.

Plots: this option allows the creation and viewing of plots generated by the software using the data files that have been opened with proper parameter files.

5.3 Results and Discussion

To determine the best stationary phase for the separation of gas oil samples, the HC-Tol column and “DNAP” column from Chapters 2 and 3 respectively, were both studied in this chapter. HC-Tol was most promising in terms of its ability to separate nitrogen group types from each other, but “DNAP” is appealing in terms of its commercial availability. “DNAP” does not separate pyrroles from pyridines, but is capable of separating nitrogen containing compounds from polycyclic aromatic hydrocarbons (PAHs). A set of 48 gas oil samples was analyzed on both columns (“distillates” and “catalysts” samples); the goal was to identify peak regions in the chromatograms that changed following distillation or hydrotreatment.

Both HC-Tol and “DNAP” displayed a series of peaks, but analysis of the gas oil samples on HC-Tol was disappointing. The peak shapes on HC-Tol were uneven and were approximately 20% of the intensity of the peaks in the “DNAP” chromatograms (Section 5.3.1). The “DNAP” chromatograms were more reproducible, and displayed four distinct peak regions (Section 5.3.2). For these reasons, “DNAP” was selected for further analysis, and MS data was collected for the “DNAP” peak regions (Section 5.3.3). The separations on HC-Tol are also discussed for completeness.

5.3.1 Separations on HC-Tol

The separation of standard compounds using HC-Tol was studied in Chapter 2, and was used to optimize the fraction collection MS analysis methods

in Chapter 4. The gas oil chromatograms on HC-Tol (Figures 5-1 and 5-2) showed a large off-scale peak between 0-5 minutes, a moderately sized peak between 5-8 minutes, and two smaller and indistinct peaks between 10-12.5 and 14-17.5 minutes. Work with model compounds (Section 2.3.4) indicated that the large peak between 0-5 minutes should contain all of the PAH compounds, while the 5-8 minute peak should be the pyrroles. The pyridine standards eluted past 20 minutes (Figure 2-7), so the remaining two peak regions on HC-Tol cannot be conclusively assigned. Preliminary work was done analyzing fractions from the HC-Tol column with positive and negative mode MS. The data from the fractions indicated that the pyrroles are concentrated in the 5-8 minutes peak region, but that the pyridines are present in every fraction of the chromatogram. Unpublished data from the National High Magnetic Field Laboratory at Florida State University showed that pyridines have a wide carbon number distribution in Athabasca bitumen products [47]. Assuming the retention on the stationary phase is occurring via the nitrogen atom, an extensive variety of alkylation surrounding the nitrogen in the gas oil samples would prevent isolation of the pyridine compounds in a small region of the chromatogram. This was further confirmed by the elution of a t-butyl pyridine standard in the PAH region of the chromatogram ($t_R \sim 1$ minute).

This being said, the signal intensity across the entire HC-Tol chromatogram can be somewhat correlated with the overall concentration of nitrogen in the sample. Figure 5-1 shows two chromatograms of distillate cuts on the HC-Tol column.

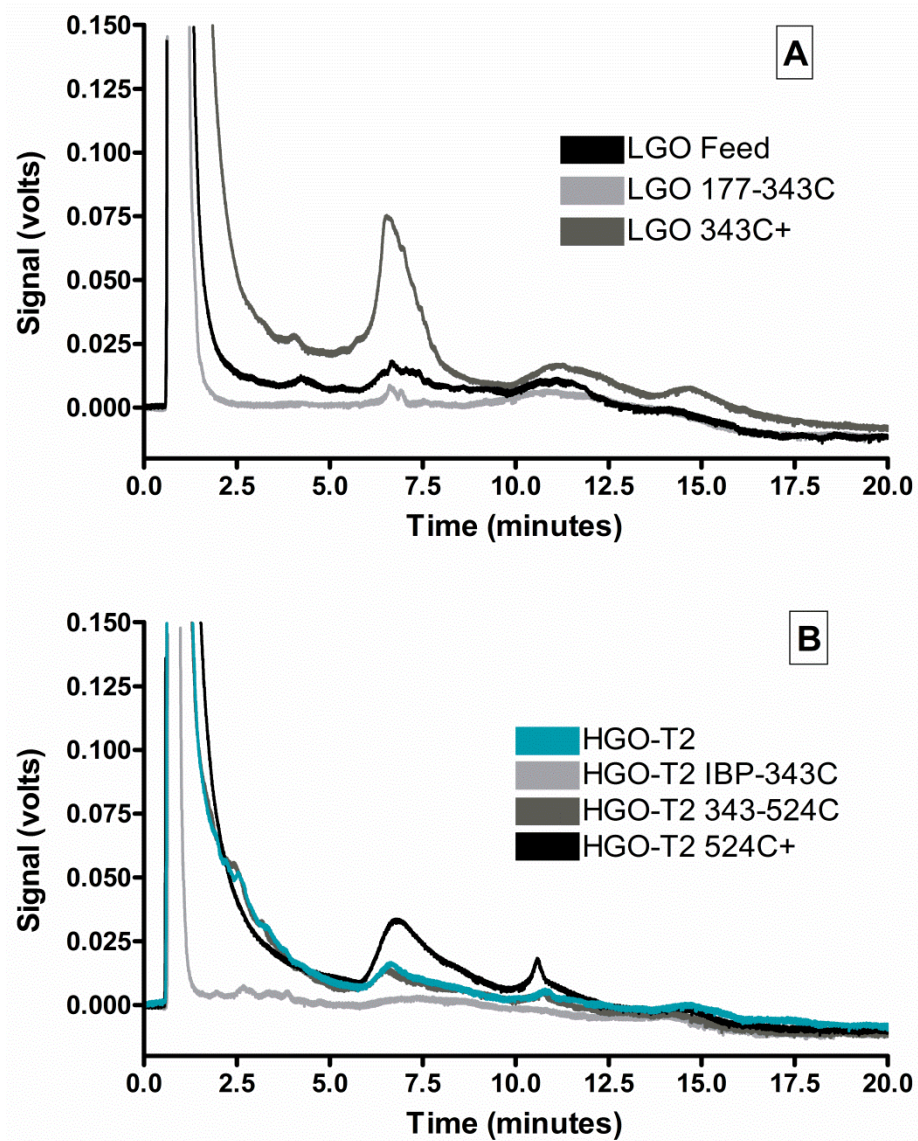


Figure 5-1. Chromatograms on HC-Tol of distillate cut gas oils. A: Light gas oil feed (black) and its distillate cuts (grey traces). B: Hydrotreated HGO (blue) and its distillate cuts (greys and black). Conditions: HC-Tol column (5.0 x 0.46 cm, 5.0 μ m particles), step gradient, 5-100% DCM in hexane, 20%/4 min. steps; T = 35°C, flow rate 1.0 mL/min, detection wavelength 254 nm.

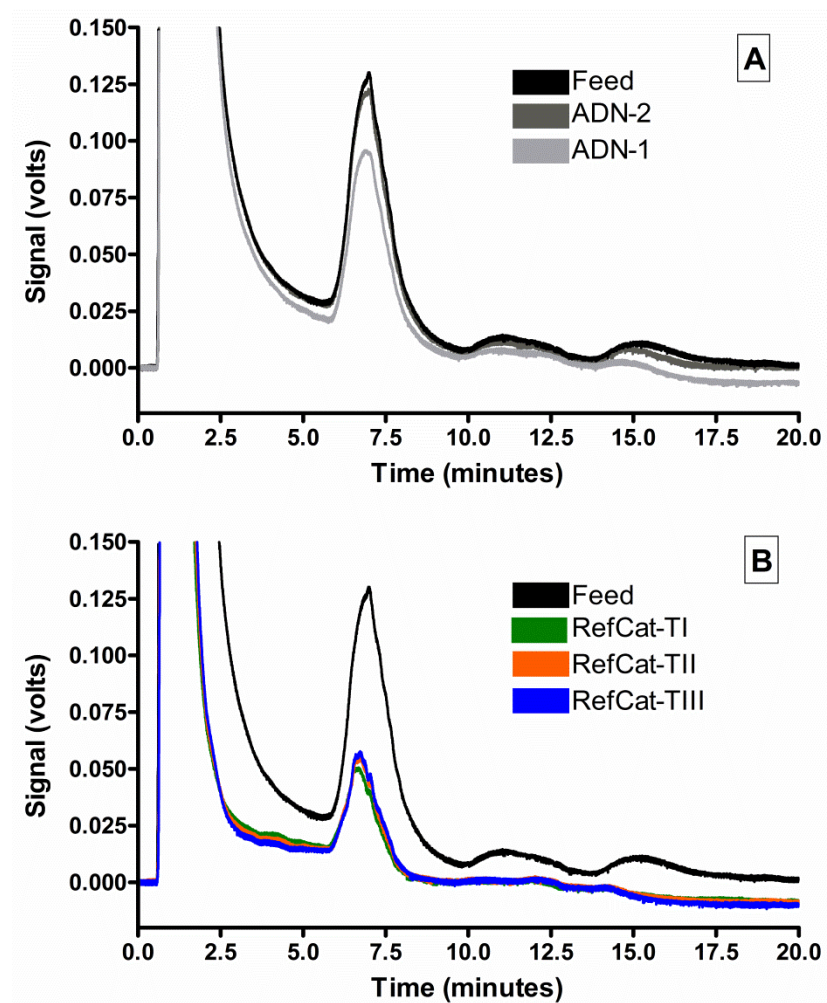


Figure 5-2. Chromatograms on HC-Tol of catalyst samples. A: HGO feed (black), ADN-1 (light grey) product and an ADN-2 (dark grey) product. B: HGO feed (black) and hydrotreated products with the same catalyst at three different temperatures (green, orange, blue). Conditions: HC-Tol column (5.0 x 0.46 cm, 5.0 μm particles), step gradient, 5-100% DCM in hexane, 20%/4 min. steps; T = 35°C, flow rate 1.0 mL/min, detection wavelength 254 nm.

Figure 5-1A is a light gas oil (LGO) feed, and two of its distillate cuts. It is apparent from the UV traces that the most aromatic species are concentrated in the higher boiling 343C+ cut. When the elemental composition of the cuts are compared to the chromatogram (Table 5-1), the 343C+ cut contains the highest concentration of nitrogen. Similarly Figure 5-1B illustrates that for the HGO the highest boiling cut (black trace, 524C+) also has the highest concentration of aromatic and nitrogen containing species.

Figure 5-2 shows two different chromatograms on HC-Tol, with gas oils from the catalyst sample set. On both the A and B chromatograms, the pyrrole peak is much more prominent than in Figure 5-1. Thus the chromatograms can be used to compare the removal of nitrogen following different treatments of the gas oil. Figure 5-2A has the HGO feed (black trace) and the products resulting from two different adsorptive treatments (ADN-1 and ADN-2) designed to remove nitrogen. If the signal intensity is taken to be equivalent to nitrogen concentration in the samples, the ADN-1 process (lightest grey trace) is much more efficient at removing nitrogen, while ADN-2 (medium grey trace) hardly affects any change. These conclusions are consistent with the elemental analysis of nitrogen in the samples (Table 5-3; Feed 3771 ppm N, ADN-1 2656 ppm N, ADN-2 3330 ppm N). Figure 5-2B is the HGO feed and three products resulting from treatment with a reference catalyst at three different temperatures. The chromatogram shows that the processes all remove a significant amount of nitrogen, but that differences between the hydrotreating temperatures cannot be discerned based on peak intensity.

Despite the somewhat poor quality of the chromatograms on HC-Tol, the data collected on this column can still be used to make a qualitative comparison of the amount of nitrogen between samples, with the best chromatogram quality resulting from the catalyst chromatograms.

5.3.2 Separations on “DNAP”

The gas oil separations on “DNAP” had better peak shapes and higher intensity than with the HC-Tol column. Using a commercially available stationary phase for further analysis is also attractive because of the ease of obtaining the column and reproducing or continuing analyses. The “DNAP” chromatograms have four peak regions: 1) 0.5-5.8 minutes; 2) 5.8-10 minutes; 3) 10-14 minutes; and 4) 14-17.5 minutes, as illustrated in Figure 5-3. Data collected from the elution of standards indicates that Fraction 1 should contain PAH compounds, as well as highly sterically hindered pyridine nitrogen species. Fraction 2 should contain some nitrogen species, as well as oxygen and sulphur species. Fraction 3 corresponds to the less sterically hindered nitrogen species. No standards eluted in the Fraction 4 time window. More information regarding the content of these fractions is discussed in Section 5.3.3.

The retention of standards on the “DNAP” column indicates that nitrogen content should be expected in Fractions 1-3. Similar to the HC-Tol column, we can correlate the relative intensity of the peaks to nitrogen content in the samples. Figure 5-4 has two chromatograms of samples from the distillate cut gas oils. Chromatogram 5-4A is a hydrotreated HGO and its distillate cuts.

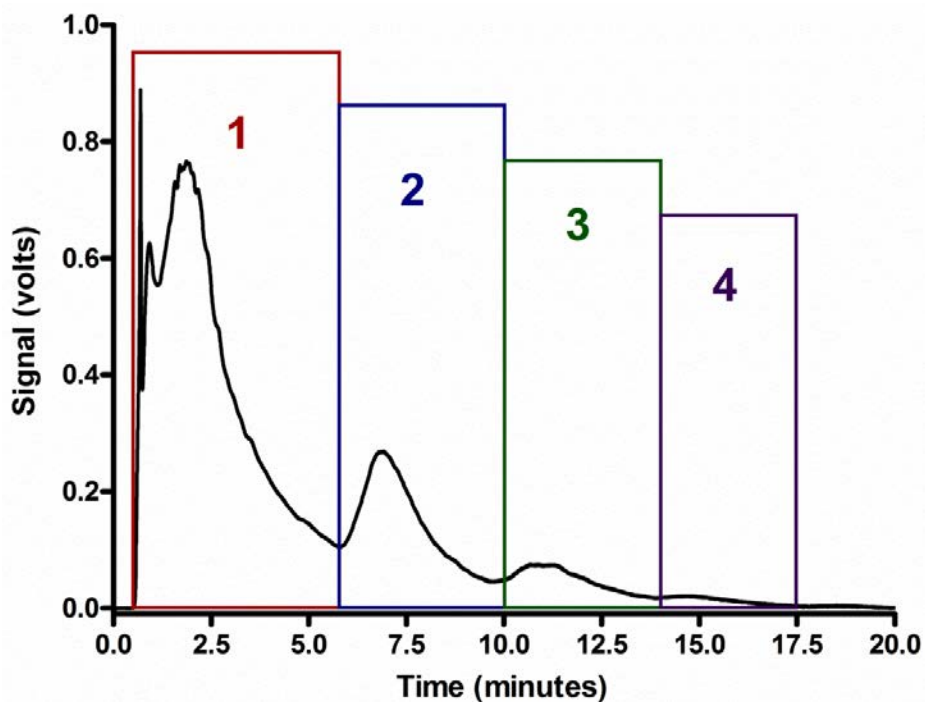


Figure 5-3. Chromatogram illustrating the four fractions collected on the “DNAP” column. Sample: HGO parent feed from the catalyst sample set. Conditions: “DNAP” column, (5.0 x 4.6 cm, 5 μ m particles), step gradient, 5-100% DCM in hexane, 20%/4 minute steps, T = 35°C, flow rate 1.0 mL/min, detection wavelength 254 nm.

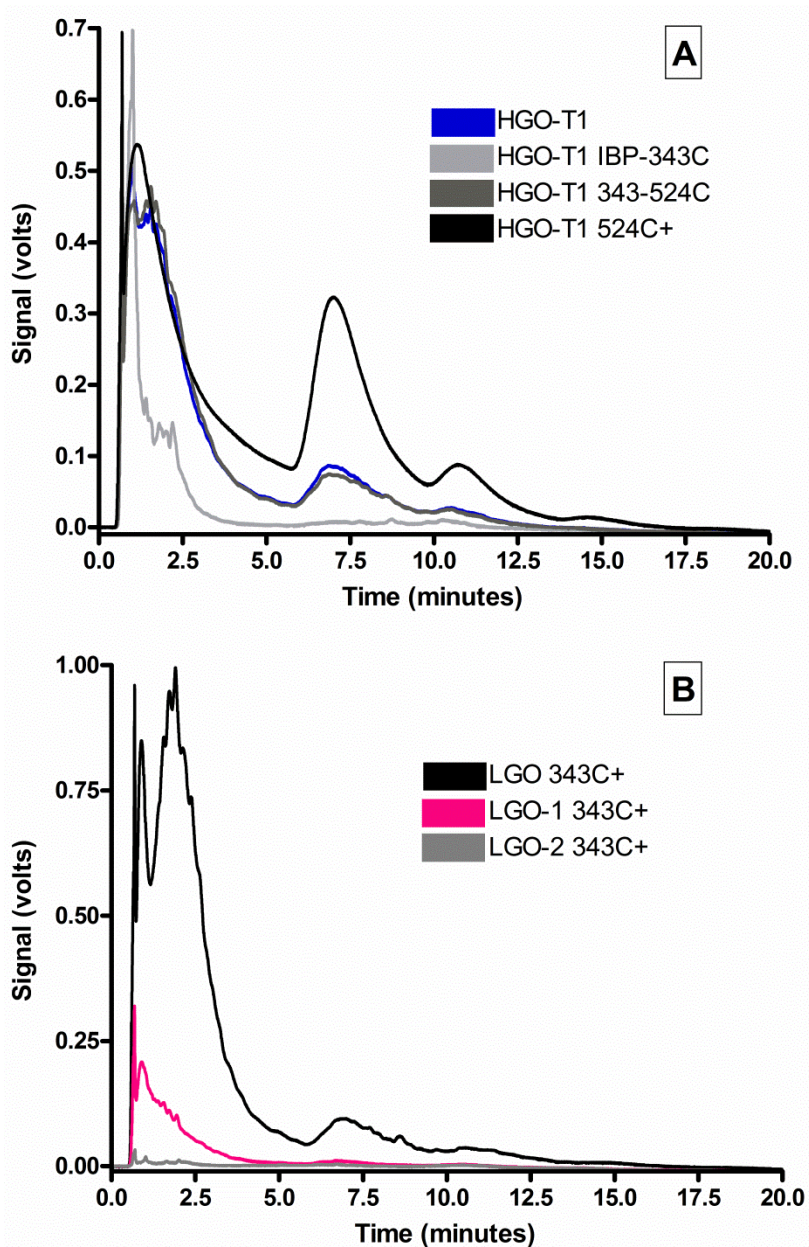


Figure 5-4. Chromatograms on “DNAP” for different gas oil distillate cuts. A: Hydrotreated heavy gas oil (blue) and its three distillate cuts (greys and black). B: The highest boiling distillate cut for a light gas oil (black), the first stage hydrotreated LGO (pink) and final stage hydrotreated LGO (grey). Conditions: “DNAP” column, (5.0 x 4.6 cm, 5 μ m particles), step gradient, 5-100% DCM in hexane, 20%/4 minute steps, T = 35°C, flow rate 1.0 mL/min, detection wavelength 254 nm.

The highest boiling distillate cut (524C+) has the highest aromatic and nitrogen content, and the lowest boiling cut (IBP-343C) has very little nitrogen content. This correlates with the elemental analysis (Table 5-2). Petroleomic analysis of gas oil distillation cuts has also shown that heteroatom content increases with boiling point, and that the molecules also become larger and more aromatic [38, 39]. Chromatogram 5-4B shows the highest boiling cut (343C+) of three different LGOs; a feed, and two hydrotreated products. From Figure 5-4B we can see that the highest boiling cut of the final hydrotreated LGO product (LGO-2) has nearly all of the nitrogen and aromatic species removed. The LGO cuts also have more species in fraction 1 than in fractions 2-4, which when matched to the retention times of standards indicates more PAH content than nitrogen containing molecules.

Figures 5-5, 5-6 and 5-7 show chromatograms of the catalyst samples on the “DNAP” column. Figure 5-5 features samples that had the adsorptive nitrogen removal treatment. Figure 5-5A compares a hydrotreated HGO (grey trace) to two HGOs that have had adsorptive denitrogenation treatment (black and red traces). Consistent with the elemental analysis data, the lower signal of the HGO-TA shows that hydrotreatment removes more nitrogen containing compounds than the two ADN treatments, and that ADN-1 removes more nitrogen than ADN-2. Figure 5-5B was plotted to see if any differences in nitrogen removal could be observed when the ADN samples were hydrotreated (ADN-1-TA and ADN-2-TA).

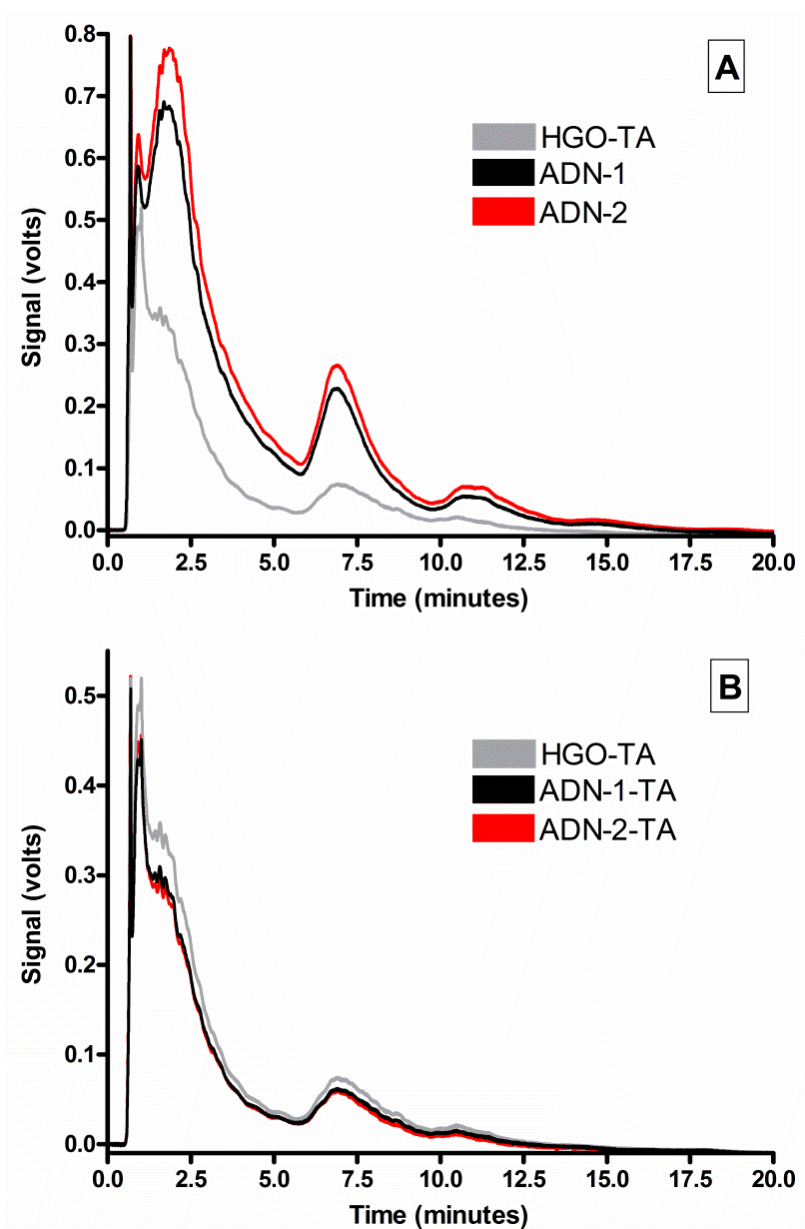


Figure 5-5. A: Overlaid chromatograms comparing hydrothermally treated samples that have had adsorptive denitrogenation treatment (ADN-1-TA, black trace and ADN-2-TA, red trace) and a hydrothermally treated sample that has had no treatment (HGO-TA, grey trace). B: Overlaid chromatograms of a hydrothermally treated HGO (grey), a hydrothermally treated HGO that has had ADN-1 treatment (black) and a hydrothermally treated HGO that has had ADN-2 treatment (red). Conditions: “DNAP” column, (5.0 x 4.6 cm, 5 μ m particles), step gradient, 5-100% DCM in hexane, 20%/4 minute steps, T = 35°C, flow rate 1.0 mL/min, detection wavelength 254 nm.

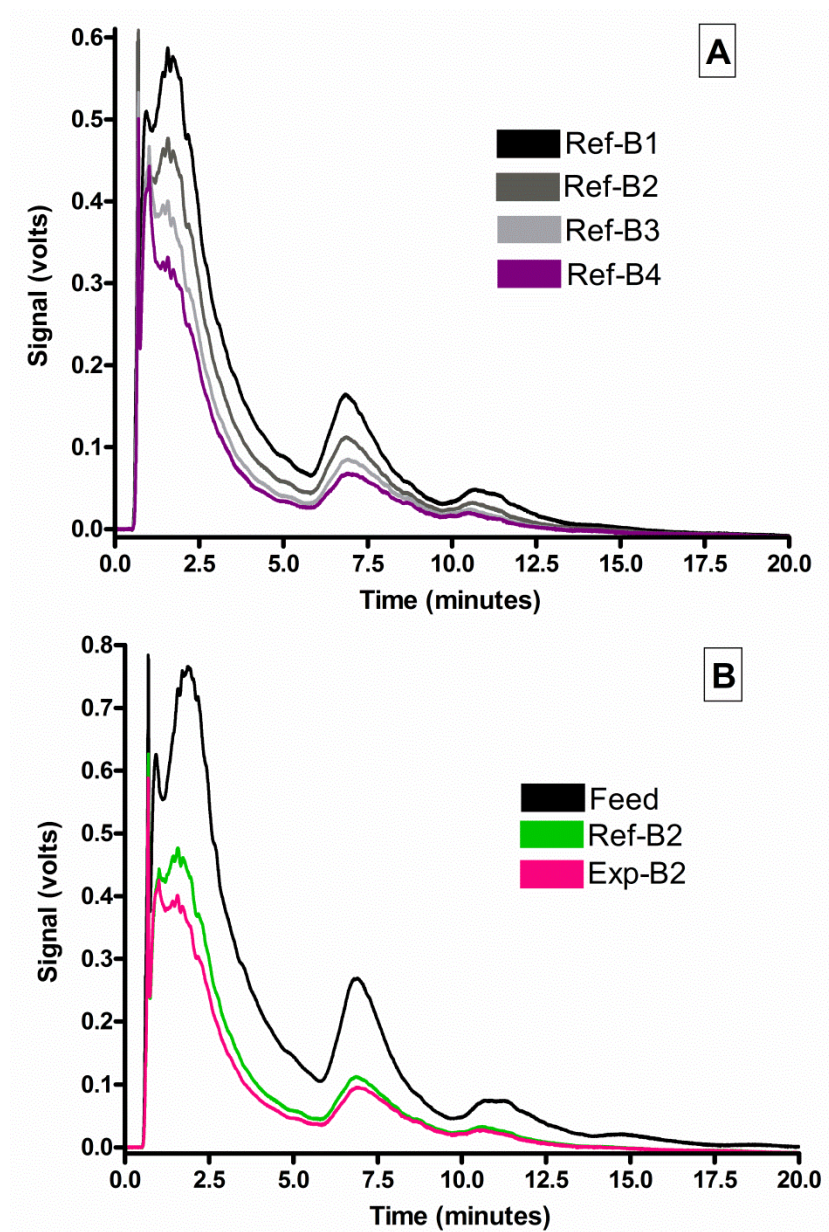


Figure 5-6. Overlaid chromatograms of samples simulating different sections of a fixed bed reactor. A: Different fixed bed sections with the same catalyst (see Table 5-3). B: The HGO feed (black) and a reference (green) and experimental (pink) catalyst in the same simulated bed section. Conditions: “DNAP” column, (5.0 x 4.6 cm, 5 μ m particles), step gradient, 5-100% DCM in hexane, 20%/4 minute steps, T = 35°C, flow rate 1.0 mL/min, detection wavelength 254 nm.

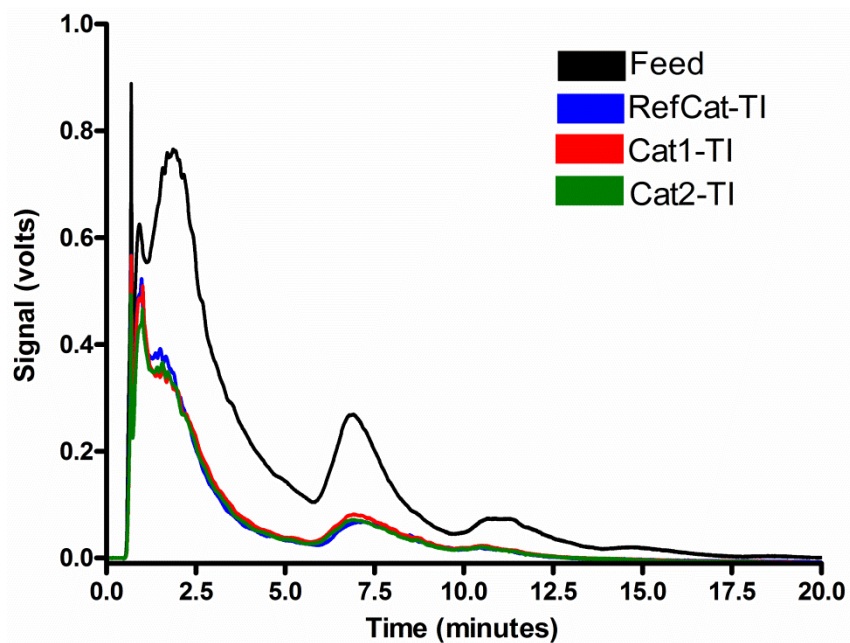


Figure 5-7. Overlaid chromatograms of the HGO feed and hydrotreated samples using different catalyst systems. Black: feed; blue: reference catalyst; red: catalyst 1; green: catalyst 2. Conditions: “DNAP” column, (5.0 x 4.6 cm, 5 μm particles), step gradient, 5-100% DCM in hexane, 20%/4 minute steps, $T = 35^\circ\text{C}$, flow rate 1.0 mL/min, detection wavelength 254 nm.

The samples in Figure 5-6 are those that simulate different sections of a fixed bed reactor. Figure 5-6A shows a progressive decrease in signal with each consecutive section of the fixed bed, corresponding to better nitrogen removal. Figure 5-6B compares a reference hydrotreating catalyst (Ref-B2) to a new experimental catalyst (Exp-B2) and their relative reduction in nitrogen compared to the HGO feed. The experimental catalyst removes more nitrogen, as indicated by its smaller overall peak area under fractions 1 and 2. Finally, Figure 5-7 shows the HGO feed in comparison to hydrotreated products of three different catalysts. The traces for the three hydrotreated products (blue, red and green) overlap almost completely, and the chromatograms do not allow for any comments to be made about the relative efficiency of nitrogen removal for these catalysts. These samples are studied in further detail in Sections 5.3.3 and 5.3.4 to see if there is a difference in the type of nitrogen compounds removed by the catalysts, and whether or not the MS data can determine these differences.

The chromatograms in this section allow for an excellent qualitative comparison of the overall nitrogen removal or concentrations between samples. Knowing the specific content of peaks in the separation will enable more in-depth analysis of the chromatograms.

5.3.3 FT-ICR MS Analysis of the “DNAP” Fractions

To determine what nitrogen species were eluting in each part of the “DNAP” chromatogram, fractions were collected for each of the regions identified in Figure 5-3. Each of these fractions was analyzed on the FT-ICR MS

system in both positive and negative mode: pyrroles are detected in negative mode through deprotonation, and pyridines are detected in positive mode through protonation [33-40, 43]. Composer software was used to identify the MS peaks in each of the fractions, and the data was collected into tables, with the heteroatom classes present in each fraction, accompanied by the range of carbon numbers, m/z range and double-bond-equivalence (DBE) range. The DBE of a molecule is a measure of the unsaturation and aromaticity – the higher the DBE, the more rings and double bonds are present in the molecule. The DBE of a compound is calculated by [48]:

$$DBE = c - \frac{h}{2} + \frac{n}{2} + 1 \quad (\text{Equation 5-1})$$

where c , h , and n are the number of carbon, hydrogen and nitrogen atoms in the molecule. The DBE values displayed for the fractions are that of the corresponding neutral molecules and not the charged ions detected by the MS. This analysis was performed for four distillate samples and four catalyst samples to determine if there are any patterns related to carbon number or DBE for the different HPLC fractions. The data is tabulated in Table 5-4 for the distillate samples and Table 5-5 for the catalyst samples.

Figure 5-8 shows a typical mass spectrum for negative mode analysis of an HPLC fraction (A) and a typical mass spectrum for positive mode analysis of an HPLC fraction (B). The contamination peaks present in B are very intense; however the Composer software has the ability to “ignore” these known peaks while analyzing the spectrum, and full peak assignments can be made when the correct parameter files are written (Section 5.2.3.1).

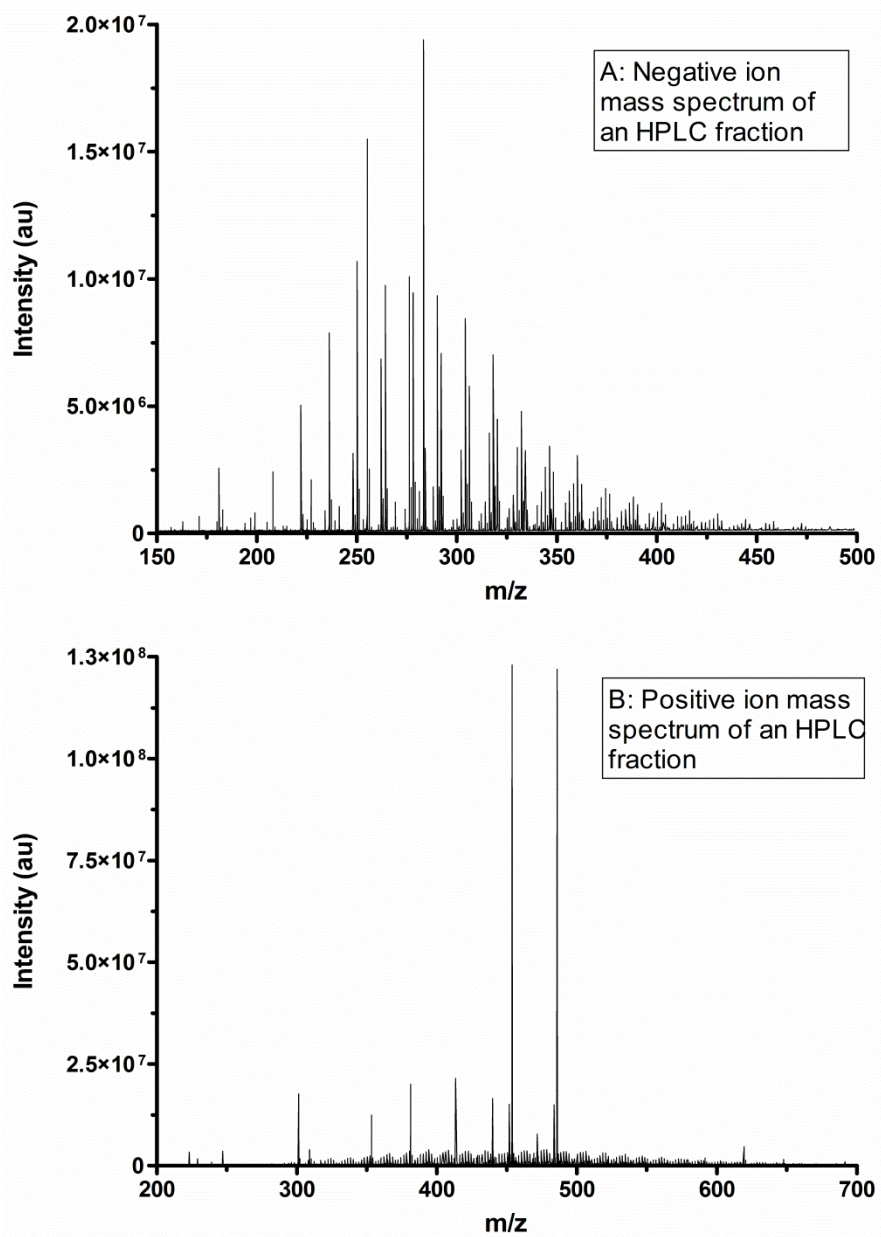


Figure 5-8. Representative mass spectra of HPLC fractions, positive and negative. The fractions were collected from the “DNAP” column; the negative mode spectrum (A) was fraction 2 from analysis of the sample Cat2-TI and the positive mode spectrum (B) was fraction 1 from analysis of the sample RefCat-TI.

Table 5-4. Dominant compound classes present in each HPLC fraction on the “DNAP” column for selected distillate cut samples, in both positive and negative mode.*

Fraction 1 (0.5-5.8 min)				
Sample	LGO-1 343C+	HGO-T1 524C+	HGO 524C+	HGO Feed
(+) Mode	N DBE 4-14 m/z 270-570, C# 18-42	N DBE 8-17 m/z 520-840, C# 37-59	N DBE 9-17 m/z 460-780, C# 30-58	N DBE 4-18 m/z 330-560, C# 22-42
	NS DBE 6-12 m/z 300-460, C# 19-30	NS[Na] DBE 6 m/z 530-770, C# 34-52	NS DBE 10-17 m/z 400-730, C# 27-51	NS DBE 7-15 m/z 340-560, C# 20-38
(-) Mode	N DBE 7-10 m/z 250-370, C# 19-27	-	-	N DBE 9-10 m/z 290-390
Fraction 2 (5.8-10 min)				
Sample	LGO-1 343C+	HGO-T1 524C+	HGO 524C+	HGO Feed
(+) Mode	N DBE 4-16 m/z 250-600, C# 20-42	N DBE 6-18 m/z 500-800, C# 36-57	N DBE 9-21 m/z 380-600, C# 30-45	N DBE 5-18 m/z 300-550, C# 19-43
	NS DBE 6-11 m/z 270-450, C# 20-30		NS DBE 16-19 m/z 390-600, C# 27-42	NS DBE 7-16 m/z 360-480, C# 20-33
(-) Mode	N DBE 7-13 m/z 220-400, C# 15-30	N DBE 9-18 m/z 360-630, C# 24-46	-	N DBE 9-14 m/z 220-480, C# 17-35
	O DBE 4-9 m/z 260-350, C# 18-27			O DBE 4-7 m/z 270-400, C# 27-42

* Compound class is listed in bold, followed by the DBE range of the compounds, the m/z range and the carbon number range (C#) for the class. The lightened grey text indicates that the compound class was detected but that the number of compounds was negligible (less than 20 individual compounds identified for each DBE class). Sample information can be found in Tables 5-1 and 5-2.

Table 5-4. Continued dominant compound classes for HPLC fractions on the “DNAP” column for selected distillate cut samples.

Fraction 3 (10-14 min)				
Sample	LGO-1 343C+	HGO-T1 524C+	HGO 524C+	HGO Feed
(+) Mode	N DBE 4-13 m/z 270-470, C# 19-34	N DBE 7-18 m/z 400-750, C# 29-53	N DBE 8-21 m/z 460-600, C# 26-44	N DBE 5-17 m/z 300-560, C# 21-42 NS DBE 9-16 m/z 300-500, C# 19-35
(-) Mode	N DBE 9-14	N DBE 13-17 m/z 320-430, C# 24-33	N DBE 13-17 m/z 300-450, C# 23-33	N DBE 9-16 m/z 200-400, C# 14-28
Fraction 4 (14-17.5 min)				
Sample	LGO-1 343C+	HGO-T1 524C+	HGO 524C+	HGO Feed
(+) Mode	OS[Na] DBE 1-4, 6-7 m/z 330-490, C# 16-30 N DBE 6-10 m/z 260-390, C# 17-28	--	-	OS[Na] DBE 1-4, 6 m/z 310-540, C# 17-33
(-) Mode	O ₂ DBE 1-7 m/z 220-460, C# 16-31	O ₂ DBE 1-7 m/z 300-420, C# 19-30	-	O ₂ DBE 1-7 m/z 150-400, C# 9-27

Table 5-5. Dominant compound classes present in each HPLC fraction on the “DNAP” column for selected catalyst samples, in both positive and negative mode.

Fraction 1 (0.5-5.8 min)				
Sample	HGO parent feed	Cat1-TI	Cat2-TI	RefCat-TI
(+) Mode	N DBE 5-17 m/z 250-730, C# 18-53	N DBE 5-14 m/z 350-680, C# 25-49	N DBE 5-16 m/z 320-690, C# 23-49	N DBE 5-14 m/z 340-660, C# 24-46
	NS DBE 9-15 m/z 270-680, C# 18-47			
(-) Mode	N DBE 9-10 m/z 300-370, C# 22-27	N DBE 9	N DBE 9-10	N DBE 7-11 m/z 280-480, C# 20-33
Fraction 2 (5.8-10 min)				
Sample	HGO parent feed	Cat1-TI	Cat2-TI	RefCat-TI
(+) Mode	N DBE 5-18 m/z 270-680, C# 20-40	N DBE 5-14 m/z 300-580, C# 20-43	N DBE 5-13 m/z 320-550, C# 23-40	N DBE 5-13 m/z 340-590, C# 24-40
	NS DBE 10-17 m/z 290-590, C# 18-41			
(-) Mode	N DBE 9-14 m/z 220-430, C# 17-30	N DBE 9-14 m/z 300-400, C# 16-29	N DBE 6-15 m/z 260-500, C# 17-36	N DBE 9-14 m/z 200-520, C# 15-36

* Compound class is listed in bold, followed by the DBE range of the compounds, the m/z range and the carbon number range (C#) for the class. The lightened grey text indicates that the compound class was detected but that the number of compounds was negligible (< 20 individual compounds identified for each DBE class). Sample information is listed in Table 5-3.

Table 5-5. Continued dominant compound classes for HPLC fractions on the “DNAP” column for selected catalyst samples.

Fraction 3 (10-14 min)				
Sample	HGO parent feed	Cat1-TI	Cat2-TI	RefCat-TI
(+) Mode	N DBE 7-14 m/z 320-500, C# 24-36	N DBE 6-11 m/z 330-550, C# 24-40	N DBE 5-14 m/z 360-600, C# 27-45	N DBE 6-12 m/z 320-580, C# 23-42
(-) Mode	N DBE 12-15 m/z 280-360, C# 21-27	N DBE 9-15 m/z 250-380, C# 18-27	N DBE 9-15 m/z 250-380, C# 17-27	N DBE 9-14 m/z 200-260, C# 16-27
Fraction 4 (14-17.5 min)				
Sample	HGO parent feed	Cat1-TI	Cat2-TI	RefCat-TI
(+) Mode	OS[H], OS[Na]	O DBE 11-12	O DBE 11-12	-
(-) Mode	-	-	-	-

These contaminants were identified and discussed in Section 4.3.2.4, and clean fractions free of the contaminants have been demonstrated. As the data analysis had already been completed when the identity of the contaminants was discovered, the choice was made to proceed with the original data.

The MS data in Tables 5-4 and 5-5 reveals that pyridine content is high in fractions 1, 2 and 3, and that the highest intensity of pyrrole species is in fraction 2, with a smaller amount in fraction 3. In negative mode, the compounds containing two oxygen atoms (O_2 species) are confined to fraction 4. Positive mode data shows that in the heavier distillate cut samples and the HGO feed, NS species co-elute with the pyridines in positive mode. Other petroleomic analyses of gas oils have reported more heteroatom classes than are observed here [37-39, 43, 49]. However the compound classes aside from the N_1 class in the literature reports are at low abundance and the dilution effect of our offline fraction analysis may make it impossible to observe these low abundance classes. Studies have also shown that following hydrotreating, the N_1 class is the dominant remaining class [35-37, 49]. Five of the samples analyzed on the MS were hydrotreated, so it is unsurprising that N_1 compounds were all that was observed for these samples.

The presence of pyridines in fractions 1-3 (Tables 5-4 and 5-5) was expected based on the retention time of standards (Section 5.3.2), however it is surprising that there is such a high intensity of pyrroles in fraction 2. Based on the standard data, it was expected that the pyrroles would be in fraction 3. The pyrrole standards analyzed were not alkylated, and if the pyrroles follow the same trend as pyridines, it is logical to assume that the pyrroles eluting in fraction 2

have a higher degree of alkylation. This is confirmed by higher carbon numbers and lower DBEs in fraction 2 than in fraction 3 (Tables 5-4 and 5-5).

The MS fraction data was studied to determine whether or not any trends could be observed between the fractions in terms of carbon number or DBE. Only the pyrroles and pyridines were examined, as they were the most prominent species and the original focus of the study. Figure 5-9 plots the relative abundance of each DBE type for pyridines (A, positive mode) and pyrroles (B, negative mode) for sample Cat1-TI. The data is plotted for fractions 1-3 for pyridines and fractions 2 and 3 for the pyrroles. The abundance plotted is that of the DBE type for N_1 species divided by the all of the other detected species. Figure 5-9A shows that the DBE distribution is similar between fractions 1 and 2 for the pyridines, and that fraction 3 does not contain any pyridines on the high or low ends of the DBE scale. This indicates that any separation occurring on the “DNAP” column for pyridines is not affected by the aromaticity of the molecules. Figure 5-9B (pyrroles) is more interesting; the pyrroles eluted in Fraction 3 are of higher DBE than in Fraction 2. This is consistent with the more alkylated pyrroles eluting in Fraction 2, and less alkylated and more aromatic pyrroles eluting in Fraction 3.

Similar to Figure 5-9, Figure 5-10 plots the carbon numbers for the pyridines (Figure 5-10A, positive mode, fractions 1-3) and the pyrroles (Figure 5-10B, negative mode, fractions 2 and 3). The y-axis on these graphs is plotted in the scale of ion intensities, to allow comparison of the intensity of peaks between the different HPLC fractions.

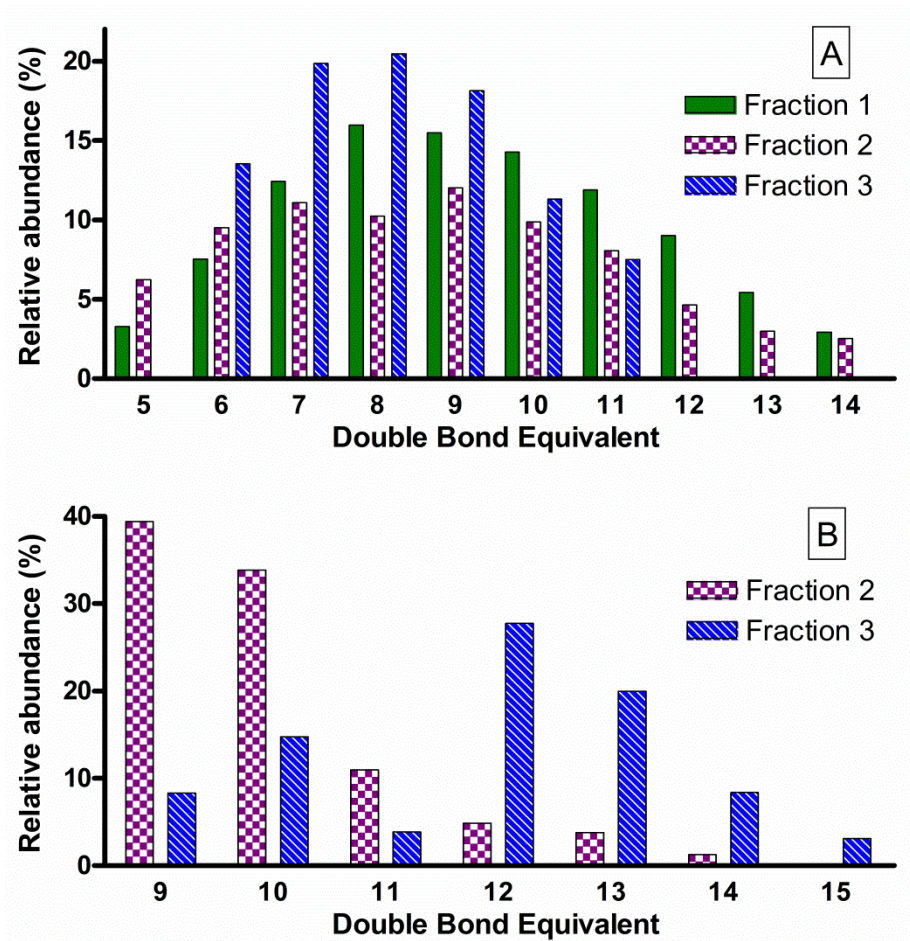


Figure 5-9. (A) Bar graph illustrating the relative abundance for each double bond equivalent (DBE) class of pyridinic nitrogen compounds in the positive mode for fractions 1-3 of sample Cat1-TI. (B) Bar graph illustrating the relative abundance for each DBE class of pyrrolic nitrogen compounds in the negative mode for fractions 2 and 3 of sample Cat1-TI. Separation was performed on the “DNAP” column, and the fractions correspond to the labelled peaks in Figure 5-3. Fraction 4 was not plotted due to the absence of any nitrogen species.

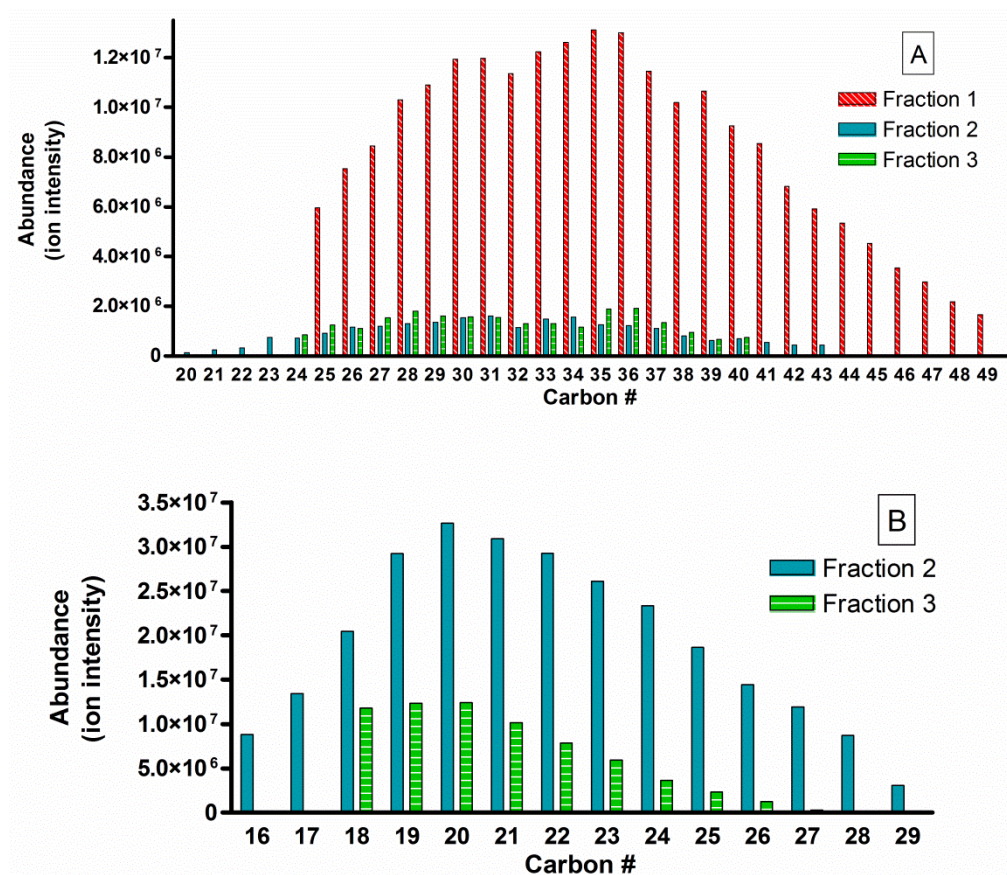


Figure 5-10. (A) Bar graph illustrating the abundance by ion intensity for each carbon number of pyridinic nitrogen compounds in the positive mode for fractions 1-3 of sample Cat1-TI. (B) Bar graph illustrating the abundance by ion intensity for each carbon number of pyrrolic nitrogen compounds in the negative mode for fractions 2 and 3 of sample Cat1-TI. Separation was performed on the “DNAP” column, and the fractions correspond to the labelled peaks in Figure 5-3. Fraction 4 was not plotted due to the absence of any nitrogen species.

The higher carbon numbers observed in fraction 1, when combined with the DBE data (Figure 5-9) is consistent with the conclusion that the pyridines in fraction 1 are more alkylated, and likely experience more steric hindrance. The reason for the higher intensity of ions in fraction 1 compared to fractions 2-3 is unknown; one possibility is that the hydrotreated sample contains an excess of highly alkylated, hydrotreatment-resistant compounds. Figure 5-10B shows that the greatest intensity of pyrrole ions is found in fraction 2, and that the higher carbon numbers are also found in fraction 2 versus fraction 3. It is also likely that there are more alkylated molecules present, giving higher ion intensity in fraction 2.

The information gained from the petroleomic data can be useful to take a more in-depth look at the chromatograms on “DNAP”. Combining the information from standard compounds and the MS data, we can conclude that the majority of the UV signal in fractions 2 and 3 can be attributed to nitrogen-containing compounds. Table 5-6 expresses the reduction of peaks 2 and 3 following different nitrogen-removal processes as a percentage of the feed sample. The adsorptive denitrogenation processes (ADN-1 and ADN-2) yield a more significant reduction in fraction 3 compared to fraction 2. The two hydrotreating processes (HGO-TA and Cat1-TI) yield comparable decreases in both fractions. We can generalize that the adsorptive processes are less effective at removing the species found in fraction 2, likely moderately alkylated pyridines, and highly alkylated pyrroles, than the hydrotreating process, and that the hydrotreating is overall more effective at reducing the nitrogen content of the samples.

Table 5-6. Reduction in HPLC d 2 and 3 on the “DNAP” column compared to the feed sample for some samples treated with nitrogen removal processes.

Sample	Peak reduction compared to feed	
	Peak 2	Peak 3
ADN-1	15%	25%
ADN-2	1%	6%
HGO-TA	72%	70%
Cat1-TI	70%	68%

Put another way, the compounds in fractions 2 and 3 are equally resistant to hydrotreating, and the fraction 2 compounds are more resistant to adsorptive denitrogenation treatment.

The MS data was also used to show how efficiently pyridines and pyrroles are removed in fractions 1-3 following the hydrotreating process. Figure 5-11 is a bar graph illustrating the abundance of nitrogen compounds for the HGO feed and two hydrotreated products (catalysts 1 and 2) for positive mode (A) and negative mode (B). The efficiency of removal of pyridinic nitrogen species (A) depends on the catalyst, with catalyst 1 removing more of the compounds in fractions 2 and 3 than catalyst 2. The effectiveness of the catalysts is not consistent from fraction to fraction, which makes it difficult to make a generalization regarding the types of compounds removed from each fraction. Figure 5-11B shows that for negative mode, the relative abundance of pyrroles is higher in the two catalyst treated samples than in the feed. This may be the result of some larger DBE pyrroles being broken down into lower DBE molecules (leaving the net abundance of pyrroles the same) during the hydrotreating process [37], or because pyrroles are less readily saturated than pyridines during hydrotreating [36]. No definite conclusions can be drawn about the removal of pyrrole compounds from fractions 2 and 3 after hydrotreating.

In summary, the petroleomic data has enabled an in-depth analysis of the “DNAP” separations, and has given us more information into the type of retention of nitrogen species occurring on the column.

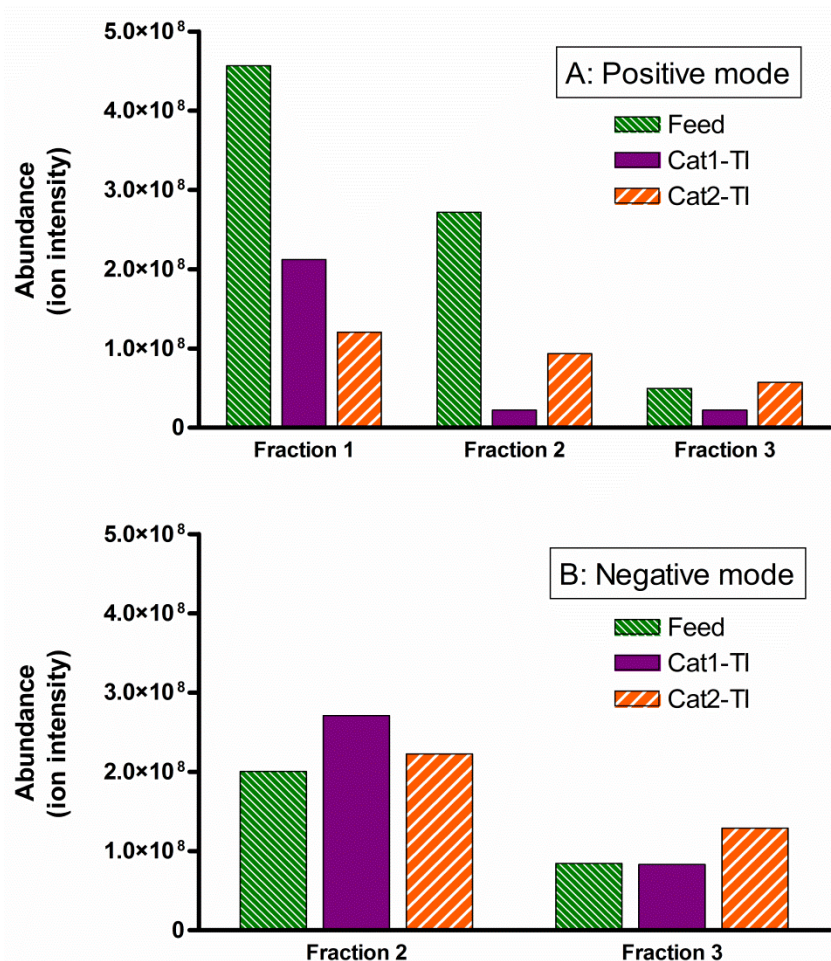


Figure 5-11. Abundance of nitrogen species by fraction for the feed and hydrotreated samples Cat1-TI and Cat2-TI. Pyridines are represented in positive mode (A) for fractions 1-3, and pyrroles are represented in negative mode (B) for fractions 2 and 3.

The separation of species in the gas oil samples with the HPLC fraction collection process makes the mass spectra analyzed simpler than in an unfractionated sample. The ESI process selectively ionizes the nitrogen containing compounds in a sample, but an ionization process such as atmospheric pressure photoionization (APPI) can ionize pyrroles, pyridines and hydrocarbons in the same spectrum [50]. In this case, the ability to isolate pyridines away from PAHs (for example, in fraction 2) would be highly beneficial to simplifying the analysis of peaks and reducing overlap in the mass spectrum.

5.3.4 Case Study: Comparing Catalysts

Figure 5-7 shows chromatograms of a feed and three hydrotreated products using three different catalysts. The discussion in Section 5.3.2 regarding this figure concluded that no differences could be seen between the three catalysts. The data collected from the MS analysis of the HPLC fractions revealed that while the overall nitrogen content may be relatively similar, the types of compounds removed are different (Figure 5-11). A closer examination of the Table 5-5 fraction data reveals that Cat1 results in pyrrole species with a DBE between 9-14, and Cat2 results in pyrroles with a DBE range of 6-15 (Fraction 2). The pyrrole species resulting from Cat2 also have a wider carbon number distribution. Fractions 1 and 2 do not show any major differences between the pyridine species, but fraction 3 also shows higher carbon numbers and a wider DBE range for Cat2.

To compare the fraction data to that of the unfractionated sample, the HGO feed and samples Cat1-TI and Cat2-TI were analyzed on the FT-ICR MS without any prior fractionation. Table 5-7 lists the detected compound classes and their carbon numbers, DBE ranges and m/z ranges for these three samples in positive and negative mode. NS species were detected in positive mode in all three samples, confirming the suspicion that the HPLC procedure dilutes these compounds below the level of detection in the HPLC fractions. The data from the unfractionated Cat1 and Cat2 shows that the DBE values of the pyridines and pyrroles are relatively the same between the catalysts, but that Cat2 results in a wider range of carbon numbers and DBE values for both species.

The results indicate that the fraction data for the pyrrole species (fraction 2) does not represent the lower carbon numbers present in the unfractionated sample for Cat2 and the lower DBE values for unfractionated Cat1. The pyridine data shows that the low carbon number pyridines present in Cat2 are not represented by the fraction data. The lower DBE and carbon numbers compounds may be of too low abundance to be detected in the diluted HPLC fractions, and this example illustrates that caution is necessary when drawing quantitative conclusions regarding DBE and carbon number from fractionated samples. The analysis of HPLC fractions enables more powerful interpretation of the chromatograms, and is a compliment to full petroleomic analysis of samples, not a replacement.

Table 5-7. Sample compositions from positive and negative mode MS analysis of an HGO feed and the products resulting from two different catalyst treatments.*

<u>Sample</u>	MS mode	
	Positive (pyridines)	Negative (pyrroles)
Feed	N[H] DBE 4-19 C# 19-45, m/z 260-620	N[H] DBE 7-17 C# 13-35, m/z 220-460
	NS[H] DBE 2-17 C# 19-42, m/z 290-600	O₂[H] DBE 1-13 C# 14-40, m/z 200-600
		O₂S[H] DBE 3-10 C# 14-33, m/z 250-540
Cat1-TI	N[H] DBE 4-15 C# 24-46, m/z 320-640	N[H] DBE 6-16 C# 15-32, m/z 220-450
	NS[H] DBE 1-7 C# 24-42, m/z 380-620	
Cat2-TI	N[H] DBE 4-16 C# 17-48, m/z 240-670	N[H] DBE 6-17 C# 13-36, m/z 180-500
	NS[H] DBE 1-6 C# 22-45, m/z 350-670	

*The compound class is listed in bold, followed by the DBE range of the compounds, the m/z range and the carbon number range (C#) for the class. The details of the samples can be found in Table 5-3.

5.4 Conclusions

This chapter demonstrated successful petroleomic analysis of HPLC fractions collected offline. The chromatograms of various hydrotreated and distillate cut gas oil samples on two different analytical columns were studied, and commercially available “DNAP” was selected for its superior peak shape and distinct peak regions, as well as its ready availability. The chromatograms and MS data showed that the chromatographic peak intensity on “DNAP” could be correlated to nitrogen content in the sample, and based on DBE and carbon number data, alkylation decreases retention of pyrroles and pyridines. “DNAP” separations can be used to judge the relative efficiency of nitrogen removal processes such as hydrotreatment and adsorptive denitrogenation treatment. Comparison of fraction data to petroleomic analysis of unfractionated samples showed that quantitative comparisons of DBE and carbon number of samples based on fraction data should be done with caution, and that the HPLC fraction analysis is not a replacement for full petroleomic studies of samples.

5.5 References

- [1] M.J. Girgis, B.C. Gates, *Industrial & Engineering Chemistry Research* **1991**, *30*, 2021-2058.
- [2] J.G. Speight, *The Chemistry and Technology of Petroleum*, 4th ed., CRC Press, 2006.
- [3] K.J. Weller, P.A. Fox, S.D. Gray, D.E. Wigley, *Polyhedron* **1997**, *16*, 3139-3163.
- [4] R. Prins, M. Jian, M. Flechsenhar, *Polyhedron* **1997**, *16*, 3235-3246.

- [5] E. Furimsky, F.E. Massoth, *Catalysis Today* **1999**, 52, 381-495.
- [6] W. Kanda, I. Siu, J. Adjaye, A.E. Nelson, M.R. Gray, *Energy & Fuels* **2004**, 18, 539-546.
- [7] Y.S. Bae, M.B. Kim, H.J. Lee, C.H. Lee, J.W. Ryu, *Aiche Journal* **2006**, 52, 510-521.
- [8] J.H. Kim, X.L. Ma, A.N. Zhou, C.S. Song, *Catalysis Today* **2006**, 111, 74-83.
- [9] M. Almarri, X.L. Ma, C.S. Song, *Industrial & Engineering Chemistry Research* **2009**, 48, 951-960.
- [10] R.P. Rodgers, T.M. Schaub, A.G. Marshall, *Analytical Chemistry* **2005**, 77, 20A-27A.
- [11] O.C. Mullins, E.Y. Sheu, A. Hammami, A.G. Marshall, *Ashphaltenes, Heavy Oils and Petroleomics*, 1st ed., Springer Science, New York, 2007.
- [12] A.G. Marshall, R.P. Rodgers, *Proceedings of the National Academy of Sciences* **2008**, 105, 18090–18095.
- [13] A.G. Marshall, C.L. Hendrickson, G.S. Jackson, *Mass Spectrometry Reviews* **1998**, 17, 1-35.
- [14] C.A. Hughey, R.P. Rodgers, A.G. Marshall, *Analytical Chemistry* **2002**, 74, 4145-4149.
- [15] Z. Wu, S. Jernstrom, C.A. Hughey, R.P. Rodgers, A.G. Marshall, *Energy & Fuels* **2003**, 17, 946-953.
- [16] M.M. Mapoleloa, R.P. Rodgers, G.T. Blakney, A.T. Yenc, S. Asomaning, A.G. Marshall, *International Journal of Mass Spectrometry* **2011**, 300, 149-157.
- [17] P.V. Hemmingsen, S. Kim, H.E. Pettersen, R.P. Rodgers, J. Sjoblom, A.G. Marshall, *Energy & Fuels* **2006**, 20, 1980-1987.

- [18] C.A. Hughey, C.S. Minardi, S.A. Galasso-Roth, G.B. Paspalof, M.M. Mapolelo, R.P. Rodgers, A.G. Marshall, D.L. Ruderman, *Rapid Communications in Mass Spectrometry* **2008**, *22*, 3968-3976.
- [19] D.F. Smith, R.P. Rodgers, P. Rahimi, A. Teclemariam, A.G. Marshall, *Energy & Fuels* **2009**, *23*, 314-319.
- [20] J.V. Headley, K.M. Peru, S. Mishra, V. Meda, A.K. Dalai, D.W. McMartin, M.M. Mapolelo, R.P. Rodgers, A.G. Marshall, *Rapid Communications in Mass Spectrometry* **2010**, *24*, 3121-3126.
- [21] C.A. Hughey, R.P. Rodgers, A.G. Marshall, K. Qian, W.K. Robbins, *Organic Geochemistry* **2002**, *33*, 743-759.
- [22] D.F. Smith, T.M. Schaub, S. Kim, R.P. Rodgers, P. Rahimi, A. Teclemariam, A.G. Marshall, *Energy & Fuels* **2008**, *22*, 2372-2378.
- [23] K. Qian, W.K. Robbins, C.A. Hughey, H.J. Cooper, R.P. Rodgers, A.G. Marshall, *Energy & Fuels* **2001**, *15*, 1505-1511.
- [24] P. Liu, C. Xu, Q. Shi, N. Pan, Y. Zhang, S. Zhao, K.H. Chung, *Analytical Chemistry* **2010**, *82*, 6601-6606
- [25] J.M. Purcell, P. Juyal, D.-G. Kim, R.P. Rodgers, C.L. Hendrickson, A.G. Marshall, *Energy & Fuels* **2007**, *21*, 2869-2874.
- [26] R.P. Rodgers, F.M. White, C.L. Hendrickson, A.G. Marshall, K.V. Andersen, *Analytical Chemistry* **1998**, *70*, 4743-4750.
- [27] D.F. Smith, G.C. Klein, A.T. Yen, M.P. Squicciarini, R.P. Rodgers, A.G. Marshall, *Energy & Fuels* **2008**, *22*, 3112-3117.
- [28] D. Borton, D.S. Pinkston, M.R. Hurt, X. Tan, K. Azyat, A. Scherer, R. Tykwinski, M. Gray, K. Qian, H.I. Kenttamaa, *Energy & Fuels* **2010**, *24*, 5548-5559.
- [29] G.C. Klein, S. Kim, R.P. Rodgers, A.G. Marshall, A. Yen, S. Asomaning, *Energy & Fuels* **2006**, *20*, 1965-1972.

- [30] G.C. Klein, S. Kim, R.P. Rodgers, A.G. Marshall, A. Yen, *Energy & Fuels* **2006**, *20*, 1973-1979.
- [31] C.S. Hsu, V.V. Lobodin, R.P. Rodgers, A.M. McKenna, A.G. Marshall, *Energy & Fuels* **2011**, *25*, 2174-2178.
- [32] P. Juyal, A.M. McKenna, Andrew Yen, R.P. Rodgers, C.M. Reddy, R.K. Nelson, A.B. Andrews, E. Atolia, S.J. Allenson, O.C. Mullins, A.G. Marshall, *Energy & Fuels* **2011**, *25*, 172-182.
- [33] K. Qian, R.P. Rodgers, C.L. Hendrickson, M.R. Emmett, A.G. Marshall, *Energy & Fuels* **2001**, *15*, 492-498.
- [34] Z. Wu, R.P. Rodgers, A.G. Marshall, J.J. Strohm, C. Song, *Energy & Fuels* **2005**, *19*, 1072-1077.
- [35] J. Fu, G.C. Klein, D.F. Smith, S. Kim, R.P. Rodgers, C.L. Hendrickson, A.G. Marshall, *Energy & Fuels* **2006**, *20*, 1235-1241.
- [36] G.C. Klein, R.P. Rodgers, A.G. Marshall, *Fuel* **2006**, *85*, 2071-2080.
- [37] T. Kekalainen, J.M.H. Pakarinen, K. Wickstrom, P. Vainiotalo, *Energy & Fuels* **2009**, *23*, 6055-6061.
- [38] D.F. Smith, P. Rahimi, A. Teclemariam, R.P. Rodgers, A.G. Marshall, *Energy & Fuels* **2008**, *22*, 3118-3125.
- [39] L.A. Stanford, S. Kim, R.P. Rodgers, A.G. Marshall, *Energy & Fuels* **2006**, *20*, 1664-1673.
- [40] Y. Zhang, C. Xu, Q. Shi, S. Zhao, K.H. Chung, D. Hou, *Energy & Fuels* **2010**, *24*, 6321-6326.
- [41] Z.K. Li, J.S. Gao, G. Wang, Q. Shi, C.M. Xu, *Industrial & Engineering Chemistry Research* **2011**, *50*, 9415-9424.
- [42] Z.K. Li, G. Wang, Q.A. Shi, C.M. Xu, J.S. Gao, *Industrial & Engineering Chemistry Research* **2011**, *50*, 4123-4132.

- [43] X. Zhu, Q. Shi, Y. Zhang, N. Pan, C. Xu, K.H. Chung, S. Zhao, *Energy & Fuels* **2011**, *25*, 281-287.
- [44] N.E. Oro, C.A. Lucy, *Journal of Chromatography A* **2010**, *1217*, 6178-6185.
- [45] N.E. Oro, C.A. Lucy, *Journal of Chromatography A* **2011**, *1218*, 7788-7795.
- [46] Magnet Lab Researchers License Critical Petroleum Data, available online at <http://www.magnet.fsu.edu/mediacenter/news/pressreleases/2008/2008july30-icr.html>, accessed on March 19, 2012.
- [47] R.P. Rodgers, Personal Communication, 2011.
- [48] F.W. McLafferty, F. Tureek, *Interpretation of Mass Spectra*, 4th ed., University Science Books, 1993.
- [49] Q. Shi, C.M. Xu, S.Q. Zhao, K.H. Chung, Y.H. Zhang, W. Gao, *Energy & Fuels* **2010**, *24*, 563-569.
- [50] J.M. Purcell, R.P. Rodgers, C.L. Hendrickson, A.G. Marshall, *Journal of the American Society for Mass Spectrometry* **2007**, *18*, 1265-1273.

CHAPTER SIX. Conclusions and Future Work

6.1 Conclusions

This thesis explored the use of normal phase high performance liquid chromatography (HPLC) for separating the nitrogen group-types found in petroleum (pyrroles and pyridines), and the further coupling of offline HPLC fractions to high resolution mass spectrometry for the detailed characterization of nitrogen compounds in gas oil samples.

6.1.1 Normal Phase HPLC

Chapter 2 studied three different HPLC stationary phases composed of hypercrosslinked polystyrene. Twenty one analytical standards representing the compounds found in petroleum samples were used to compare the retention of a polymeric hypercrosslinked polystyrene phase (HGN), and two custom-synthesized phases consisting of a polymer layer on silica, HC-C₈ and HC-Tol. All three types of phase have unique selectivity for model petroleum compounds. The custom HC phases had previously never been used under normal phase conditions. Plots of retention factor versus solvent strength showed that they act under an adsorptive retention mechanism, with the specific adsorption site remaining unknown. This was opposite to the previously reported partitioning mechanism observed under reversed phase conditions. The HGN phase also retained via adsorption, with the dominant analyte-stationary phase interaction being π - π . This was consistent with previously published literature.

Under the conditions used in Chapter 2, the HGN and HC-C₈ columns irreversibly retained pyridine compounds, making these phases unsuitable for the study of nitrogen group types. The HC-Tol column demonstrated useful and unique selectivity for model petroleum compounds, separating PAHs, pyrroles and pyridines into three distinct groups in under 25 minutes, with the use of a step gradient. Sulphur and oxygen containing compounds eluted with the PAH compounds. Under different gradient conditions oxygen compounds may also be separated by type. The HC-Tol column showed very weak retention of PAH compounds, making it ideal for the study of polar petroleum compounds.

Chapter 3 continued the overarching goal of achieving a nitrogen group type HPLC separation. While the HC-Tol column in Chapter 2 provided the separation we were looking for, the stationary phase needs to be synthesized in-house, and as such is unavailable for use by companies or research groups without synthetic and column-packing capabilities. Three commercially available columns were studied in Chapter 3. Work was continued with the HGN phase, and a biphenyl phase was also selected for its structural similarity to the HGN phase. Finally, a dinitrophenyl phase “DNAP” was also selected; the “DNAP” phase is sold for petroleum analysis, but no literature separations were available to judge its suitability for our needs.

When isopropyl alcohol was used as a strong solvent on HGN instead of dichloromethane, all model compound groups were eluted. A linear gradient of isopropyl alcohol in hexane on HGN demonstrated that gas oil samples could be separated based on their aromaticity and polarity. This separation enables a non-

quantitative assessment of the aromatic and polar content in a sample, but no group-type separation was achieved. The biphenyl phase had no retention of model petroleum compounds under normal phase conditions, so work was not continued with this phase. The “DNAP” phase could not separate pyrroles from pyridines, but is selective for nitrogen containing compounds, separating them from PAHs, as well as oxygen and sulphur compounds. No irreversible retention of gas oil samples was observed on this phase, and the group type separation capabilities on “DNAP” made it the best choice from this chapter for further studies of nitrogen compounds in petroleum.

6.1.2 High Resolution Mass Spectrometry

The latter half of this thesis focused on the development of methods to analyze HPLC fractions collected offline on a Fourier Transform Ion Cyclotron Resonance mass spectrometer (FT-ICR MS). This pairing was non-trivial, as the extra sample handling steps introduced during the fraction collection can introduce contaminants. Chapter 4 describes the protocols necessary to minimize interference and optimize concentrations of HPLC fractions for MS analysis. To improve signal, HPLC fractions must be concentrated and re-dissolved, with the addition of formic acid for positive mode analysis and ammonium hydroxide for negative mode analysis. Sources of contamination included the molecular sieves used to dry normal phase solvents, detergents, and plastics. A contamination with a 0.8 mass defect resulting from the clustering of iron with formate ions was also observed. The formate-iron clusters have not been previously reported in any

literature, and their source was likely the stainless steel present in the HPLC system. Fortunately, the clusters are unstable and easily broken up and removed. Two other previously unreported contamination peaks resulting from palmitoylglycerol and stearoylglycerol are also discussed.

Chapter 5 brings together parts of all the knowledge gained throughout the course of this thesis. Chapter 5 uses HPLC to separate nitrogen compounds, followed by petroleomic analysis of the HPLC fractions to study the nitrogen compounds present in samples. The HC-Tol column from Chapter 2 and the “DNAP” column from Chapter 3 were both studied as a means of fractionating samples. Separations of gas oil samples on “DNAP” had more distinct peak regions, and better intensity and peak shape than on HC-Tol; thus the “DNAP” column was chosen for full petroleomic analysis of fractions. The chromatograms on “DNAP” showed four peak regions, whose relative intensities could be correlated to the nitrogen content in the samples. A wide variety of distillate cut gas oils and treated heavy gas oils were analyzed on “DNAP”.

The HPLC fractions collected from “DNAP” were analyzed on the FT-ICR MS with electrospray ionization (ESI) in both positive and negative mode to determine pyrrole (negative mode) and pyridine (positive mode) content of each of the four peak regions. Pyrroles are concentrated in peaks 2 and 3, while the pyridines elute in peaks 1-3. More alkylated nitrogen compounds elute earlier than their less alkylated counterparts, and nitrogen compounds in peaks 2 and 3 are equally resistant to hydrotreating, while the peak 2 compounds are more resistant to adsorptive denitrogenation treatment. Comparison of the fraction data

to unfractionated samples indicated that the dilution effect of HPLC analysis makes the fraction data unsuitable for quantitative comparisons of nitrogen removal in terms of carbon number and double bond equivalents.

In summary, the analysis of nitrogen containing compounds in gas oil samples was improved by developing nitrogen specific HPLC separations and advanced MS methods for the determination of species present in HPLC peak regions. The comprehensive petroleomic MS analysis of samples represents how far analytical technology has progressed, and the recent research in this area shows that interest is active and ongoing. The methods developed in this thesis are a stepping stone to further work, and demonstrate the possibilities for improved analysis when combining two powerful analytical techniques. This being said, it is important to remember that there is always a need for simple and straightforward techniques for analysis of petroleum samples, and methods should be developed with the least complicated procedure possible. The hope is that with continued on-going research in this area that a complete separation of nitrogen group types in a real sample can be achieved in a single HPLC separation.

6.2 Future Work

6.2.1 Improving HPLC Separations

For the separation of standard compounds, the HC-Tol column provided the best selectivity (Chapter 2). The column separates with an adsorptive mechanism via the nitrogen atom in the molecules. The problem with developing further separations with this column is the lack of understanding of the retention

mechanism on the column. There are unanswered questions, including why the HC-C₈ phase shows different retention for pyridine compounds compared to HC-Tol, and why HC-Tol is so selective for different types of nitrogen compounds. While these features of HC-Tol may be partially attributed to differences in the underlying silica and compounds used in the synthesis of the phase [1], we still do not know for sure.

Current research in the Lucy group is using linear solvation energy relationships (LSERs) to study the nature of the HC-Tol column. LSERs are used to break down the retention on a column into five terms, each of which represents a different parameter of the solute: polarizability (*E*), dipolarity (*S*), hydrogen bond donating ability (*A*), hydrogen bond accepting ability (*B*), and molecular size (*V*) [2, 3]. These terms are displayed in Equation 6-1, where SP usually represents log *k* for chromatography [2]:

$$SP = c + eE + sS + aA + bB + vV \quad (\text{Equation 6-1})$$

Through the determination of *c*, *e*, *s*, *a*, *b* and *v* using linear regression, it is hoped that the LSERs can give importance to and insight into the interactions between solutes and the column. The more a parameter contributes to retention, the higher its numerical value. Preliminary work on the HC-Tol column has indicated that *b* (hydrogen bond accepting ability of the solute) is significant for the retention of nitrogen-containing compounds. The knowledge of the nature of the interaction occurring between the nitrogen-containing compounds and the stationary phase would benefit future synthetic design of columns. Understanding what is causing retention of pyrroles and pyridines would allow for purposeful modification and

design of future stationary phases in an effort to better isolate pyridines within a region on the chromatogram.

A general challenge presented to thorough HPLC method development of petroleum samples is the lack of available analytical standards to predict the retention of compounds on a stationary phase. The lack of commercially available standards also is a problem for MS development [4]. Many of the compounds found in petroleum, especially the samples from Athabasca bitumen, are highly aromatic and alkylated [4, 5]. While compounds such as acridine and carbazole are easily available through chemical suppliers, compounds with additional rings and alkylation are difficult to obtain. A recent publication has reported the synthesis of highly alkylated pyrene and N-phenylcarbazole molecules, with molecular weights approaching ~1000 amu [6]. The synthesis of model asphaltene compounds has also been reported [7-9]. These publications give hope that someday alkylated model petroleum compounds will be easily available for both HPLC and MS studies. As shown throughout this thesis, it is difficult to predict the behavior of actual samples on a stationary phase with the standards currently available. Studying the retention of model compounds with sequential alkylation and ring number would show conclusively how steric hindrance around the nitrogen atom in a molecule affects interaction with the stationary phase. An extended suite of model compounds would also enable a more accurate prediction of ionization efficiencies in MS analyses (Section 6.2.4).

6.2.2 Petroleomic Data Analysis

The petroleomic data in Chapter 5 was analyzed using a commercial software program designed to assign compounds to peaks in a mass spectrum of a petroleum sample (Composer, produced by Sierra Analytics). Correct interpretation of the mass spectrum could be seen as the most important part of the data analysis, as incorrect assignments give a completely different interpretation of the data. While the Composer software is designed to make analysis of mass spectra simpler, in the case of analyzing HPLC fractions, optimizing the software for the reduced peak series found in the fractions was a difficult challenge. Publications from multiple groups doing petroleomic analysis have demonstrated that data analysis is possible using the raw data files and home-written functions in Microsoft Excel [10-13], including the analysis of HPLC fractions [14].

When the data is processed with home-written files, there exists the flexibility to plot or display the data any way desired, including contour plots, bar graphs, and dot plots [10-12, 14, 15]. Composer allows the output of figures, but the user is limited to the graph options within the program. There is also a concern that the Composer program parameters can be easily manipulated to give a result that is incorrect, and that someone who does not thoroughly understand the parameters may proceed with incorrect peak assignments. Throughout the course of using Composer over a period of approximately ten months, countless software bugs were discovered, and although future updates may fix these, there is a lack of confidence in the program overall. Discussions with other users of the

program have revealed similar conclusions [16]. Writing our own files to analyze the data would be initially time consuming, but it would save the licensing fee for the Composer software (~\$10 000/year) and give much more flexibility in assigning peaks and displaying the data in terms of ion abundance, carbon number and double bond equivalents.

6.2.3 Different MS Ionization Methods

The initial work done with petroleomics used electrospray ionization (ESI) [12, 17, 18], and ESI is used exclusively in this thesis. ESI is attractive because it selectively ionizes polar compounds like those containing nitrogen through proton transfer reactions to create negative ($[M-H]^-$) and positive ($[M+H]^+$) ions [12, 19, 20]. Non-polar compounds such as aromatics are not ionized and do not complicate the analysis [18]. In recent years, the push has been toward using ionization methods such as atmospheric pressure photoionization (APPI) [21-24]. The ionization process for APPI creates ions through photoionization, typically using a vacuum ultraviolet gas discharge lamp [21, 25]. A dopant such as toluene is often added, as it has a low ionization energy and can create analyte ions through collisions and charge exchange [26]. The APPI process creates both proton-transfer ions and radical cations, allowing the ionization of species with low polarity, or non-polar species [21, 22, 27, 28]. Using APPI to analyze the fractions collected from “DNAP” would make it possible to see what the full content of the chromatogram is, and not just where the nitrogen compounds are eluting. While the analytical standards suggest that the PAHs are eluting in peak

1, it is impossible to know if this is the case without further analysis. The information gained from APPI analysis would make the correlation of peak intensity to relative nitrogen content more accurate, as the percentage of the peaks that can be attributed to solely nitrogen species could be calculated.

Unfortunately, the use of an APPI source is not currently possible for the FT-ICR MS instrument available at the University of Alberta. The company that manufactures the instrument has discontinued software and hardware support for an APPI source on the FT-MS, and the addition of this type of source would require modifications that are not feasible on a shared instrument. Recent work by Alan Marshall and Ryan Rodgers has demonstrated that ESI spectra that are comparable to APPI spectra can be obtained through the addition of special additives to samples [29, 30]. In negative mode, a strong base such as tetramethylammonium hydroxide can be used to deprotonate very non-polar molecules, including hydrocarbons, and in positive mode silver triflate can be added to complex non-polar molecules with Ag^+ to create a positive charge. These additives add charge to molecules that are normally not ionized in ESI, and allow the user to “see” them in a mass spectrum. This method of analysis is more accessible than the addition of a new ionization source, and would be an easy extension of the work experimentally (the addition of strong base or complexing reagent to samples in place of ammonium hydroxide/formic acid). These more information-dense mass spectra would be an interesting comparison to traditional ESI mass spectra, and would likely require method validation to show that effective ionization of hydrocarbons is taking place.

6.2.4 Response Factors and Quantitative Analysis

One of the things missing in petroleomic analysis is quantitative analysis of peaks in a mass spectrum [28]. Due to the complexity of petroleum samples and their resulting mass spectra, this has presented a challenge that has yet to be met by the scientific community. A project of this nature could easily be a number of chapters in a Ph.D. thesis, or even an entire thesis work in itself. None of the ionization techniques available for MS ionize analytes with the same efficiency, making it difficult to correlate ion intensity with analyte concentration in solution [31, 32]. The ideal way to quantify an analyte is to measure the MS response of a standard compound in relation to its concentration [33]. A single petroleum spectrum can contain upwards of 11 000 distinct chemical species, making it impossible to calibrate response with analytical standards [34]. Work done by Chalcraft et al. has demonstrated that it is possible to predict the ionization efficiency of compounds without analytical standards in capillary electrophoresis (CE) ESI-MS [32]. Their method developed a multivariate model of solute parameters derived from molecular structure to predict relative response factors of metabolites. The model required the use of 58 analytical standards to create a training set (47 metabolites) for the model and a test set to validate the model (10 metabolites), with one compound acting as an internal standard.

In the future, it may be possible to apply experiments of this nature to petroleomic analysis. The selection of an appropriate set of model compounds for predicting response factors is a possible obstacle, as the commercial availability of analytical standards for petroleum is poor (Section 6.2.1). It is likely that many

standards used would have to be custom made in a synthetic lab. To develop the quantitation methods, pre-fractionated petroleum samples would be an ideal starting point, with the intent of building on the model to analyze samples of increasing complexity. Despite the difficulties in proceeding with quantitative analysis, the information gained would be worth the time invested. Knowing the content of a sample as well as compound concentrations would make petroleomics a truly comprehensive technique.

6.2.5 Perspective on Current Research

When developing new analytical methodologies, it should be considered how the techniques can be applied to real-world problems. As a scientist, and especially a graduate student, it can be far too easy to get caught up in the small experimental problems and details, while forgetting to step back and look at the big picture. Instead of asking “how do I get this value?” or “how do I optimize this parameter?” it can be instructive and refreshing to ask “what does this mean?” and “how can this information be used to solve a problem?” Giving the work relevance can add perspective and motivation when a project or idea seems to be stalled.

As traditional oil and gas reserves become depleted, heavy oil and oil sands are now an increasingly popular source of fuel and petroleum products [15, 35, 36]. The complex nature of oil sands deposits presents interesting challenges for the extraction and upgrading of oil sands bitumen [36-39]. Current issues facing the industry are both environmental and economic in nature. Improving

the extraction of bitumen with lower temperature and reduced water consumption is of current concern [40-42], as is the reduction of the fine tailings produced [43, 44]. On the upgrading side, designing better catalysts for the treatment of heavy products is important to reduce both waste and atmospheric emissions [35, 45, 46]. As the technology of industrial processes evolves and advances, so too must the analytical methods supporting the research and development. In a world where oil production needs to constantly adapt to new obstacles and environmental concerns, chemists are needed to tackle difficult analytical problems with enthusiasm and creativity.

6.3 References

- [1] Y. Zhang, Y.M. Huang, P.W. Carr, *Journal of Separation Science* **2011**, *34*, 1407-1422.

- [2] M. Vitha, P.W. Carr, *Journal of Chromatography A* **2006**, *1126*, 143-194.

- [3] F.Z. Oumada, M. Roses, E. Bosch, M.H. Abraham, *Analytica Chimica Acta* **1999**, *382*, 301-308.

- [4] C.S. Hsu, V.V. Lobodin, R.P. Rodgers, A.M. McKenna, A.G. Marshall, *Energy & Fuels* **2011**, *25*, 2174-2178.

- [5] M.R. Gray, J.H. Masliyah, *Extraction and Upgrading of Oil Sands Bitumen*, Calgary, AB, 2009.

- [6] M.A. Francisco, R. Garcia, B. Chawla, C. Yung, K. Qian, K.E. Edwards, L.A. Green, *Energy & Fuels* **2011**, *25*, 4600-4605.

- [7] F. Rakotondradany, H. Fenniri, P. Rahimi, K.L. Gawrys, P.K. Kilpatrick, M.R. Gray, *Energy & Fuels* **2006**, *20*, 2439-2447.

- [8] X.L. Tan, H. Fenniri, M.R. Gray, *Energy & Fuels* **2008**, *22*, 715-720.
- [9] H. Sabbah, A.L. Morrow, A.E. Pomerantz, O.C. Mullins, X.L. Tan, M.R. Gray, K. Azyat, R.R. Tykwinski, R.N. Zare, *Energy & Fuels* **2010**, *24*, 3589-3594.
- [10] T. Kekalainen, J.M.H. Pakarinen, K. Wickstrom, P. Vainiotalo, *Energy & Fuels* **2009**, *23*, 6055-6061.
- [11] Q. Shi, C.M. Xu, S.Q. Zhao, K.H. Chung, Y.H. Zhang, W. Gao, *Energy & Fuels* **2010**, *24*, 563-569.
- [12] K. Qian, R.P. Rodgers, C.L. Hendrickson, M.R. Emmett, A.G. Marshall, *Energy & Fuels* **2001**, *15*, 492-498.
- [13] C.S. Hsu, K.N. Qian, Y.N.C. Chen, *Analytica Chimica Acta* **1992**, *264*, 79-89.
- [14] X. Zhu, Q. Shi, Y. Zhang, N. Pan, C. Xu, K.H. Chung, S. Zhao, *Energy & Fuels* **2011**, *25*, 281-287.
- [15] O.C. Mullins, E.Y. Sheu, A. Hammami, A.G. Marshall, *Ashphaltenes, Heavy Oils and Petroleomics*, 1st ed., Springer Science, New York, 2007.
- [16] S. Lababidi, Personal Communication, 2011.
- [17] K. Qian, W.K. Robbins, C.A. Hughey, H.J. Cooper, R.P. Rodgers, A.G. Marshall, *Energy & Fuels* **2001**, *15*, 1505-1511.
- [18] D.L. Zhan, J.B. Fenn, *International Journal of Mass Spectrometry* **2000**, *194*, 197-208.
- [19] J.B. Fenn, M. Mann, C.K. Meng, S.F. Wong, C.M. Whitehouse, *Mass Spectrometry Reviews* **1990**, *9*, 37-70.
- [20] R.P. Rodgers, T.M. Schaub, A.G. Marshall, *Analytical Chemistry* **2005**, *77*, 20a-27a.

- [21] J.M. Purcell, C.L. Hendrickson, R.P. Rodgers, A.G. Marshall, *Analytical Chemistry* **2006**, 78, 5906-5912.
- [22] J.M. Purcell, C.L. Hendrickson, R.P. Rodgers, A.G. Marshall, *Journal of the American Society for Mass Spectrometry* **2007**, 18, 1682-1689.
- [23] J.M. Purcell, R.P. Rodgers, C.L. Hendrickson, A.G. Marshall, *Journal of the American Society for Mass Spectrometry* **2007**, 18, 1265-1273.
- [24] A.M. McKenna, J.M. Purcell, R.P. Rodgers, A.G. Marshall, *Energy & Fuels* **2010**, 24, 2929-2938.
- [25] D.B. Robb, T.R. Covey, A.P. Bruins, *Analytical Chemistry* **2000**, 72, 3653-3659.
- [26] M. Tubaro, E. Marotta, R. Seraglia, P. Traldi, *Rapid Communications in Mass Spectrometry* **2003**, 17, 2423-2429.
- [27] J.A. Syage, M.D. Evans, *Spectroscopy* **2001**, 16, 14-21.
- [28] A.G. Marshall, R.P. Rodgers, *Proceedings of the National Academy of Sciences of the United States of America* **2008**, 105, 18090-18095.
- [29] A.G. Marshall, G.T. Blakney, M.R. Emmett, C.L. Hendrickson, R.P. Rodgers, Recent Advances in Fourier Transform Ion Cyclotron Resonance Mass Spectrometry, Pittcon Conference, Orlando, FL, 2010.
- [30] A.G. Marshall, P. Juyal, R.P. Rodgers, Electrospray Ionization Mass Spectrometry Methodology, Florida State University Research Foundation, United States, 2012.
- [31] F.W. McLafferty, F. Tureek, *Interpretation of Mass Spectra*, 4th ed., University Science Books, 1993.
- [32] K.R. Chalcraft, R. Lee, C. Mills, P. Britz-McKibbin, *Analytical Chemistry* **2009**, 81, 2506-2515.

- [33] D.A. Skoog, F.J. Holler, T.A. Nieman, *Principles of Instrumental Analysis*, 5th ed., Brooks/Cole, 1998.
- [34] C.A. Hughey, R.P. Rodgers, A.G. Marshall, *Analytical Chemistry* **2002**, *74*, 4145-4149.
- [35] J. Fu, G.C. Klein, D.F. Smith, S. Kim, R.P. Rodgers, C.L. Hendrickson, A.G. Marshall, *Energy & Fuels* **2006**, *20*, 1235-1241.
- [36] S.H. Ng, J.S. Wang, C. Fairbridge, Y.X. Zhu, Y.J. Zhu, L.Y. Yang, F.C. Ding, S. Yui, *Energy & Fuels* **2004**, *18*, 172-187.
- [37] S. Ng, Y.X. Zhu, A. Humphries, L.G. Zheng, F.C. Ding, T. Gentzis, J.P. Charland, S. Yui, *Energy & Fuels* **2002**, *16*, 1196-1208.
- [38] S. Ng, Y.X. Zhu, A. Humphries, L.G. Zheng, F.C. Ding, L.Y. Yang, S. Yui, *Energy & Fuels* **2002**, *16*, 1209-1221.
- [39] S.H. Ng, J.S. Wang, C. Fairbridge, Y.X. Zhu, L.Y. Yang, F.C. Ding, S. Yui, *Energy & Fuels* **2004**, *18*, 160-171.
- [40] X.G. Li, W.J. Sun, G.Z. Wu, L. He, H. Li, H. Sui, *Energy & Fuels* **2011**, *25*, 5224-5231.
- [41] J. Masliyah, Z.J. Zhou, Z.H. Xu, J. Czarnecki, H. Hamza, *Canadian Journal of Chemical Engineering* **2004**, *82*, 628-654.
- [42] J. Long, J. Drelich, Z.H. Xu, J.H. Masliyah, *Canadian Journal of Chemical Engineering* **2007**, *85*, 726-738.
- [43] Y.M. Xu, T. Dabros, J.M. Kan, *Process Safety and Environmental Protection* **2008**, *86*, 268-276.
- [44] E.K. Quagraine, H.G. Peterson, J.V. Headley, *Journal of Environmental Science and Health Part A - Toxic/Hazardous Substances & Environmental Engineering* **2005**, *40*, 685-722.

[45] E. Furimsky, *Industrial & Engineering Chemistry Research* **2009**, 48, 2752-2769.

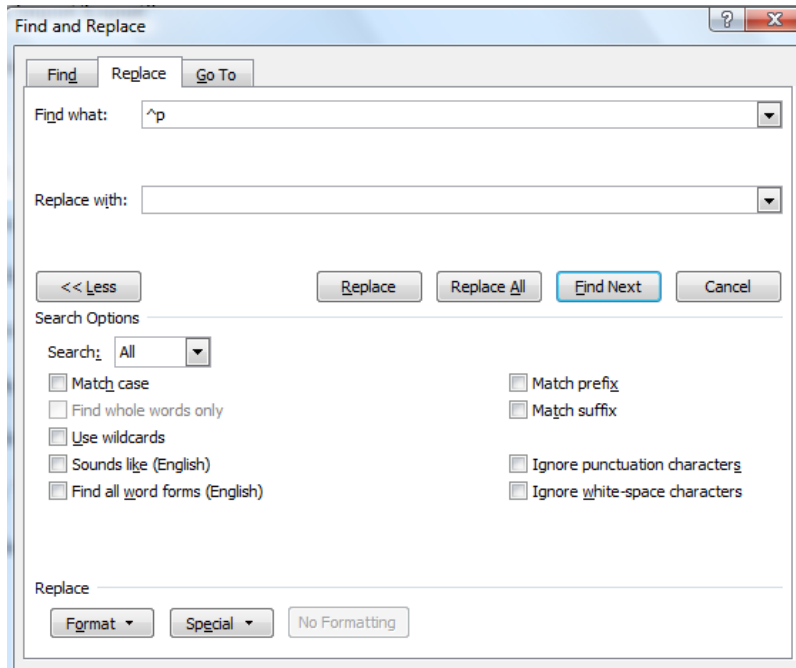
[46] A. Marafi, A. Stanislaus, E. Furimsky, *Catalysis Reviews-Science and Engineering* **2010**, 52, 204-324.

APPENDIX A. Exporting Chromatograms from Varian's Star Workstation and Mass Spectra from Bruker's DataAnalysis for Re-plotting

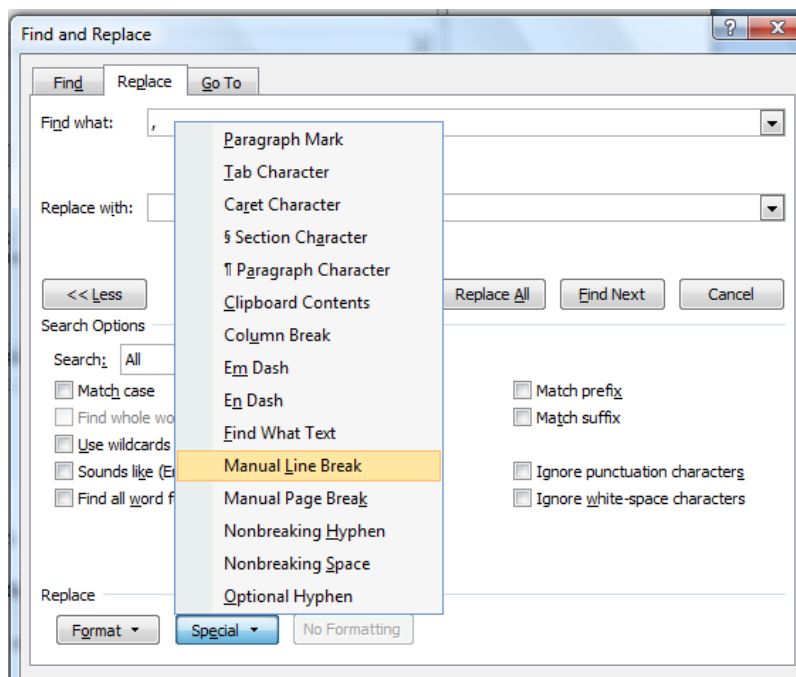
A.1 Exporting Chromatograms

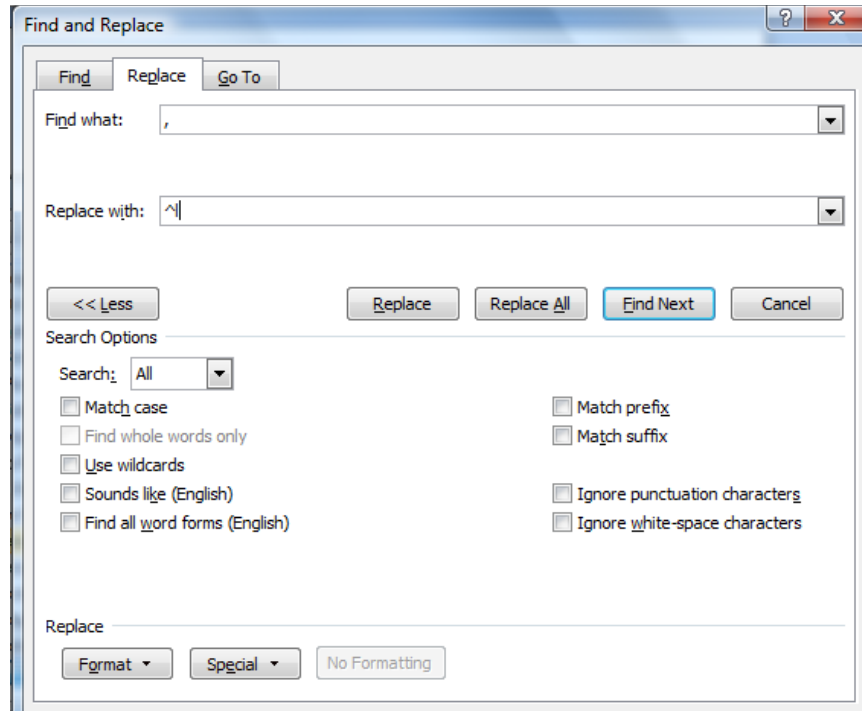
To export chromatograms from Varian's Star Workstation, the data points need to be formatted properly to fit in one column for plotting. The data points that are exported from Star Workstation are that of intensity (the y-axis) in volts, and are output in a multi-line format that will not copy and paste properly into a single column. To export and format data points:

- Open chromatogram to be plotted in Interactive Graphics
- Right click on the chromatogram while it is open in Interactive Graphics
- Select "AIA Import/Export"
- Select "Varian to AIA" and save the file with name and location of choice
- In the "AIA Import/Export" window, select "AIA to Text File" and select the file just saved to convert it to a *.txt format; save text file with name and location of choice
- Open the *.txt file in Notepad
- Copy *only* the body of numbers into a new Word file
- In Word, select the option to "Show mark-up" (Ctrl+Shift+8 or ¶ button)
- Use Word's "Replace" function:
 - Replace All "^p" with nothing; this removes all of the paragraph breaks



Replace All “,” with a manual line break (found under the “Special” pull-down menu at the bottom of the Replace window); this moves each number to a line of its own





- All numbers should now be in a single column
- Copy and paste this column of numbers into a new Excel worksheet
- Make a “Time” column in the Excel worksheet
 - Start at zero, and add data points based on the sampling rate
 - For example, data collected every 0.05s would add 0.0008333 min for every data point
 - Fill the column with Time data points in minutes; for example, if cell A1 is 0, then A2 would be “=A1+0.0008333” and A3 would be “=A2+0.0008333”
- There should now be two columns of data, one of time in minutes and one of intensity in volts

- Excel often crashes when trying to plot large data sets; it is highly recommended that a program such as GraphPad Prism be used to plot the figures

A.2 Exporting Mass Spectra

Bruker's DataAnalysis allows you to save a mass spectrum as an image file, but the axis labels are small and the resolution is low. Re-plotting the spectrum gives a higher quality image and more freedom with displaying the data. Similar to the chromatograms, the data points output by DataAnalysis need to be formatted properly to be plotted. To export and plot data points:

- Open DataAnalysis and open the mass spectrum to be plotted
- From the top menu bar, select File→Export→Mass Spectrum...
- Save the spectrum with name and location of choice, as file format "Mass Spectrum XML File (*.xml)"
- Open the *.xml file; it can be viewed in Internet Explorer
- Copy and paste the text between the two tags <ms_peaks> and </ms_peaks> into a new Word document:

```
<ms_peaks>
<pk res="657052" algo="FTMS" fwhm="0.000285923" a="12.9734" sn="5.2639" i="99299" mz="187.86615726"/>
<pk res="732471" algo="FTMS" fwhm="0.000256567" a="12.3932" sn="4.02233" i="82346.8" mz="187.92814587"/>
<pk res="702304" algo="FTMS" fwhm="0.000267605" a="21.1026" sn="4.12591" i="83761.1" mz="187.94038599"/>
<pk res="678091" algo="FTMS" fwhm="0.000272243" a="10.3726" sn="4.0295" i="82444.7" mz="187.99616652"/>
<pk res="796982" algo="FTMS" fwhm="0.000235948" a="9.97882" sn="4.10396" i="83461.3" mz="188.04626038"/>
<pk res="608719" algo="FTMS" fwhm="0.000308963" a="26.5245" sn="4.33632" i="86634" mz="188.0717624"/>
<pk res="548773" algo="FTMS" fwhm="0.000342869" a="17.8046" sn="4.57302" i="89865.9" mz="188.15723160"/>
<pk res="516680" algo="FTMS" fwhm="0.000364197" a="29.2322" sn="5.48366" i="102299" mz="188.1732997"/>
<pk res="701265" algo="FTMS" fwhm="0.000268543" a="14.6904" sn="4.7143" i="91794.8" mz="188.32026086"/>
<pk res="575651" algo="FTMS" fwhm="0.000327209" a="24.1198" sn="4.09713" i="83368.1" mz="188.35816486"/>
<pk res="832380" algo="FTMS" fwhm="0.00022658" a="5.24663" sn="4.0322" i="82481.5" mz="188.60085929"/>
<pk res="625528" algo="FTMS" fwhm="0.000301907" a="8.55189" sn="4.06618" i="82945.3" mz="188.85126260"/>
<pk res="699533" algo="FTMS" fwhm="0.000269973" a="7.896" sn="4.76622" i="92503.6" mz="188.85526952"/>
<pk res="632786" algo="FTMS" fwhm="0.000298761" a="13.311" sn="4.44322" i="88093.3" mz="189.05188019"/>
<pk res="659389" algo="FTMS" fwhm="0.000287102" a="11.2254" sn="4.21188" i="84934.6" mz="189.31175019"/>
<pk res="629091" algo="FTMS" fwhm="0.000301082" a="22.2559" sn="4.09744" i="83372.1" mz="189.40821827"/>
<pk res="789972" algo="FTMS" fwhm="0.000239826" a="7.62641" sn="4.70554" i="91674.8" mz="189.45593023"/>
<pk res="466852" algo="FTMS" fwhm="0.00040582" a="18.9917" sn="4.34882" i="86804.3" mz="189.45798624"/>
</ms_peaks>
```

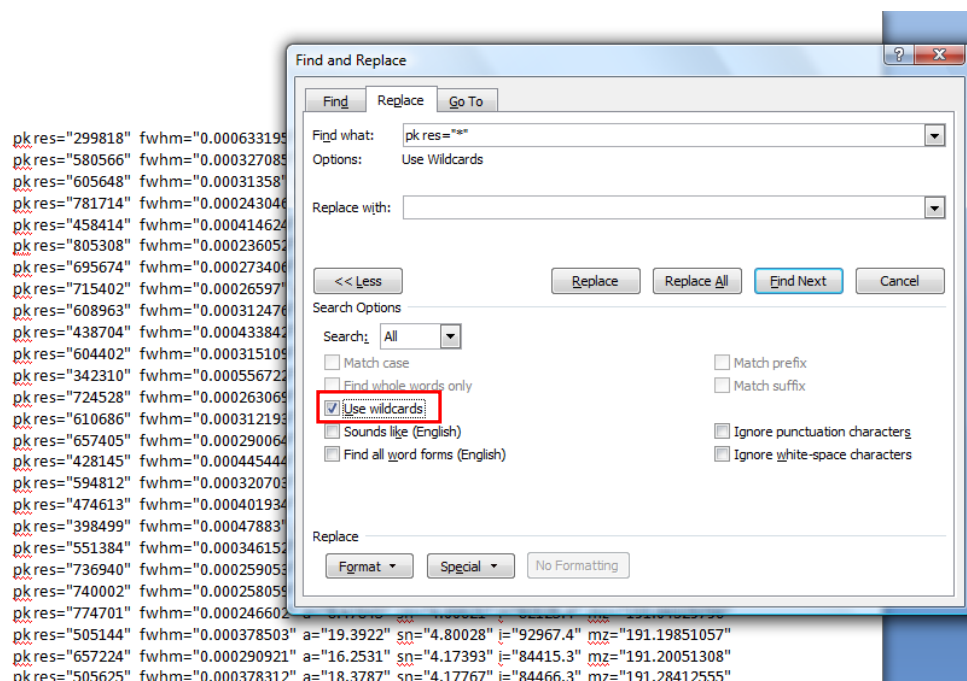
- The formatting will be lost when it is copied into Word:

```
<pk res="299818" algo="FTMS" fwhm="0.000633195" a="21.0114" sn="4.18544" i="84573.4"
mz="189.84337537"/><pk res="580566" algo="FTMS" fwhm="0.000327085" a="35.9957" sn="4.56119"
i="89703.8" mz="189.89435216"/><pk res="605648" algo="FTMS" fwhm="0.00031358" a="20.6375"
sn="4.51767" i="89109.5" mz="189.91897752"/><pk res="781714" algo="FTMS" fwhm="0.000243046"
a="18.2868" sn="5.21721" i="98660.8" mz="189.99266590"/><pk res="458414" algo="FTMS"
fwhm="0.000414624" a="24.3925" sn="4.51531" i="89077.3" mz="190.06967328"/><pk res="805308"
algo="FTMS" fwhm="0.000236052" a="15.2647" sn="4.35876" i="86939.7" mz="190.09497305"/><pk
res="695674" algo="FTMS" fwhm="0.000273406" a="2.51466" sn="4.57006" i="89824.7"
mz="190.20165122"/><pk res="715402" algo="FTMS" fwhm="0.00026597" a="11.7661" sn="4.23058"
i="85189.5" mz="190.27566234"/><pk res="608963" algo="FTMS" fwhm="0.000312476" a="15.9297"
sn="4.96728" i="95248.2" mz="190.28631600"/><pk res="438704" algo="FTMS" fwhm="0.000433842"
a="19.9107" sn="4.0701" i="82998.3" mz="190.32837832"/><pk res="604402" algo="FTMS"
fwhm="0.000315109" a="18.547" sn="4.10718" i="83504.4" mz="190.45260677"/><pk res="342310"
algo="FTMS" fwhm="0.000556722" a="33.2001" sn="4.48986" i="88729.5" mz="190.57174561"/><pk
res="724528" algo="FTMS" fwhm="0.000263069" a="14.9351" sn="4.06986" i="82994.9"
mz="190.60102049"/><pk res="610686" algo="FTMS" fwhm="0.000312193" a="14.17654" sn="4.02411"
i="82370.1" mz="190.65194863"/><pk res="657405" algo="FTMS" fwhm="0.000290064" a="25.6954"
sn="5.31069" i="99936.8" mz="190.68937609"/><pk res="428145" algo="FTMS" fwhm="0.000445444"
a="17.6754" sn="4.65967" i="91047.9" mz="190.71482400"/><pk res="594812" algo="FTMS"
fwhm="0.000320703" a="13.4612" sn="4.25466" i="85517.9" mz="190.75756599"/><pk res="474613"
algo="FTMS" fwhm="0.000401934" a="24.5012" sn="4.5779" i="89931.4" mz="190.76321511"/><pk
res="398499" algo="FTMS" fwhm="0.00047883" a="24.9834" sn="4.77283" i="92592.9"
mz="190.81328260"/><pk res="551384" algo="FTMS" fwhm="0.000346152" a="22.1327" sn="5.31342"
i="99974" mz="190.86247891"/><pk res="736940" algo="FTMS" fwhm="0.000259053" a="15.321"
sn="4.11279" i="83580.7" mz="190.90645333"/><pk res="740002" algo="FTMS" fwhm="0.000258059"
a="14.2313" sn="4.02636" i="82400.7" mz="190.96423913"/><pk res="774701" algo="FTMS"
fwhm="0.000246602" a="8.47845" sn="4.00621" i="82125.4" mz="191.04329796"/><pk res="505144"
algo="FTMS" fwhm="0.000378503" a="19.3922" sn="4.80028" i="92967.4" mz="191.19851057"/><pk
res="657224" algo="FTMS" fwhm="0.000290921" a="16.2531" sn="4.17393" i="84415.3"
mz="191.20612040"/><pk res="866685" algo="FTMS" fwhm="0.000370313" i="844287" i="447787"
```

- Open the Replace menu, and Replace All “/>”with a manual line break (found under the “Special” pull-down menu at the bottom of the Replace window); this puts each data point on one line

```
<pk res="299818" algo="FTMS" fwhm="0.000633195" a="21.0114" sn="4.18544" i="84573.4"
mz="189.84337537"
<pk res="580566" algo="FTMS" fwhm="0.000327085" a="35.9957" sn="4.56119" i="89703.8"
mz="189.89435216"
<pk res="605648" algo="FTMS" fwhm="0.00031358" a="20.6375" sn="4.51767" i="89109.5"
mz="189.91897752"
<pk res="781714" algo="FTMS" fwhm="0.000243046" a="18.2868" sn="5.21721" i="98660.8"
mz="189.99266590"
<pk res="458414" algo="FTMS" fwhm="0.000414624" a="24.3925" sn="4.51531" i="89077.3"
mz="190.06967328"
<pk res="805308" algo="FTMS" fwhm="0.000236052" a="15.2647" sn="4.35876" i="86939.7"
mz="190.09497305"
<pk res="695674" algo="FTMS" fwhm="0.000273406" a="2.51466" sn="4.57006" i="89824.7"
mz="190.20165122"
<pk res="715402" algo="FTMS" fwhm="0.00026597" a="11.7661" sn="4.23058" i="85189.5"
mz="190.27566234"
<pk res="608963" algo="FTMS" fwhm="0.000312476" a="15.9297" sn="4.96728" i="95248.2"
mz="190.28631600"
<pk res="438704" algo="FTMS" fwhm="0.000433842" a="19.9107" sn="4.0701" i="82998.3"
mz="190.32837832"
<pk res="604402" algo="FTMS" fwhm="0.000315109" a="18.547" sn="4.10718" i="83504.4"
mz="190.45260677"
<pk res="342310" algo="FTMS" fwhm="0.000556722" a="33.2001" sn="4.48986" i="88729.5"
mz="190.57174561"
<pk res="724528" algo="FTMS" fwhm="0.000263069" a="14.9351" sn="4.06986" i="82994.9"
mz="190.60102049"
<pk res="610686" algo="FTMS" fwhm="0.000312193" a="14.17654" sn="4.02411" i="82370.1"
mz="190.65194863"
<pk res="657405" algo="FTMS" fwhm="0.000290064" a="25.6954" sn="5.31069" i="99936.8"
mz="190.68937609"
<pk res="428145" algo="FTMS" fwhm="0.000445444" a="17.6754" sn="4.65967" i="91047.9"
mz="190.71482400"
<pk res="594812" algo="FTMS" fwhm="0.000320703" a="13.4612" sn="4.25466" i="85517.9"
mz="190.75756599"
<pk res="474613" algo="FTMS" fwhm="0.000401934" a="24.5012" sn="4.5779" i="89931.4"
mz="190.76321511"
<pk res="398499" algo="FTMS" fwhm="0.00047883" a="24.9834" sn="4.77283" i="92592.9"
mz="190.81328260"
<pk res="551384" algo="FTMS" fwhm="0.000346152" a="22.1327" sn="5.31342" i="99974"
mz="190.86247891"
<pk res="736940" algo="FTMS" fwhm="0.000259053" a="15.321" sn="4.11279" i="83580.7"
mz="190.90645333"
<pk res="740002" algo="FTMS" fwhm="0.000258059" a="14.2313" sn="4.02636" i="82400.7"
mz="190.96423913"
<pk res="774701" algo="FTMS" fwhm="0.000246602" a="8.47845" sn="4.00621" i="82125.4"
mz="191.04329796"
<pk res="505144" algo="FTMS" fwhm="0.000378503" a="19.3922" sn="4.80028" i="92967.4"
mz="191.19851057"
<pk res="657224" algo="FTMS" fwhm="0.000290921" a="16.2531" sn="4.17393" i="84415.3"
mz="191.20612040"
<pk res="866685" algo="FTMS" fwhm="0.000370313" i="844287" i="447787"
```

- The two values from these lines of data that are important are i (intensity) and m/z (mass to charge); the rest of the information will be deleted
- Open the Replace window and Replace All “algo=“FTMS”” with nothing
- Replace all “<” with nothing
- To remove the remaining extra data, the Replace function needs to have “Use wildcards” selected
- Replace All “pk res=“*”” with nothing; selecting wildcards tells Word to substitute the * with any numbers between the quotation marks



- Replace All “fwhm=“*”” with nothing; do the same for the “a” and “sn” values
- Uncheck “Use wildcards”
- Replace All quotation marks “ with nothing

- Replace All “i=” with nothing
- Replace All “mz=” with Tab Character (^t, found in the Special dropdown menu)
- The data should now be two columns of numbers, with the intensity in the first column and mass to charge in the second column
- Copy and paste the data into an Excel worksheet
- Move the intensity data to the left of the mass-to-charge data, as it will be plotted on the y-axis
- As with the chromatograms, it is highly recommended to use GraphPad Prism to plot the mass spectrum